

FINITE ELEMENT MODELLING, EARTHQUAKE ANALYSIS, AND
STRUCTURAL HEALTH MONITORING OF THE ORTAHISAR CASTLE

A THESIS SUBMITTED TO
THE GRADUATE SCHOOL OF NATURAL AND APPLIED SCIENCES
OF
MIDDLE EAST TECHNICAL UNIVERSITY

BY

OSMAN GÖKSU

IN PARTIAL FULFILLMENT OF THE REQUIREMENTS
FOR
THE DEGREE OF MASTER OF SCIENCE
IN
CIVIL ENGINEERING

AUGUST 2015

Approval of the thesis:

**FINITE ELEMENT MODELLING, EARTHQUAKE ANALYSIS AND
STRUCTURAL HEALTH MONITORING OF ORTAHISAR CASTLE**

submitted by **OSMAN GÖKSU** in partial fulfillment of the requirements for the
degree of **Master of Science in Civil Engineering Department, Middle East
Technical University** by,

Prof. Dr. Gülbin Dural Ünver
Dean, Graduate School of **Natural and Applied Sciences** _____

Prof. Dr. Ahmet Cevdet Yalçın
Head of Department, **Dept. of Civil Engineering** _____

Prof. Dr. Ahmet Türer
Supervisor, **Dept. of Civil Engineering, METU** _____

Examining Committee Members:

Prof. Dr. Oğuzhan Hasançebi
Civil Engineering Dept., METU _____

Prof. Dr. Ahmet Türer
Civil Engineering Dept., METU _____

Prof. Dr. Kağan Tuncay
Civil Engineering Dept., METU _____

Asst. Prof. Dr Saeid Kazamzadeh Azad
Civil Engineering Dept., Atılım University _____

Prof. Dr. Tamer Topal
Geological Engineering Dept., METU _____

Date: _____

I hereby declare that all information in this document has been obtained and presented in accordance with academic rules and ethical conduct. I also declare that, as required by these rules and conduct, I have fully cited and referenced all material and results that are not original to this work.

Name, Last name : OSMAN GÖKSU

Signature :

ABSTRACT

FINITE ELEMENT MODELLING, EARTHQUAKE ANALYSIS AND STRUCTURAL HEALTH MONITORING OF ORTAHISAR CASTLE

Göksu, Osman
M.S., Department of Civil Engineering
Supervisor: Prof. Dr. Ahmet Türer
August 2015, 86 pages

Ortahisar Castle is one of the valuable historic sites in Turkey at Cappadocia region. Besides being the largest fairy chimney, its irregular shape makes it difficult to carry out structural evaluation studies. This thesis targets a) to generate a detailed 3D Finite Element Model (FEM) of Ortahisar Castle for the purpose of structural evaluation under earthquake, wind, and temperature loads and b) evaluate collected data from 48 crack meters, one accelerometer, one temperature & humidity sensor, one anemometer, and one wind direction vane installed on the Castle. The FEM of the Castle is formed by using data obtained from 3D laser scanning of the Castle, which is then calibrated by checking against experimentally obtained natural vibration frequencies of the Castle. The stress results obtained from structural analyses are checked with Coulomb-Mohr Theory and Modified-Mohr Theory to see if the material capacity of the Castle is exceeded or not. Collected long term health monitoring data is post-processed into time-amplitude graphs and relevant conclusions are drawn. As a result 97.5% of all members have stresses smaller than 10% of their material capacity under earthquake loads.

Keywords: 3D Laser Scanning, 3D Finite Element Modelling, Structural Health Monitoring, Historical Structures, Coulomb-Mohr Theory, Modified-Mohr Theory

ÖZ

ORTAHİSAR KALESİ'NİN SONLU ELEMANLAR MODELLEMESİ, DEPREM ANALİZİ VE YAPISAL SAĞLIK İZLEMESİ

Göksu, Osman
Yüksek Lisans, İnşaat Mühendisliği Bölümü
Tez Yöneticisi: Prof. Dr. Ahmet Türer
Ağustos 2015, 86 sayfa

Kapakdokya Bölgesinde bulunan Ortahisar Kalesi, Türkiye'nin en değerli tarihsel sahalarından biridir. En büyük peribacası olmasının yanı sıra, düzensiz bir şekle sahip olması; kalenin yapısal değerlendirme çalışmalarını zorlaştırmaktadır. Bu tezin amaçları a) detaylı bir 3 boyutlu (3D) sonlu elemanlar modelinin (FEM) oluşturulması b) kale üzerinde bulunan 48 çatlak ölçer, 1 ivmeölçer, 1 sıcaklık ve nemölçer, 1 rüzgâr hızı ölçer ve 1 rüzgâr yön ölçerin oluşturduğu sensör ağından gelen bilgilerin değerlendirmesidir. Kalenin deneyler sonucu elde edilen doğal salınım frekanslarıyla kalibre edilmiş sonlu elemanlar modeli, kalenin 3 boyutlu lazer taraması sonucu elde edilen bilgiler kullanılarak oluşturulmuştur. Yapılan yapısal analizlerin sonuçlarının değerlendirilmesi Coulomb-Mohr ve Modified-Mohr teorileri kullanılarak yapılmıştır ve kalenin malzeme kapasitesinin aşıp aşılmadığı değerlendirilmiştir. Uzun dönemde toplanan yapısal sağlık izleme verileri derlenerek zaman-değişim grafikleri çizilmiş ve bu grafiklerden elde edilen sonuçlar değerlendirilmiştir. Deprem yükleri altında kaleyi oluşturan elemanların 97,5%'sinin stres değerleri malzeme kapasitelerinin 10%'nun altında kalmaktadır.

Anahtar Kelimeler: 3 Boyutlu Lazer Taraması, 3 Boyutlu Sonlu Elemanlar Modellemesi, Yapısal Sağlık İzlemesi, Tarihi Yapılar, Coulomb-Mohr Teorisi, Modified-Mohr Teorisi

To My Family

ACKNOWLEDGEMENTS

This thesis was completed under the supervision of Prof. Dr. Ahmet Türer. I would like to thank him before than others. The studies, done during the thesis, could not be completed without his labor. He is the best supervisor I have ever met. I also want to thank him for his patience during the thesis. I will carry the honor of working with him during my life.

I also would like to thank Prof. Dr. Tamer Topal for his support during the field works at Ortahisar Castle. His studies about the Castle were illuminated my way during thesis studies and his ideas were improved the quality of the thesis.

I would like to thank you Mr. Evren Küçükdoğan who is the responsible architect of Ortahisar Castle. The information, which he shared, is a key role on this thesis. His cooperation made the studies fast.

I want to thank you Middle East Technical University Scientific Research Project Coordination Unit (BAP) to apply the project, BAP-03-03-2015-003.

I also owe thanks to Prof. Dr. Kağan Tuncay. He has an important role in my career. His support, enthusiasm and, scientific perspective are main factors on my success at bachelor education.

My deepest thanks belong to my family. My parents, Meral and Suat Göksu, my sister, Ayşegül Güleş, my brother in law, Bülent Güleş and, my niece, İpek Güleş always show their support, labor and encouragement during all my life.

I would like to express my deep appreciation to Burak Bulut. He has been one of my best friend for 8 years. We all together completed not only bachelor education but also master education. I cannot forget your importance at this thesis and my life.

I also want to thank my sincere close friends, Ali Efesoy, Banu Özbaş, Berk Bal, Burak Tabağ, Samet Erdoğan, Seçkin Mete and, Umur Gündüz. Their friendship is always with me. Their support and ideas have important roles in my life.

I want to express my deep appreciation to my longtime close friends, Alp Yürümez, Muzaffer Karaman, Muhammet Çubukcı, Samet Gürler, Seda Babayiğit, Ufuk Parlak, and Yağmur Ünal. I owe them the best days in my life.

Lastly but not least, I would like to thank my childhood friends, Erdem İşlek and Eren Işık. I cannot ignore their support during my life.

I also want to thank Ozan Orhan for his cooperation. He was very helpful to me during the thesis study.

TABLE OF CONTENTS

ABSTRACT	v
ÖZ	vii
ACKNOWLEDGEMENTS	xi
TABLE OF CONTENTS	xiii
LIST OF TABLES	xv
LIST OF FIGURES	xvi
CHAPTERS	
1. INTRODUCTION	1
1.1. General	1
1.2. Literature Review	4
1.3. Objectives and Scope	8
2. FINITE ELEMENT MODELLING OF ORTAHISAR CASTLE.....	11
2.1. 3D Laser Scanning of Ortahisar Castle	11
2.2. Organization of Coordinates of the Castle	13
2.3. Importing Dots of the Castle to SAP2000.....	17
2.4. Drawing Finite Element Model of the Castle.....	19
2.5. Determination of Modulus of Subgrade Reaction.....	21
2.6. Natural Frequencies of Ortahisar Castle	22
2.7. Definition of Load Patterns and Load Cases in SAP2000	23
2.8. Load Combinations	28

2.9.	MATLAB Code	32
2.10.	Coulomb-Mohr Theory and Modified-Mohr Theory	33
2.11.	Difficulties Encountered During the Analysis	34
2.12.	Analysis Results	35
3.	STRUCTURAL HEALTH MONITORING STUDIES ON THE CASTLE.....	59
3.1.	Importance of Structural Health Monitoring for Historical Structures	59
3.2.	Sensor Types Used at Ortahisar Castle.....	60
3.2.1.	Crack Meter (LVDT)	60
3.2.2.	Accelerometer	61
3.2.3.	Anemometer	61
3.2.4.	Wind Direction Vane	62
3.2.5.	Temperature and Humidity Sensor	63
3.2.6.	Data logger	63
3.3.	Location of LVDTs on the Castle.....	63
3.4.	Graphical Data Obtaining From LVDTs	64
3.5.	Evaluation of Data Obtaining From LVDTs	68
	CONCLUSION	81
	REFERENCES.....	85

LIST OF TABLES

TABLES

Table 1 Coordinates of Surface Dots	16
Table 2 Natural Frequencies	23
Table 3 Wind Velocity and Wind Pressure (TS 498)	25
Table 4 Stress Results Under DL, U1, and U2	38

LIST OF FIGURES

FIGURES

Figure 1 General View of Ortahisar Castle	1
Figure 2 Location of Cappadocia Region and Study Area.....	3
Figure 3 All 18 different slices shown together with one of the 2D plots	12
Figure 4 View of the Castle From East-West Axis	13
Figure 5 Cross Section of the Castle	17
Figure 6 Cross Sections at Different Elevations	18
Figure 7 Material Properties of Tuff	20
Figure 8 Spring Configuration of the Castle	21
Figure 9 Result of Records from Accelerometer 5	23
Figure 10 Response Spectrum of the Castle.....	27
Figure 11 Coulomb-Mohr and Modified-Mohr Theories	34
Figure 12 Analysis Results of Earthquake Loads with Fixed Supports (144 cases)..	36
Figure 13 Analysis Results of Earthquake Loads with Springs at the base (144 cases).	36
Figure 14 Analysis Results of Wind Loads (36 cases).....	37
Figure 15 Analysis Results of Temperature Loads (2 cases)	37
Figure 16 Global Coordinates of FEM.....	38
Figure 17 Global Coordinates of a Solid.....	39
Figure 18 Temperature Load Analysis of a Rectangular Pris	41
Figure 19 FEM of the Castle	42
Figure 20 S33 Dead Load Stresses (kPa)	43
Figure 21 S33 *Envelope Min Stresses (kPa)	44
Figure 22 S33 *Envelope Max Stresses (kPa)	45
Figure 23 S22 *Envelope Min Stresses (kPa)	46
Figure 24 S22 *Envelope Max Stresses (kPa)	47

Figure 25 S11 *Envelope Min Stresses (kPa).....	48
Figure 26 S11 *Envelope Max Stresses (kPa).....	49
Figure 27 S12 *Envelope Max Stresses (kPa).....	50
Figure 28 S12 *Envelope Min Stresses (kPa).....	51
Figure 29 S13 *Envelope Max Stresses (kPa).....	52
Figure 30 S13 *Envelope Min Stresses (kPa).....	53
Figure 31 S23 *Envelope Min Stresses (kPa).....	54
Figure 32 S23 *Envelope Max Stresses (kPa).....	55
Figure 33 Von-Mises Stress Under Temperature Summer Loads	56
Figure 34 Von-Mises Stress Under Temperature Winter Loads.....	57
Figure 35 Number of Solids in Confidence Intervals According to Earthquake Analysis.....	58
Figure 36 Inside and Outside View of LVDT.....	61
Figure 37 C3 Anemometer.....	62
Figure 38 NRG200P Vane	62
Figure 39 LVDTs Location from North of the Castle.....	65
Figure 40 LVDTs Location from East of the Castle	66
Figure 41 LVDTs Location from West of the Castle.....	67
Figure 42 Sensors No.1 No.4 Change of Crack Width.....	72
Figure 43 Sensors No.6 No.8 Change of Crack Width.....	73
Figure 44 Sensors No.11 No.12 Change of Crack Width.....	74
Figure 45 Sensors No.13 No.14 Change of Crack Width.....	75
Figure 46 Sensors No.15 No.16 Change of Crack Width.....	76
Figure 47 Sensors No.18 No.19 Change of Crack Width.....	77
Figure 48 Sensors No.20 No.29 Change of Crack Width.....	78
Figure 49 Sensors No.30 No.32 Change of Crack Width.....	79
Figure 50 Sensors No.7 No.44 Change of Crack Width.....	80

CHAPTER 1

INTRODUCTION

1.1. General

Heritage does not only mean transfer of the cultural tangibles to the next generations but also sharing culture and history of the humankind is a way of legating. Protecting old structures, which have historical and cultural value for humankind, is one way for legating to next generations. These type of structures are also important for touristic activities. Ortahisar Castle is located in the Cappadocia Region, Turkey (Figure 1) and is the main subject of this thesis.



Figure 1 General View of Ortahisar Castle

The Cappadocia Region, consisting of Niğde, Nevşehir, and Kayseri, is one of the most charming touristic sites because of its magnificent and peerless landforms and historical heritage. The total area of Cappadocia Region is 5000 km² (Topal and Doyuran, 1995). The Cappadocia Region is one of the World Heritage List sites because of its significant historical, cultural and touristic features (Ulusay et al., 2006). Aydan and Ulusay (2003) mentioned that there are many underground cities and settlements which are more than 1500 years old in the Cappadocia Region. Topal and Doyuran (1995) illustrated that a number of stratovolcanoes, numerous calderas, and thousands of morphologically distinct earth pillars in other words fairy chimneys make the Cappadocia Region unique in the world. The fairy chimneys are the most important structures that is why more than 2 million tourists visit Cappadocia region in one year (Tunusluoğlu and Zorlu, 2008). Topal and Doyuran (1995) informed that as a result of differential erosion and weathering of ash flow tuffs deposited, the fairy chimneys came into existence.

Ortahisar Castle is located at the center of the Cappadocia Region at Ortahisar province of Nevşehir (Figure 2). The height of the Castle is 64 meters and is the highest fairy chimney in Turkey. According to Kamberoğlu (2012), Ortahisar Castle is an important structure in this region because of its location which makes the Castle visible from anywhere in the Ürgüp region (Figure 2). The castle had been used as sanctuary for local people during the Hittite Empire and caves in the the Castle were first carved by Hittites. After Hittite Empire period, the Castle had been continued to be used as a castle for other empires such as Byzantine, and Ottoman Empire. Topal and Doyuran (1995) mentioned that because of cave dwellings the fairy chimneys were excavated and the fairy chimneys were inhabited by Byzantines. Kamberoğlu (2012) illustrated that according to macro form of Ortahisar, the first zone of occupation started at the high elevation of the Castle and it went on into the surrounding skirts of the Castle. At the present day, the Castle is no more occupied by residents and solely used for touristic purposes. But not all parts of the Castle can be visited by tourists because of poor structural condition of the Castle. However, a restoration and strengthening

project was started in 2012. Within the scope of the project, damaged parts of the Castle posing source of danger are strengthened and a structural health monitoring system is installed on the Castle. Therefore, this thesis explored calibrated, three dimensional (3D) Finite Element Modelling (FEM) of the Castle, for the purpose of structural evaluation against earthquakes, wind, and temperature forces. Each one of the finite element members was individually checked if Columb-Mohr failure criteria was met to see if cracks will occur. Additional work was carried out for dynamic testing and calibration of the analytical model. Furthermore, a large sensor network collected data was evaluated for 48 crack meters, one accelerometer, one temperature & humidity sensor, one anemometer, and one wind direction vane.

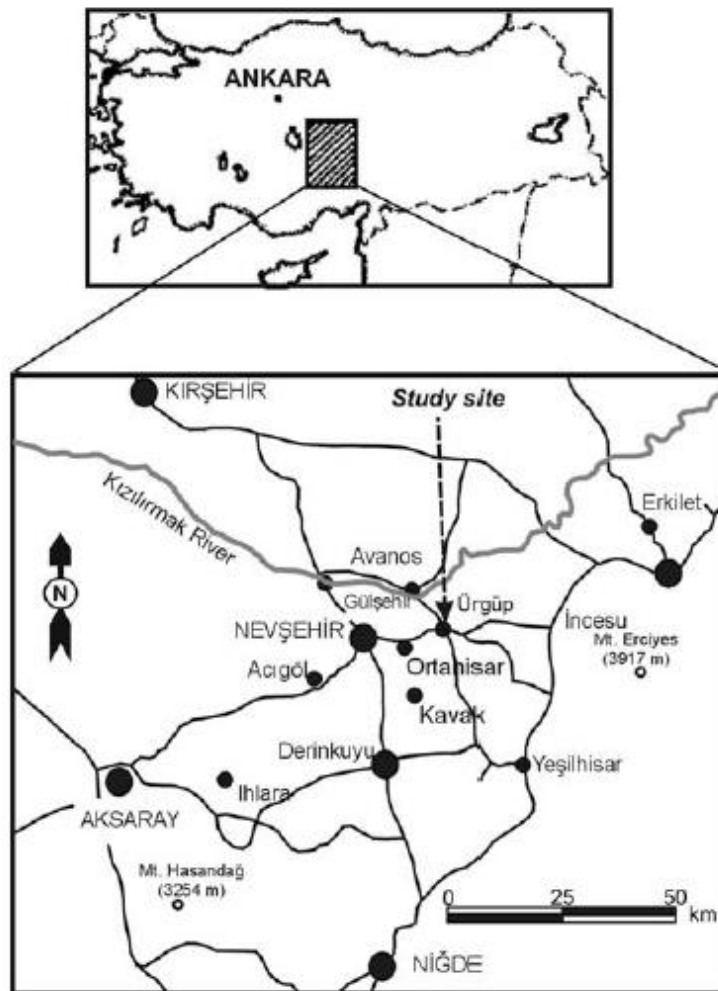


Figure 2 Location of Cappadocia Region and Study Area

1.2. Literature Review

Although Ortahisar Castle is the largest Fairy Chimneys in Nevşehir Region, there are limited number of academic studies on them. The existing ones are generally about the geological situation of the Castle most of the articles about Cappadocia Region are mainly dealing with geotechnical, geoenvironmental and geological problems of the region. There are limited resources about structural health monitoring and finite element modelling of the Castle to use at the thesis literature review part of the thesis. For this reason, the articles about SHM and FEM of historical structures are reviewed in general. The academic studies not only about the Castle and Ortahisar but also the Cappadocia Region, SHM, and FEM are used during the literature search of thesis. Herein after, brief summaries of these studies are explained.

Doyuran (1976) made a research about environmental and geologic problems of Ortahisar Castle. The aim of the research is considering rock fall from the Castle in a geologic approach, which threaten local people and tourists. Firstly, Doyuran (1976) explored the geology of Ortahisar region and cracks on the Castle. The reason of cracks on the Castle was founded as rain water leakage into rocks. When rain water leaks into the rocks, the water freezes because of winter conditions and volume of the frozen water increases, expanding the cracks. Doyuran (1976) reported that because of increment of cracks dimensions, rock fall can occur although there have not been any recent rock fall. A rock fall may cause loss of life. Therefore, reducing impact area of rock fall to a minimum instead of preventing the rock falls is advised. Doyuran (1976) mentioned that there are three ways to reduce the impact area of rock fall. The first one is vacating the residential houses in the region. Secondly, the region obtained from vacating should be covered with talus to prevent second jump of downthrown rock. Lastly, Doyuran (1976) suggested that retaining walls should be constructed around the impact region to block little particles to bounce from the fall, which might damage houses around the region.

Topal and Doyuran (1995) made research about the geological engineering characteristics of the tuffs of Kavak member discontinues on the development of the Fairy chimneys. Topal and Doyuran (1995) illustrated that the tuffs of the Kavak member of the Ürgüp formation is the main material of the Fairy chimneys in the Cappadocia Region. The formation of the fairy chimneys is controlled by the joints. Erosion along the joints affect the formation of the fairy chimneys (Topal and Doyuran, 1995). Topal and Doyuran (1995) mentioned that surface runoff water based erosion is more effective than wind actions at the formation of the fairy chimneys; lack of vegetation, steep topography and low permeability of the bed rock are also important parameters.

Aydan and Ulusay (2003) were dealing with the geotechnical and geoenvironmental characteristics of man-made underground structures in Cappadocia. They made several experiments like Schmidt hammer tests to determine the characteristic properties of Cappadocia tuff. The authors also tried to find a relationship between the environmental conditions such as temperature, humidity and behavior of the tuff. According to Aydan and Ulusay (2003), it is found that the Cappadocia tuffs are prone to temperature and humidity. Uniaxial compressive strength of Cappadocia tuffs can also be accepted as partially weak to very weak.

Ulusay et al. (2006) studied the environmental and engineering geological problems of deserted rock-hewn settlement in Ürgüp. Ulusay et al. (2006) investigated nearly 1200 rock-hewn underground openings and existing historical structures. Since the study region is in Cappadocia, they discovered that the rock material type is tuff and tuffites similar to Aydan and Ulusay's previous work (2003). In addition to Aydan and Ulusay's article in 2003; in their publication dated 2006, they also suggested corrective solutions for the structural problems. The study of Ulusay et al. (2006) included various problems such as block fall, rock fall, and erosion. To increase the stability of underground cave roofs, they advised to use timber beams as supporters, which is also a traditional method in Cappadocia. Strong prismatic tuff blocks can be constructed for weak entrances of openings. Individual blocks can be divided in to

smaller pieces and removed from the study area to ensure the necessary safety against rock fall.

Tunusluoğlu and Zorlu (2008) conducted rock fall hazard assessment in Ortahisar. They grouped problems of Ortahisar Castle in two groups which are natural effects and anthropogenic effects. Doyuran (1976) also grouped the problems of Ortahisar in the same way. The main purpose of Tunusluoğlu and Zorlu is investigating rock fall hazard of the Castle. Firstly, fieldwork research was done. This research consists of determination of location rocks, dimensions of blocks, an exhaustive discontinuity survey, description of topographic and morphologic characteristics, and location of fallen blocks. After that the cross-sections of the Castle were obtained and 2D rock fall analyses were made. Tunusluoğlu and Zorlu (2008) mentioned that the main reason for rock falls is changing in forces acting on a rock because of climatic and biological events; however, at Ortahisar Castle, reasons for a rock fall can be wind erosion, freeze thaw process and water influence. 2D rock fall analyses' results show that any falling block reaches high velocities at the bottom generating a very dangerous phenomenon. Tunusluoğlu and Zorlu (2008) also prepared a run out distance zone whose area is nearly 30,000m². They advised that the Castle and its surrounds should be closed for uncontrolled touristic activities considering the run out zone to reduce any loss of lives.

Kamberoğlu (2012) also evaluated the case of Ortahisar in her master thesis. The academic study mainly focuses social situation of Ortahisar, tourism facilities, city planning and economic facilities in Ortahisar. According to Kamberoğlu (2012), Ortahisar is settled around the Castle and all touristic activities in Ortahisar is occurred because of Ortahisar Castle that proves the importance of the Castle again. The records of Ministry of Tourism and Culture show that more than 600,000 tourists visited this region in 2009 annually which is a good income for local people of Ortahisar.

Guarnieri et al. (2013) illustrated that structural analysis of a historical structure is made to identify the probable state of danger and estimate the future behavior of the

structure. Finite Element Modelling (FEM) is used widely in structural analysis of historical structures. Guarnieri et al. (2013) mentioned that three-dimensional mesh generated from laser scanning data was used to obtain FEM model of the Olympic Theatre. Static and dynamic analyses were done with the FEM model according to Italian regulations.

Chellini et al. (2014) mentioned that because of great socioeconomic, historical, and intrinsic value of cultural heritage buildings, the interest in minimizing seismic hazard for these types of structures grew enduringly. Historical structures are mainly complex structures since they are built on the past design criteria, construction methods, and technical knowledge. Chellini et al. (2014) made a study about evaluation of seismic vulnerability of Santa Maria del Mar Church using terrestrial laser scanning three-dimensional survey and finite element analysis. Response spectrum analysis was used and two different collapse scenarios were analyzed by changing inclinations of cracks. Chellini et al. (2014) concluded that design seismic action can overturn the facade upper part of the church.

Lima et al. (2008) illustrated that one of the most powerful ways to manage infrastructures is structural health monitoring. Lima et al. (2008) made a scientific research about structural health monitoring of one historical building. The SHM system has 19 displacement sensors and 5 temperature sensors. The duration of data obtained from SHM system is 1 year. Lima et al. (2008) aimed to get information about the structure and find new techniques for restoration of the historical structure.

According to Marazzi et al. (2011), structural health monitoring (SHM) techniques to control and consideration of monumental structures was very important. A handled SHM study is a way to increase information about structural conditions of a monument and problems of the monument. Therefore, SHM can be used to select the most appropriate restoration response to satisfy required safety level. Marazzi et al. (2011) studied about experimental comparison between two techniques to measure the

crack widths whose origin is settlement. Marazzi et al. (2011) concluded that manual measurements and optical measurements have a very good agreement between them.

1.3. Objectives and Scope

Historical structures are very important for cultural heritage. Ramoset al. (2010) mentioned that conservation of cultural and architectural heritage is a necessary concern in the cultural life of contemporary societies. Hossein and Tabrizi (2010) illustrated that imperfect knowledge about structural conditions of historical buildings is an important problem for many cities in the world. Since there are no structural drawings of historic structures, it is not possible to determine original material, dimensions, and behavior of these structures, which make structural health monitoring very important. In other words, structural health monitoring (SHM) is accepted as one of keys to ensure safety of historical structures (Damonte et al., 2007). Therefore, application of structural health monitoring on the Ortahisar Castle and monitoring the Castle's vital responses are one of the major objectives of this thesis. The monitoring work is carried out using a number of crack meters or LVDTs to measure possible changes in crack widths. Since the Castle has numerous cracks on its surface, the cracks should be monitored by using a large number of LVDTs. The LVDTs are connected to a data logger, which is used to communicate with the sensor, make measurement, convert to digital format, record the data, and transfer the data to a computer. The data consists of change of crack widths in time; therefore, obtaining data from the data logger is used for evaluating crack widths changes.

The second objective of the thesis is to make a comprehensive evaluation of the overall behavior of the Castle using detailed finite element modelling of Ortahisar Castle. The behavior of the Castle under an earthquake, wind or temperature load is a critical problem and needs to be considered. 3D finite element model of the Castle is generated using 3D laser scanning data by using solid members and afterwards

earthquake and wind loads are defined for structural analysis to obtain deflections and stresses. The expected response of the Castle against most important loads of nature are evaluated by FEM. The analytical model is also calibrated using dynamic measurements taken from the top level of the Castle.

Finally, the thesis is written to make relevant suggestions for future work.

The structural health monitoring system of Ortahisar Castle consists of LVDTs, accelerometers, data logger, battery, solar panel, and remote communication modem. The readily available monitoring system has been used in this thesis. The measurement data are sent to a computer with help of direct connection cable or remote communication by GSM modem, and post process works start at the computer. The change of crack widths are plotted using time versus crack width graphs. If the crack widths change dramatically, this change can be understood from the graphs and rock fall initiation can be sensed well ahead of time.

3D laser scanning is used to determine the dimensions of the Castle since there are not any architectural drawings. FEM is prepared by using the results of 3D laser scanning and SAP2000 analysis software. Earthquake loads, wind loads, and temperature loads are applied on the analytical model and the model is analyzed. Behavior of the Castle under earthquake load wind load, and temperature load is obtained, structural performance of the Castle is evaluated using the analysis results of the detailed 3D finite element model.

CHAPTER 2

FINITE ELEMENT MODELLING OF ORTAHISAR CASTLE

2.1. 3D Laser Scanning of Ortahisar Castle

The finite element modeling studies require geometric dimensions of the structure to be modelled. The Ortahisar Castle has no well-defined geometric shape and mostly has an amorphous shape. Fortunately, 3D laser scanning of the Castle was carried out in the past and FEM studies have taken advantage of that data. 3D laser scanning is a method which is used to obtain any geometric shape of physical objects by sending laser lights to the object. At the end of scanning, point clouds are collected, each point is described by using xyz coordinate system, and the shape of the object can be extracted from the point clouds. However, the point clouds in the format of xyz coordinate system of Ortahisar Castle could not be obtained; only slices of 3D points in 2D planes at AutoCAD (computer aided design programme) drawings of the Castle were found and used (Figure 3). In a previous unrelated study, the Castle's point cloud was used to generate 2D plots of 18 slices that are 10° degree away from each other. Each one of the slices were separately stored in drawing files. If all 18 drawing files are combined together, an approximate 3D plot of the Castle can be obtained. These 2D plots were used to generate the 3D FEM of the Castle.

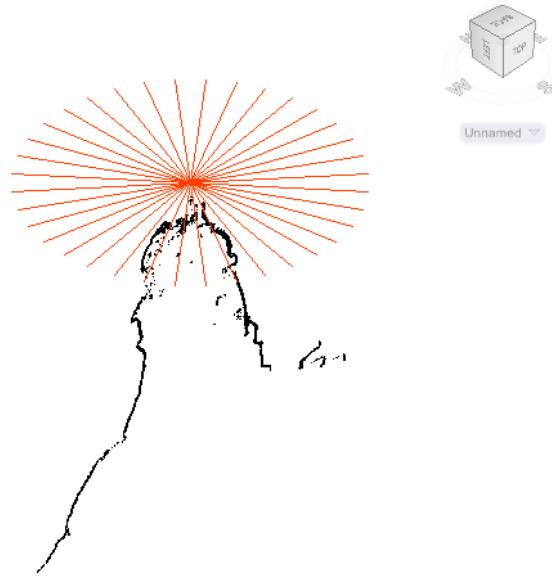


Figure 3 All 18 different slices shown together with one of the 2D plots

As it can be seen in Figure 3, red lines are the cutting axes. The name of first axis is east-west axis and the others are named as east-west 10° , east-west 20° etc. until the angle between axis reaches to 80° . Afterwards, north-south axis starts and same denotation is used again. Figure 4 shows the Castle from east-west axis. The black dots in the Figure demonstrate surface of the Castle at the direction of the axis. Each one of the dots is obtained from 3D laser scanning. 3D location of each one of the dots are determined from their 2D coordinate and angle of the plane with respect to East or North. However, the coordinates of the dots could now be directly obtained from the AutoCAD file and reading each coordinate manually was taking too much time and effort. Instead, NetCAD (computer aided design programme), which is a GIS application that can read AutoCAD files, is used to get coordinates of each dot at each drawing file.

Firstly, the AutoCAD drawing file is imported to NetCAD. NetCAD loads information inside the drawing file. Secondly, all dots inside the drawing file are categorized by their coordinates inside NetCAD. Thirdly, the categorization by coordinate system is exported as an excel file. This procedure carried out using NETCAD was necessary to extract xyz coordinates of all dots that form the outer

surface of the Castle. The next step is importing these dots to SAP2000; however, before that the dots are arranged in such an order that the solid members can be easily generated. Since the available data of 2D planes slices the Castle like a cake into 18 planes, all these dots need to be reorganized and combined to generate the Castle as a whole in 3D.



Figure 4 View of the Castle From East-West Axis

2.2. Organization of Coordinates of the Castle

NetCAD just gives coordinates of dots but the order of the dots are mixed. In other words, which dot represents which part of the Castle is pretty much unknown when starting from a 2D data file. Therefore, dots need to be arranged in a 3D coordinate system. As it is mentioned above, drawing files are named in two main category which are east-west and north-south directions. East-west direction is accepted as x-direction, south-west direction is accepted as y-direction and height of the Castle is accepted as

z-direction. The drawing files, whose names begin with east-west, are used to get x-direction and z-direction of dots in the local coordinate system. The drawing files, whose names begin with north-south, are used to get y-direction and z-direction of dots in their own local coordinate system. Values of z-axis of dots are the same for both readings; however, values of x and y axes are different from each other which means correlation is needed between values of x and y axis of dots. Center point of the Castle is found and coordinate of the center point of the Castle is read with using NetCAD. X axis value of center point is subtracted from all x axis values of dots that were read from drawing files that had names beginning with east-west direction. The same procedure is repeated for y axis values of drawing files that have names begin with north-south direction. Result of correlation gives coordinates of dots in z-axis and new x' and y' axes. After that point, arranging dots with the new axis is carried out. The dots belong to the surface of the Castle at intervals of 10° but there are not 36 drawings files; there are only 18 drawing files. Therefore, a vertical line from the center that divides the figure into two parts are used to generate 18 additional planes. The left part of East-West plots represents west part or left part of the North-South plot represents south part of the Castle. The difference between east and west or north and south is 180° . For instance; a file, whose name is east-west 0° , has surface dots of the Castle at 0° and 180° or north-south 50° has surface dots of the Castle at 140° from East and 320° from East. This logic is used to prepare Table 1.

Values in white boxes at Table 1 shows values obtained from 3D laser scanning. As it can be seen from Table 1, all of the 2D slices do not start at the same elevation as well as they don't finish at the same elevation. There are two reasons for this misreading. The first one is that, the Castle consists of different elevations at the base and they do not match when the cutting plane is turned with different angles. The second reason is about the quality of 3D laser scanner which may skip some of the measurement points of the Castle. Therefore, mismatching of missing values in Table 1 are filled manually which are shown by colorful boxes. An example for calculation of purple boxes in Table 1 is given below. As an example, the radius of 60° and 80° are known at same elevation but 70° radius is missing. The valued is filled by taking

linear average of these two values. Similarly, the missing data may be regenerated using values of the neighboring elevations.

$$\text{Value 1 (in white boxes)} = 56,33542 \quad \text{Value 2 (in white boxes)} = 52,66067 \quad (\text{Eqn. 1})$$

$$\text{1st Unknown (in purple boxes)} = \frac{(56,33542+52,66067)}{2} = 54,49805 \quad (\text{Eqn. 2})$$

2.3. Importing Dots of the Castle to SAP2000

Finite element modelling of the Castle is prepared by using structural analysis program whose name is SAP2000. At SAP2000, a model can be generated in three different ways; these ways are 1) model by using lines for frames, shell members for areas, and 3) solid members for three dimensional volumes. Solid modelling is chosen for the FEM of the Castle since the structure is formed by solid tuff rock. Solid members consist of 8 nodes since they are 3D objects. At SAP2000, the nodes are described as joints with their values in x, y, z axis. As a first step, format using by SAP2000 to create solid models is learnt. The format is exported to Excel from SAP2000 since coordinates of surface dots of the Castle is saved as an Excel file. Eight joints with their coordinates need to be described to create solid member; however, as it can be seen from Table 1, the joints have only 2 coordinates which are in z-axis and x' or y'-axis. The lack of coordinate and the format that SAP2000 uses are main reasons to develop a code. The code is developed by Macro, which works under Excel. First aim or task of the code is obtaining coordinates of joints in x and y axis. Simple trigonometry is used for this process. The values in white and colorful boxes at Table 1 are multiplied with cosine and sine of angles on the first row of Table 1; hereby all coordinates of the joints are obtained in 3D Cartesian coordinates. Second task of the code is to sort the coordinates of dots that SAP2000 can generate solid model of the Castle. The sorting procedure starts from bottom of the Castle and starts from 0° at each level. By the time degree reaches 350° from 0° , all solids at any level are created (Figure 5 and Figure 6) and solids at the level top of the previous one are started to create from 0° to 350° again. This procedure finishes when all of the solids are created.

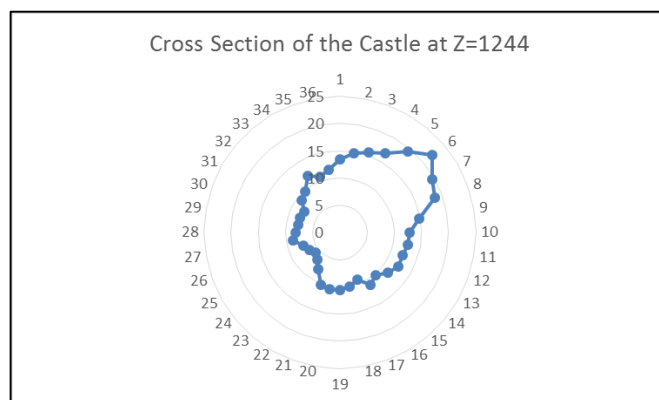


Figure 5 Cross Section of the Castle

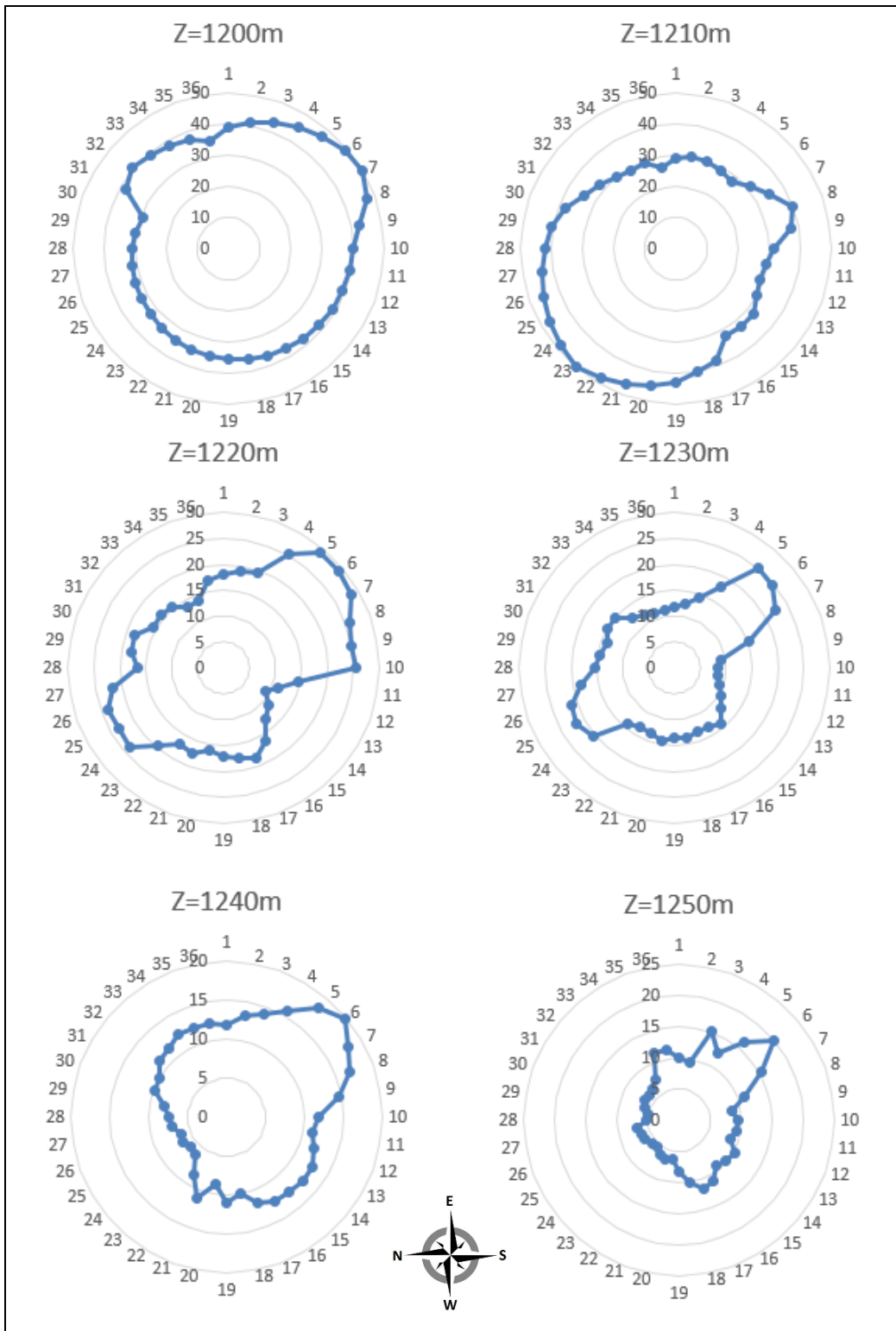


Figure 6 Cross Sections at Different Elevations

2.4. Drawing Finite Element Model of the Castle

The coordinates of dots are prepared according to SAP2000 solid joint order format before they are transferred to SAP2000. The transfer is made by copying the coordinates of dots from excel to SAP2000. FEM of the Castle is obtained only in general form as the transfer is completed. Definitions of materials, solids, load cases, and load combination are done as next steps. There are two important issues to mention at this step: The first important issue is definition of material properties. Although the Castle may have heterogeneous type material property distribution, the material properties are defined the same for all members assuming the correlation with dynamic measurements will be used for calibration and this will take care of changing material properties as a single smeared material property. The elastic modulus obtained from the material tests in the literature is 1.3 to 1.5 GPa. However, these values may be general and may refer to material that was exposed to weather conditions. The material of the Castle is original and kept inside the castle and analytical model calibration studies have shown that a 0.7 GPa for the modulus of elasticity gave better results. The reason to calibrate the modulus of elasticity is that the Castle has caves inside which cannot be modelled; moreover, the cracks at inside and outside of the Castle cannot be modelled. Since the cracks and the caves inside and surface of the Castle cannot be modelled, modulus of elasticity of Cappadocian tuff is reduced to 0.7 GPa. In addition to modulus of elasticity, additional parameters such as weight per unit volume and Poisson's ratio need to be defined in the SAP2000 analysis software. Weight per unit volume (17.37 kN/m^3), Poisson's ratio of tuff (0.27), and thermal expansion coefficient ($6.3 \times 10^{-6} \text{ 1/}^\circ\text{C}$) are entered according to material test reports made at field.

Second important issue is boundary conditions of the Castle's model. Choosing the right type of support effects result of structural analysis considerably. The Castle is located on tuff foundation. Foundation on a fixed support is hypothetical; however, it may be better to assign spring coefficients for the tuff base instead of a fixed support. Therefore, two kind of models are prepared. First model has fixed end supports with all degrees of freedom are restrained and the second model has springs instead of fixed

supports. The reasons for preparing two models are to compare results of two models and to be on the safe side during analysis by taking the worst case scenario. Modulus of elasticity of the Castle’s material is an unknown for both models and also spring constants are another unknown for model with springs. Modulus of elasticity is decided according to the model with fixed supports. The E value which gives similar result with natural frequencies is accepted as modulus of elasticity of the Castle material and it is used for both of models. The same E value gave even better match with the dynamic test results when springs were used. The determination of spring constant for second model is explained in Section 2.4. The material properties of tuff for the Castle are shown in Figure 7.

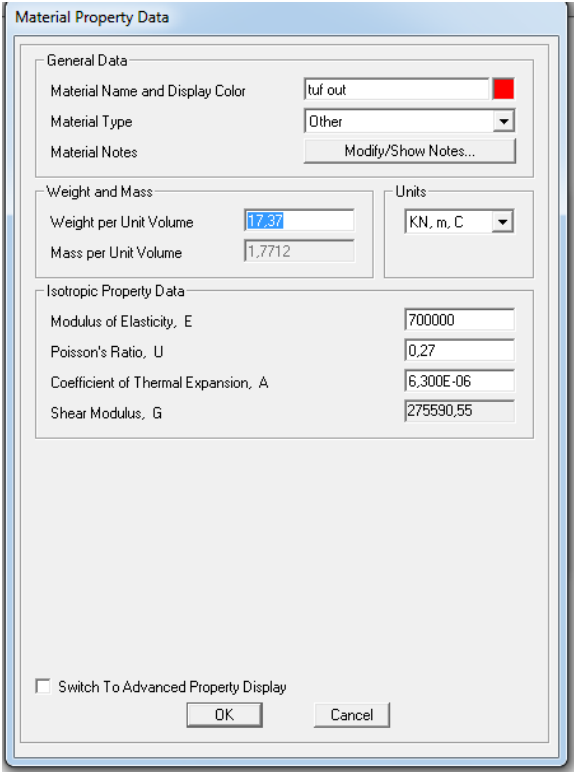


Figure 7 Material Properties of Tuff

Dimensions of solids are set automatically according to the results of developed macro program; however, the mesh is too coarse and it can be seen that solids need to be divided into smaller pieces to get more accurate solutions. Therefore, a solid is

divide into 4 pieces in the radial direction. The total number of solids forming the Castle is 105984 after further meshing. Fix supports and springs are used separately at the bottom joints of the Castle to satisfy the connection between the Castle and ground surface.

2.5. Determination of Modulus of Subgrade Reaction

Modulus of subgrade reaction (k_s) is the value which is used to define spring constant at support of the Castle. The Castle lays on tuff settlement; therefore, using only fixed supports is not a good estimation. Two different FEM of the Castle are prepared with fix supports and springs. A comparison is done using two models. Modulus of subgrade reaction is chosen as 12000 kN/m^3 according to soil property of combination of bed rock and tuff. The combination is classified as loose dense sand whose modulus of subgrade reaction is between $4800\text{-}16000 \text{ kN/m}^3$. After defining subgrade reaction, tributary area method is used to define spring coefficient in SAP2000 since the k_s cannot be described to all area of bottom of the Castle as same value. The spring values obtained from tributary area method are defined in SAP2000 (Figure 8).

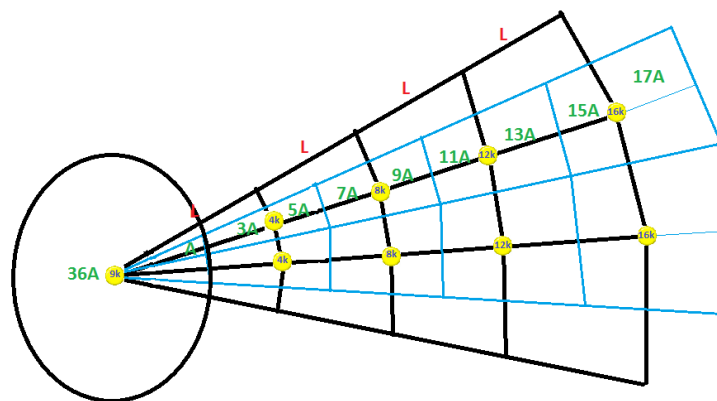


Figure 8 Spring Configuration of the Castle

2.6. Natural Frequencies of Ortahisar Castle

One of the main topics of the thesis is finite element modelling of the Castle and making earthquake and wind analysis with FEM. Therefore, generating a realistic FEM of the Castle is the key point for the accuracy of the analyses. Dimensions, material properties, and boundary conditions need to be modelled as correct as possible as to generate a realistic model of the Castle. The dimensions of the model is obtained after arranging data obtained from 3D laser scanning but defining material properties of the Castle is a problem for FEM; however, rooms and tunnels inside the castle could not be modelled. Modulus of elasticity in the literature is about 1.4 GPa; however, the region where the field tests are made is a small part of the Castle and modulus of elasticity of other parts of the Castle might show difference. For this reason, natural frequencies of the Castle is used to determine the material properties. In order to state that the model is reliable, similarities between natural frequencies of model and natural frequencies obtained from field tests are required to be consistent. Several models are prepared at SAP2000 with different modulus elasticity values. The model whose frequencies has best match with measured natural frequencies of the Castle is chosen as FEM of the Castle.

Natural frequencies of a structure can be obtained by help of accelerometers. Accelerometers record change in position of the structure and the record data is used to get the natural frequencies of the structure. Fast Fourier Transform (FFT) is one way to obtain natural frequencies and FFT is used at this analysis. FFT is an algorithm which is used to compute a sequence's discrete Fourier transform. A sensitive accelerometer was used to make 6 individual records of ambient dynamic response of the castle at the roof level (Figure 9). The first two readings could not give any meaningful results since they were taken to test the instruments and their durations were too short. Results of all records are analyzed with FFT using MATLAB commands and natural frequencies of the Castle are obtained. Arithmetic mean of similar peak frequencies are calculated, which is accepted as the test result and modal frequencies of SAP models with different modulus of elasticity are compared with the

test result. The best match is obtained with a model whose modulus elasticity is 0.7 GPa as it can be seen in Table 2.

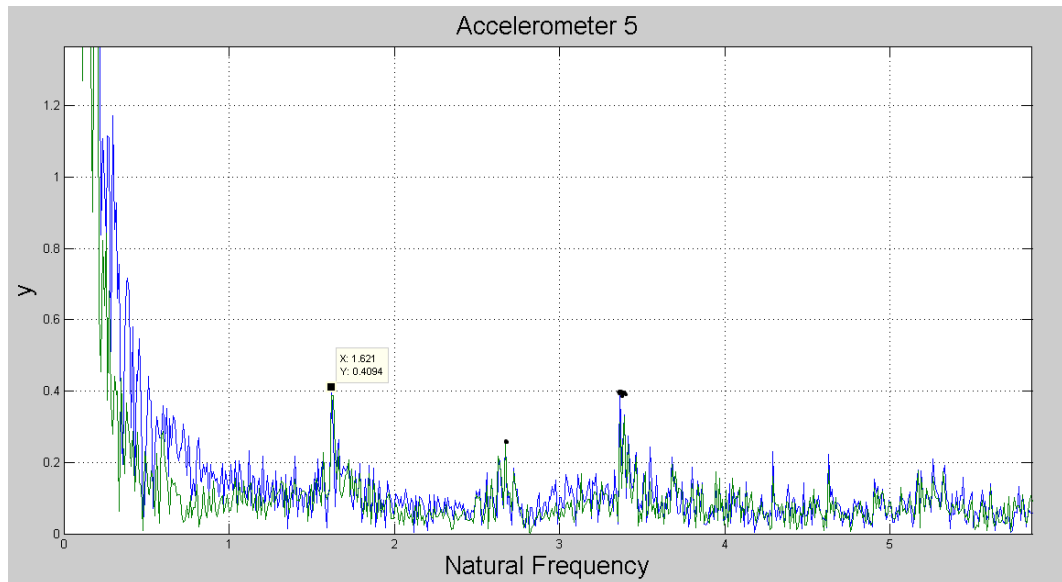


Figure 9 Result of Records from Accelerometer 5

Table 1 Natural Frequencies

		Natural Frequencies						Test Results
Modes	SAP	1 st Record	2 nd Record	3 rd Record	4 th Record	5 th Record	6 th Record	
1	1,64	0	0	1,633	1,64	1,621	1,633	1,63
2	2,25	0	0	2,122			2,183	2,15
3	3,36	0	0	2,656	2,66	2,671	2,655	2,66
4	4,77	0	0	3,385	3,51	3,364	3,36	3,40
5	4,84	0	0	5,096	5,1			5,10
6	5,01					5,26	5,258	5,26
7	6,73					6,67		6,67

2.7. Definition of Load Patterns and Load Cases in SAP2000

A structure can be effected by different types of loads such as: dead load, live load, wind load, temperature load, and earthquake load; however, in this thesis only

dead load, wind load, temperature load, and earthquake loads are considered for the FEM studies. There is limited touristic activity and surface that can be effected by live load is limited; therefore, live load is not considered during the analyses.

A load is firstly described as a load pattern to SAP2000 after it is described as a load case and the loads of the Castle are defined according to this procedure. SAP2000 can automatically calculate amount of dead load after defining material properties of solids. It is only needed to define dead load as a load pattern, indicate the gravity, and define relevant load case.

Wind load calculations are done according to TS498; however, wind load is described as a pressure and applied perpendicular to exterior surface of the Castle. SAP2000 automatically calculates wind load by multiplying wind load pressure and the surface area effected by the pressure. Since wind does not blow from one direction, wind loads are calculated at each 10° intervals starting from 0° to 350°. For instance; W110, described as load pattern at SAP2000, means that wind blows to the Castle with angle of 110° from East. Calculation of wind pressure, applied to the exterior surface of solids, is done using formulas mentioned at TS498. The wind load calculation is done using Excel for each direction of wind load. Firstly, exterior solids numbers are listed with their elevations from ground and coordinates of their joints in Excel. Normal vector of surface area is calculated from coordinates of joints to calculate the angle between the wind load and surface area. C_p , q are wind related parameters available in TS498. Wind pressure (w) acting perpendicular to the surface is calculated using Equation 3.

$$w = C_p * q \quad (\text{Eqn. 3})$$

Where:

w = wind pressure kN/m^2

q = wind pressure without absorption coefficient kN/m^2

C_p = absorption coefficient

Wind pressure coefficients (q) are taken from Table 3 which is also available in the TS648 code.

Table 2 Wind Velocity and Wind Pressure (TS 498)

Elevation from Ground (m)	Velocity of Wind – v (m/s)	q (kN/m ²)
0-8	28	0.5
9-20	36	0.8
21-100	42	1.1
>100	46	1.3

After using the formula and angles between the surface and wind directions, wind pressures are obtained for all exterior surface areas of the Castle, which means 3311 wind loads are calculated for each case. Since there are 36 wind load cases, 11196 loads must be entered to SAP2000. The simple way for this procedure is updating s2k file, text based input file name for SAP2000, for each case and importing s2k files to SAP2000 program. Therefore, 36 s2k files are created from the results of Excel and they are imported to SAP2000 one by one.

There are two different cases for temperature loading, which are temperature loads generated in winter and temperature load generated in summer. The common point of these two cases that the loads are applied to the Castle up to 10 cm inside from the surface. The temperature at the region in winter and in summer is chosen according to reports prepared by Turkish State Meteorological Service. Therefore; -20°C is used for winter temperature load and 20°C is used for summer temperature load. Additional 20°C is also applied to the southern part of the Castle under summer temperature loading.

Earthquake load calculation is done using response spectrum method. Ortahisar is in the 3rd degree seismic zone which means that effective ground acceleration coefficient (A_0) is taken as 0.20. Spectrum characteristic periods are taken as 0.10 seconds for T_A and 0.30 seconds for T_B according to Z1 local site soil class since the

Castle is settled on tuff settlement. According to A_0 , T_A , and T_B , response spectrum curve is drawn and imported to SAP2000 (Figure 9). Damping ratio is calculated as 0.006 according to Half-power Bandwidth Method. The response spectrum curve is used to describe two main load cases, U1 and U2 in SAP2000. U1 and U2 are the earthquake loads which effect the Castle in x-direction and y-directions. Their scale factor is 1.962 which is obtained by multiplication of gravitational acceleration and A_0 . Earthquakes may affect the Castle in different directions. A similar procedure with wind load is applied for earthquake loads, too. New load cases are described at every 10° angles from 0° to 170° . Differently from wind loads, earthquake loads are not described at SAP2000 since it is complex and makes SAP2000 give errors. A code is developed in MATLAB to capture results of SAP2000 for x and y direction earthquakes and MATLAB code for different earthquake directions acting on the Castle were calculated externally. Since the model is a linear one, combination of load cases in different directions gave correct results. To prove this idea, the results of earthquake coming with an angle of 110° with x-direction are calculated in SAP2000 and MATLAB routine and gave the same results. The code creates combinations, explained below, with resulting stresses of each solids obtaining from U1, U2, and dead load and gives resulting stresses of solids according to the combinations. The resulting stresses of U1, U2, and dead load are obtained as a list after running SAP2000 input file. The list is imported to MATLAB.

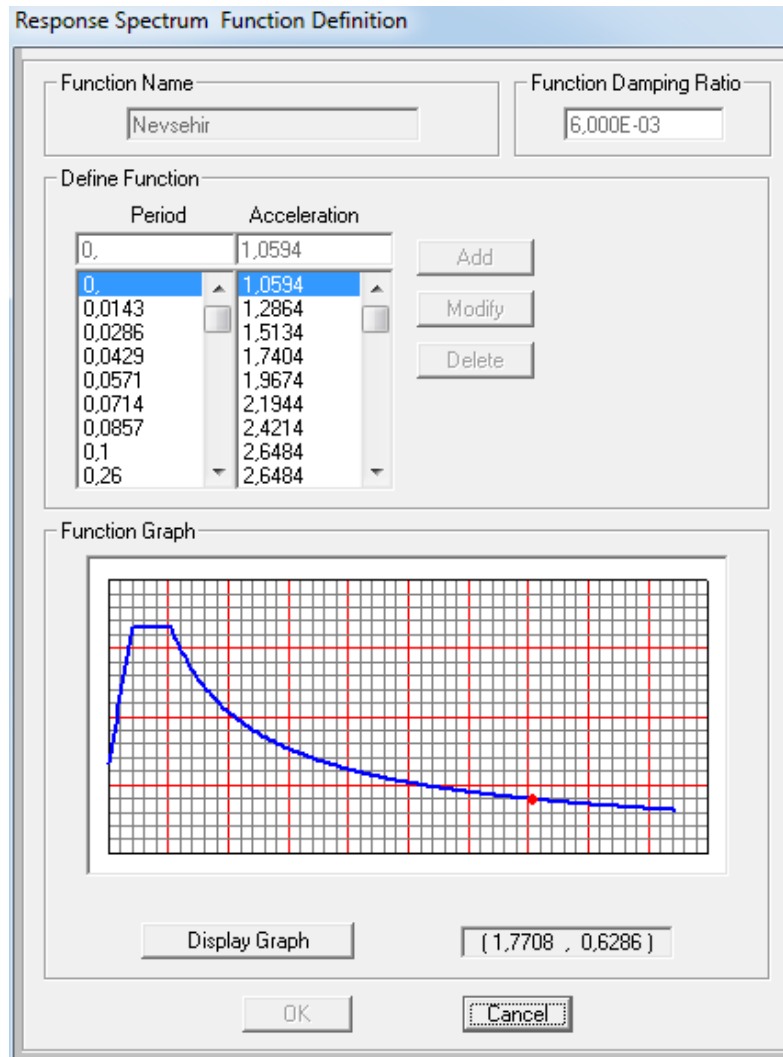


Figure 10 Response Spectrum of the Castle

2.8. Load Combinations

In this section, load combinations that are used for analysis of FEM of the Castle are listed. There are 39 combinations at SAP2000 which are wind load, dead load, and temperature load combinations and 144 combinations at MATLAB which are earthquake load combinations. To sum up, 183 combinations are created for analysis of the Castle.

DL	DL+W350
TEMPwinter	TEMPsummer
DL+W0	$DL+[U1\cos 0+U2\sin 0]+0.3[U1\cos(0+\pi/2)+U2\sin(0+\pi/2)]$
DL+W10	$DL+[U1\cos 10+U2\sin 10]+0.3[U1\cos(10+\pi/2)+U2\sin(10+\pi/2)]$
DL+W20	$DL+[U1\cos 20+U2\sin 20]+0.3[U1\cos(20+\pi/2)+U2\sin(20+\pi/2)]$
DL+W30	$DL+[U1\cos 30+U2\sin 30]+0.3[U1\cos(30+\pi/2)+U2\sin(30+\pi/2)]$
DL+W40	$DL+[U1\cos 40+U2\sin 40]+0.3[U1\cos(40+\pi/2)+U2\sin(40+\pi/2)]$
DL+W50	$DL+[U1\cos 50+U2\sin 50]+0.3[U1\cos(50+\pi/2)+U2\sin(50+\pi/2)]$
DL+W60	$DL+[U1\cos 60+U2\sin 60]+0.3[U1\cos(60+\pi/2)+U2\sin(60+\pi/2)]$
DL+W70	$DL+[U1\cos 70+U2\sin 70]+0.3[U1\cos(70+\pi/2)+U2\sin(70+\pi/2)]$
DL+W80	$DL+[U1\cos 80+U2\sin 80]+0.3[U1\cos(80+\pi/2)+U2\sin(80+\pi/2)]$
DL+W90	$DL+[U1\cos 90+U2\sin 90]+0.3[U1\cos(90+\pi/2)+U2\sin(90+\pi/2)]$
DL+W100	$DL+[U1\cos 100+U2\sin 100]+0.3[U1\cos(100+\pi/2)+U2\sin(100+\pi/2)]$
DL+W110	$DL+[U1\cos 110+U2\sin 110]+0.3[U1\cos(110+\pi/2)+U2\sin(110+\pi/2)]$
DL+W120	$DL+[U1\cos 120+U2\sin 120]+0.3[U1\cos(120+\pi/2)+U2\sin(120+\pi/2)]$
DL+W130	$DL+[U1\cos 130+U2\sin 130]+0.3[U1\cos(130+\pi/2)+U2\sin(130+\pi/2)]$
DL+W140	$DL+[U1\cos 140+U2\sin 140]+0.3[U1\cos(140+\pi/2)+U2\sin(140+\pi/2)]$
DL+W150	$DL+[U1\cos 150+U2\sin 150]+0.3[U1\cos(150+\pi/2)+U2\sin(150+\pi/2)]$
DL+W160	$DL+[U1\cos 160+U2\sin 160]+0.3[U1\cos(160+\pi/2)+U2\sin(160+\pi/2)]$
DL+W170	$DL+[U1\cos 170+U2\sin 170]+0.3[U1\cos(170+\pi/2)+U2\sin(170+\pi/2)]$
DL+W180	$DL+0.3[U1\cos 0+U2\sin 0]+[U1\cos(0+\pi/2)+U2\sin(0+\pi/2)]$
DL+W190	$DL+0.3[U1\cos 10+U2\sin 10]+[U1\cos(10+\pi/2)+U2\sin(10+\pi/2)]$
DL+W200	$DL+0.3[U1\cos 20+U2\sin 20]+[U1\cos(20+\pi/2)+U2\sin(20+\pi/2)]$
DL+W210	$DL+0.3[U1\cos 30+U2\sin 30]+[U1\cos(30+\pi/2)+U2\sin(30+\pi/2)]$
DL+W220	$DL+0.3[U1\cos 40+U2\sin 40]+[U1\cos(40+\pi/2)+U2\sin(40+\pi/2)]$
DL+W230	$DL+0.3[U1\cos 50+U2\sin 50]+[U1\cos(50+\pi/2)+U2\sin(50+\pi/2)]$
DL+W240	$DL+0.3[U1\cos 60+U2\sin 60]+[U1\cos(60+\pi/2)+U2\sin(60+\pi/2)]$
DL+W250	$DL+0.3[U1\cos 70+U2\sin 70]+[U1\cos(70+\pi/2)+U2\sin(70+\pi/2)]$
DL+W260	$DL+0.3[U1\cos 80+U2\sin 80]+[U1\cos(80+\pi/2)+U2\sin(80+\pi/2)]$
DL+W270	$DL+0.3[U1\cos 90+U2\sin 90]+[U1\cos(90+\pi/2)+U2\sin(90+\pi/2)]$
DL+W280	$DL+0.3[U1\cos 100+U2\sin 100]+[U1\cos(100+\pi/2)+U2\sin(100+\pi/2)]$
DL+W290	$DL+0.3[U1\cos 110+U2\sin 110]+[U1\cos(110+\pi/2)+U2\sin(110+\pi/2)]$

$DL+W300 \quad DL+0.3[U1\cos 120+U2\sin 120]+[U1\cos(120+\pi/2)+U2\sin(120+\pi/2)]$
 $DL+W310 \quad DL+0.3[U1\cos 130+U2\sin 130]+[U1\cos(130+\pi/2)+U2\sin(130+\pi/2)]$
 $DL+W320 \quad DL+0.3[U1\cos 140+U2\sin 140]+[U1\cos(140+\pi/2)+U2\sin(140+\pi/2)]$
 $DL+W330 \quad DL+0.3[U1\cos 150+U2\sin 150]+[U1\cos(150+\pi/2)+U2\sin(150+\pi/2)]$
 $DL+W340 \quad DL+0.3[U1\cos 160+U2\sin 160]+[U1\cos(160+\pi/2)+U2\sin(160+\pi/2)]$
 $DL+0.3[U1\cos 170+U2\sin 170]+[U1\cos(170+\pi/2)+U2\sin(170+\pi/2)]$
 $DL+[U1\cos 0+U2\sin 0]-0.3[U1\cos(0+\pi/2)+U2\sin(0+\pi/2)]$
 $DL+[U1\cos 10+U2\sin 10]-0.3[U1\cos(10+\pi/2)+U2\sin(10+\pi/2)]$
 $DL+[U1\cos 20+U2\sin 20]-0.3[U1\cos(20+\pi/2)+U2\sin(20+\pi/2)]$
 $DL+[U1\cos 30+U2\sin 30]-0.3[U1\cos(30+\pi/2)+U2\sin(30+\pi/2)]$
 $DL+[U1\cos 40+U2\sin 40]-0.3[U1\cos(40+\pi/2)+U2\sin(40+\pi/2)]$
 $DL+[U1\cos 50+U2\sin 50]-0.3[U1\cos(50+\pi/2)+U2\sin(50+\pi/2)]$
 $DL+[U1\cos 60+U2\sin 60]-0.3[U1\cos(60+\pi/2)+U2\sin(60+\pi/2)]$
 $DL+[U1\cos 70+U2\sin 70]-0.3[U1\cos(70+\pi/2)+U2\sin(70+\pi/2)]$
 $DL+[U1\cos 80+U2\sin 80]-0.3[U1\cos(80+\pi/2)+U2\sin(80+\pi/2)]$
 $DL+[U1\cos 90+U2\sin 90]-0.3[U1\cos(90+\pi/2)+U2\sin(90+\pi/2)]$
 $DL+[U1\cos 100+U2\sin 100]-0.3[U1\cos(100+\pi/2)+U2\sin(100+\pi/2)]$
 $DL+[U1\cos 110+U2\sin 110]-0.3[U1\cos(110+\pi/2)+U2\sin(110+\pi/2)]$
 $DL+[U1\cos 120+U2\sin 120]-0.3[U1\cos(120+\pi/2)+U2\sin(120+\pi/2)]$
 $DL+[U1\cos 130+U2\sin 130]-0.3[U1\cos(130+\pi/2)+U2\sin(130+\pi/2)]$
 $DL+[U1\cos 140+U2\sin 140]-0.3[U1\cos(140+\pi/2)+U2\sin(140+\pi/2)]$
 $DL+[U1\cos 150+U2\sin 150]-0.3[U1\cos(150+\pi/2)+U2\sin(150+\pi/2)]$
 $DL+[U1\cos 160+U2\sin 160]-0.3[U1\cos(160+\pi/2)+U2\sin(160+\pi/2)]$
 $DL+[U1\cos 170+U2\sin 170]-0.3[U1\cos(170+\pi/2)+U2\sin(170+\pi/2)]$
 $DL-0.3[U1\cos 0+U2\sin 0]+[U1\cos(0+\pi/2)+U2\sin(0+\pi/2)]$
 $DL-0.3[U1\cos 10+U2\sin 10]+[U1\cos(10+\pi/2)+U2\sin(10+\pi/2)]$
 $DL-0.3[U1\cos 20+U2\sin 20]+[U1\cos(20+\pi/2)+U2\sin(20+\pi/2)]$
 $DL-0.3[U1\cos 30+U2\sin 30]+[U1\cos(30+\pi/2)+U2\sin(30+\pi/2)]$
 $DL-0.3[U1\cos 40+U2\sin 40]+[U1\cos(40+\pi/2)+U2\sin(40+\pi/2)]$
 $DL-0.3[U1\cos 50+U2\sin 50]+[U1\cos(50+\pi/2)+U2\sin(50+\pi/2)]$
 $DL-0.3[U1\cos 60+U2\sin 60]+[U1\cos(60+\pi/2)+U2\sin(60+\pi/2)]$
 $DL-0.3[U1\cos 70+U2\sin 70]+[U1\cos(70+\pi/2)+U2\sin(70+\pi/2)]$
 $DL-0.3[U1\cos 80+U2\sin 80]+[U1\cos(80+\pi/2)+U2\sin(80+\pi/2)]$
 $DL-0.3[U1\cos 90+U2\sin 90]+[U1\cos(90+\pi/2)+U2\sin(90+\pi/2)]$
 $DL-0.3[U1\cos 100+U2\sin 100]+[U1\cos(100+\pi/2)+U2\sin(100+\pi/2)]$
 $DL-0.3[U1\cos 110+U2\sin 110]+[U1\cos(110+\pi/2)+U2\sin(110+\pi/2)]$
 $DL-0.3[U1\cos 120+U2\sin 120]+[U1\cos(120+\pi/2)+U2\sin(120+\pi/2)]$
 $DL-0.3[U1\cos 130+U2\sin 130]+[U1\cos(130+\pi/2)+U2\sin(130+\pi/2)]$
 $DL-0.3[U1\cos 140+U2\sin 140]+[U1\cos(140+\pi/2)+U2\sin(140+\pi/2)]$
 $DL-0.3[U1\cos 150+U2\sin 150]+[U1\cos(150+\pi/2)+U2\sin(150+\pi/2)]$
 $DL-0.3[U1\cos 160+U2\sin 160]+[U1\cos(160+\pi/2)+U2\sin(160+\pi/2)]$
 $DL-0.3[U1\cos 170+U2\sin 170]+[U1\cos(170+\pi/2)+U2\sin(170+\pi/2)]$
 $DL+0.3[U1\cos 0+U2\sin 0]-[U1\cos(0+\pi/2)+U2\sin(0+\pi/2)]$

$DL+0.3[U1\cos10+U2\sin10]-[U1\cos(10+\pi/2)+U2\sin(10+\pi/2)]$
 $DL+0.3[U1\cos20+U2\sin20]-[U1\cos(20+\pi/2)+U2\sin(20+\pi/2)]$
 $DL+0.3[U1\cos30+U2\sin30]-[U1\cos(30+\pi/2)+U2\sin(30+\pi/2)]$
 $DL+0.3[U1\cos40+U2\sin40]-[U1\cos(40+\pi/2)+U2\sin(40+\pi/2)]$
 $DL+0.3[U1\cos50+U2\sin50]-[U1\cos(50+\pi/2)+U2\sin(50+\pi/2)]$
 $DL+0.3[U1\cos60+U2\sin60]-[U1\cos(60+\pi/2)+U2\sin(60+\pi/2)]$
 $DL+0.3[U1\cos70+U2\sin70]-[U1\cos(70+\pi/2)+U2\sin(70+\pi/2)]$
 $DL+0.3[U1\cos80+U2\sin80]-[U1\cos(80+\pi/2)+U2\sin(80+\pi/2)]$
 $DL+0.3[U1\cos90+U2\sin90]-[U1\cos(90+\pi/2)+U2\sin(90+\pi/2)]$
 $DL+0.3[U1\cos100+U2\sin100]-[U1\cos(100+\pi/2)+U2\sin(100+\pi/2)]$
 $DL+0.3[U1\cos110+U2\sin110]-[U1\cos(110+\pi/2)+U2\sin(110+\pi/2)]$
 $DL+0.3[U1\cos120+U2\sin120]-[U1\cos(120+\pi/2)+U2\sin(120+\pi/2)]$
 $DL+0.3[U1\cos130+U2\sin130]-[U1\cos(130+\pi/2)+U2\sin(130+\pi/2)]$
 $DL+0.3[U1\cos140+U2\sin140]-[U1\cos(140+\pi/2)+U2\sin(140+\pi/2)]$
 $DL+0.3[U1\cos150+U2\sin150]-[U1\cos(150+\pi/2)+U2\sin(150+\pi/2)]$
 $DL+0.3[U1\cos160+U2\sin160]-[U1\cos(160+\pi/2)+U2\sin(160+\pi/2)]$
 $DL+0.3[U1\cos170+U2\sin170]-[U1\cos(170+\pi/2)+U2\sin(170+\pi/2)]$
 $DL-[U1\cos0+U2\sin0]+[U1\cos(0+\pi/2)+U2\sin(0+\pi/2)]$
 $DL-[U1\cos10+U2\sin10]+0.3[U1\cos(10+\pi/2)+U2\sin(10+\pi/2)]$
 $DL-[U1\cos20+U2\sin20]+0.3[U1\cos(20+\pi/2)+U2\sin(20+\pi/2)]$
 $DL-[U1\cos30+U2\sin30]+0.3[U1\cos(30+\pi/2)+U2\sin(30+\pi/2)]$
 $DL-[U1\cos40+U2\sin40]+0.3[U1\cos(40+\pi/2)+U2\sin(40+\pi/2)]$
 $DL-[U1\cos50+U2\sin50]+0.3[U1\cos(50+\pi/2)+U2\sin(50+\pi/2)]$
 $DL-[U1\cos60+U2\sin60]+0.3[U1\cos(60+\pi/2)+U2\sin(60+\pi/2)]$
 $DL-[U1\cos70+U2\sin70]+0.3[U1\cos(70+\pi/2)+U2\sin(70+\pi/2)]$
 $DL-[U1\cos80+U2\sin80]+0.3[U1\cos(80+\pi/2)+U2\sin(80+\pi/2)]$
 $DL-[U1\cos90+U2\sin90]+0.3[U1\cos(90+\pi/2)+U2\sin(90+\pi/2)]$
 $DL-[U1\cos100+U2\sin100]+0.3[U1\cos(100+\pi/2)+U2\sin(100+\pi/2)]$
 $DL-[U1\cos110+U2\sin110]+0.3[U1\cos(110+\pi/2)+U2\sin(110+\pi/2)]$
 $DL-[U1\cos120+U2\sin120]+0.3[U1\cos(120+\pi/2)+U2\sin(120+\pi/2)]$
 $DL-[U1\cos130+U2\sin130]+0.3[U1\cos(130+\pi/2)+U2\sin(130+\pi/2)]$
 $DL-[U1\cos140+U2\sin140]+0.3[U1\cos(140+\pi/2)+U2\sin(140+\pi/2)]$
 $DL-[U1\cos150+U2\sin150]+0.3[U1\cos(150+\pi/2)+U2\sin(150+\pi/2)]$
 $DL-[U1\cos160+U2\sin160]+0.3[U1\cos(160+\pi/2)+U2\sin(160+\pi/2)]$
 $DL-[U1\cos170+U2\sin170]+0.3[U1\cos(170+\pi/2)+U2\sin(170+\pi/2)]$
 $DL-[U1\cos0+U2\sin0]-0.3[U1\cos(0+\pi/2)+U2\sin(0+\pi/2)]$
 $DL-[U1\cos10+U2\sin10]-0.3[U1\cos(10+\pi/2)+U2\sin(10+\pi/2)]$
 $DL-[U1\cos20+U2\sin20]-0.3[U1\cos(20+\pi/2)+U2\sin(20+\pi/2)]$
 $DL-[U1\cos30+U2\sin30]-0.3[U1\cos(30+\pi/2)+U2\sin(30+\pi/2)]$
 $DL-[U1\cos40+U2\sin40]-0.3[U1\cos(40+\pi/2)+U2\sin(40+\pi/2)]$
 $DL-[U1\cos50+U2\sin50]-0.3[U1\cos(50+\pi/2)+U2\sin(50+\pi/2)]$
 $DL-[U1\cos60+U2\sin60]-0.3[U1\cos(60+\pi/2)+U2\sin(60+\pi/2)]$
 $DL-[U1\cos70+U2\sin70]-0.3[U1\cos(70+\pi/2)+U2\sin(70+\pi/2)]$

$DL-[U1\cos 80+U2\sin 80]-0.3[U1\cos(80+\pi/2)+U2\sin(80+\pi/2)]$
 $DL-[U1\cos 90+U2\sin 90]-0.3[U1\cos(90+\pi/2)+U2\sin(90+\pi/2)]$
 $DL-[U1\cos 100+U2\sin 100]-0.3[U1\cos(100+\pi/2)+U2\sin(100+\pi/2)]$
 $DL-[U1\cos 110+U2\sin 110]-0.3[U1\cos(110+\pi/2)+U2\sin(110+\pi/2)]$
 $DL-[U1\cos 120+U2\sin 120]-0.3[U1\cos(120+\pi/2)+U2\sin(120+\pi/2)]$
 $DL-[U1\cos 130+U2\sin 130]-0.3[U1\cos(130+\pi/2)+U2\sin(130+\pi/2)]$
 $DL-[U1\cos 140+U2\sin 140]-0.3[U1\cos(140+\pi/2)+U2\sin(140+\pi/2)]$
 $DL-[U1\cos 150+U2\sin 150]-0.3[U1\cos(150+\pi/2)+U2\sin(150+\pi/2)]$
 $DL-[U1\cos 160+U2\sin 160]-0.3[U1\cos(160+\pi/2)+U2\sin(160+\pi/2)]$
 $DL-[U1\cos 170+U2\sin 170]-0.3[U1\cos(170+\pi/2)+U2\sin(170+\pi/2)]$
 $DL-0.3[U1\cos 0+U2\sin 0]-[U1\cos(0+\pi/2)+U2\sin(0+\pi/2)]$
 $DL-0.3[U1\cos 10+U2\sin 10]-[U1\cos(10+\pi/2)+U2\sin(10+\pi/2)]$
 $DL-0.3[U1\cos 20+U2\sin 20]-[U1\cos(20+\pi/2)+U2\sin(20+\pi/2)]$
 $DL-0.3[U1\cos 30+U2\sin 30]-[U1\cos(30+\pi/2)+U2\sin(30+\pi/2)]$
 $DL-0.3[U1\cos 40+U2\sin 40]-[U1\cos(40+\pi/2)+U2\sin(40+\pi/2)]$
 $DL-0.3[U1\cos 50+U2\sin 50]-[U1\cos(50+\pi/2)+U2\sin(50+\pi/2)]$
 $DL-0.3[U1\cos 60+U2\sin 60]-[U1\cos(60+\pi/2)+U2\sin(60+\pi/2)]$
 $DL-0.3[U1\cos 70+U2\sin 70]-[U1\cos(70+\pi/2)+U2\sin(70+\pi/2)]$
 $DL-0.3[U1\cos 80+U2\sin 80]-[U1\cos(80+\pi/2)+U2\sin(80+\pi/2)]$
 $DL-0.3[U1\cos 90+U2\sin 90]-[U1\cos(90+\pi/2)+U2\sin(90+\pi/2)]$
 $DL-0.3[U1\cos 100+U2\sin 100]-[U1\cos(100+\pi/2)+U2\sin(100+\pi/2)]$
 $DL-0.3[U1\cos 110+U2\sin 110]-[U1\cos(110+\pi/2)+U2\sin(110+\pi/2)]$
 $DL-0.3[U1\cos 120+U2\sin 120]-[U1\cos(120+\pi/2)+U2\sin(120+\pi/2)]$
 $DL-0.3[U1\cos 130+U2\sin 130]-[U1\cos(130+\pi/2)+U2\sin(130+\pi/2)]$
 $DL-0.3[U1\cos 140+U2\sin 140]-[U1\cos(140+\pi/2)+U2\sin(140+\pi/2)]$
 $DL-0.3[U1\cos 150+U2\sin 150]-[U1\cos(150+\pi/2)+U2\sin(150+\pi/2)]$
 $DL-0.3[U1\cos 160+U2\sin 160]-[U1\cos(160+\pi/2)+U2\sin(160+\pi/2)]$
 $DL-0.3[U1\cos 170+U2\sin 170]-[U1\cos(170+\pi/2)+U2\sin(170+\pi/2)]$

The first two cases are belongs to temperature loading. The other 36 combinations are about wind load combinations, which are defined in accordance with TS498. Dead load and wind loads acting with angles of 0° to 350° from East in counter clock wise are sum up for each combinations and resultant loads are applied to the Castle. Other 144 combinations are obtained in accordance with National Earthquake Hazards Reduction Program (NEHRP) and Federal Emergency Management Agency (FEMA) and in essence can also be found in American Association of State Highway and Transportation (AASTHO) as well. In all EQ related load definitions coming with 10° intervals, 100% of main direction (U1) earthquake load and 30% of transverse direction (U2) earthquake load are defined and applied to the Castle at the same time.

Similarly, total of 8 combinations are created for EQ being multiplied with -1, indicating the negative effects (compression and tension) at the same time. The transverse 30% combination is also multiplied with -1 and combined with the main loading directions. The 30% transverse direction actually defined to count for different EQ application angles. In this study, this procedure is repeated for 10 degree increments generating new axes (x' and y') to stay on the safe side. Basic coordinate transformation is used to define x' and y' axes by multiplication of U1 and U2 with sinus and cosines belongs to angle of the new axis.

2.9. MATLAB Code

MATLAB is used to develop a code for creating combinations mentioned in Chapter 2 and analyzing results of the combinations. The code firstly reads data obtained from SAP2000 analyses results of dead load, U1, and U2. The data can be read from text file by MATLAB. Secondly, the code generates 144 combinations which are about different combination of earthquake loads. Then, results of 144 combinations are obtained as normal and shear stresses. The normal stresses are σ_x , σ_y , σ_z and the shear stresses are τ_{xy} , τ_{xz} , τ_{yz} . These stresses are used to obtain principal stresses of each solids of the Castle. At this point, the code uses the formulas shown in Equations 4 till 14 to get the principal stresses.

$$I_1 = \sigma_x + \sigma_y + \sigma_z \text{ (Eqn. 4)}$$

$$I_2 = \sigma_x\sigma_y + \sigma_x\sigma_z + \sigma_y\sigma_z - \tau_{xy}^2 - \tau_{xz}^2 - \tau_{yz}^2 \text{ (Eqn. 5)}$$

$$I_3 = \sigma_x\sigma_y\sigma_z + 2\tau_{xy}\tau_{xz}\tau_{yz} - \sigma_x\tau_{yz}^2 - \sigma_y\tau_{xz}^2 - \sigma_z\tau_{xy}^2 \text{ (Eqn. 6)}$$

$$R = \frac{1}{3}I_1^2 - I_2 \text{ (Eqn. 7)}$$

$$S = \left(\frac{1}{3}R\right)^{\frac{1}{2}} \text{ (Eqn. 8)}$$

$$Q = \frac{1}{3}I_1I_2 - I_3 - \frac{2}{27}I_1^3 \text{ (Eqn. 9)}$$

$$T = \left(\frac{1}{3}R^3\right)^{\frac{1}{2}} \text{ (Eqn. 10)}$$

$$\alpha = \cos^{-1}\left(-\frac{Q}{2T}\right) \text{ (Eqn. 11)}$$

$$\sigma_a = 2S \left[\cos\left(\frac{\alpha}{3}\right) \right] + \frac{1}{3}I_1 \text{ (Eqn. 12)}$$

$$\sigma_b = 2S \left\{ \cos\left[\left(\frac{\alpha}{3}\right) + 120^\circ\right] \right\} + \frac{1}{3}I_1 \text{ (Eqn. 13)}$$

$$\sigma_c = 2S \left\{ \cos\left[\left(\frac{\alpha}{3}\right) + 240^\circ\right] \right\} + \frac{1}{3}I_1 \text{ (Eqn. 14)}$$

σ_a , σ_b , σ_c are the principles stresses of a solid of the Castle. The maximum one is σ_1 , the minimum one is σ_3 , and the middle one is σ_2 . At the end of the code, (18×8×13248=) 1907712 principal stresses are found for each load combinations and this is the main reason for using MATLAB instead of SAP2000 during the earthquake analyses of the Castle. Definition of load cases in SAP2000 is more difficult, takes more time to run, and principal stresses cannot be obtained in SAP2000.

2.10. Coulomb-Mohr Theory and Modified-Mohr Theory

Cappadocian tuff is a brittle material which is suitable to be evaluated with using Coulomb-Mohr Theory. Another version of Coulomb-Mohr Theory is the Modified-Mohr Theory, which has slight difference in the shear region. Both of these theories are based on maximum normal-stress theory. The ultimate tensile strength, S_{ut} , is the limit of σ_1 for tensile strength on the other hand the ultimate compressive strength, S_{uc} , is the limit of σ_3 for compressive strength. The difference between Coulomb-Mohr Theory and Modified-Mohr Theory is the limit of case when σ_1 is in tension and σ_3 is in compression. The Coulomb-Mohr Theory is relatively more conservative compared to the Modified-Mohr Theory by decreasing the limits of ultimate strengths. These theories are used to evaluate the analysis results of the Castle. Each solids' principle stresses obtained from results of 183 combinations are analyzed according to

Coulomb-Mohr Theory and Modified-Mohr Theory and plotted on a 2D graph as shown in Figure 11.

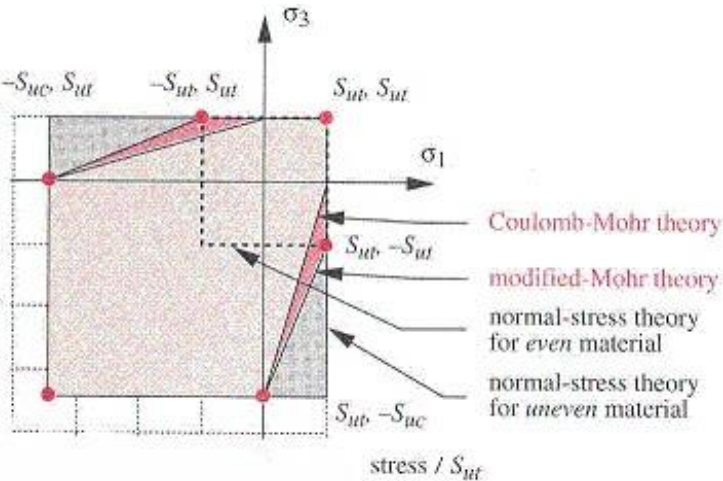


Figure 11 Coulomb-Mohr and Modified-Mohr Theories

2.11. Difficulties Encountered During the Analysis

Preparing FEM of the Castle has difficulties at stages of drawing, defining conditions, and analyzing. The Castle has an irregular shape, which is very difficult to define FEM. This problem leads to develop a code which reads coordinates of the Castle as single dots and transfers the dots to create solids for FEM of the Castle.

The second problem is defining material properties and load combinations of FEM of the Castle. Since the cracks and the caves cannot modelled, calibration was done to get more realistic model. The calibration is done only for modulus of elasticity to count for existing cracks. The third problem is about temperature loading at Sap2000. The results of temperature loads at SAP2000 has a relationship with how fine or coarsely the solid members are meshed in SAP2000. If coarse meshing for solids is used, the calculated temperature load at SAP2000 is higher than hand calculated realistic values. Since the FEM used at this thesis is coarse because of computer limitations, the temperature loads calculated at SAP2000 is higher than the values calculated by hand. Smaller models with fine meshing showed close agreement with the theoretical hand

calculation. However, this difference can be accepted since the stress values are higher than values calculated by hand therefore, the results are on the safe side. Another problem is number of loading combinations: MATLAB code is develop to solve the extensive number of load combinations problem for SAP2000.

The last problem is faced at analyzing step: SAP2000 runs each analysis in an hour or more and sometimes gives error during the analysis which causes loss of time

2.12. Analysis Results

The analysis results are studied to see if the castle is safe against EQ, wind, and temperature loads. A criteria is needed to consider the analysis results: The Coulomb-Mohr Theory and Modified-Mohr Theory are chosen for evaluating the results. EQ results obtained from SAP2000 and post processed in MATLAB to obtain principal stresses are plotted on Coulomb-Mohr Theory and Modified-Mohr Theory graphs (Figure 12 and Figure 13). The plotted data are principal stresses of each one of the solids which are separately plotted for all 183 load combinations as explained in Section 2.6. The wind load combination results are also post processed and plotted in Figure 14 while the temperature load results are plotted in Figure 15. If the plotted data remains inside the boundaries defined by both theories, then those solid members can be accepted safe against 183 load combinations including EQ, wind, and temperature loading. Only a few members have stresses exceeding the tensile capacity of the material (Figure 12) for the fixed case modeling condition. When the base rock stiffness is defined using springs or when the wind load is acting on the Castle, the stressed do not exceed the capacity of the material and remain within the boundaries (Figures 13 and 14). Temperature loading results show that a solid member located at the top of the Castle with high aspect ratio has stresses exceeding the tensile capacity of the material (Figure 15). This may be due to modeling properties and even if one member exceeds the limits, the overall castle remains intact.

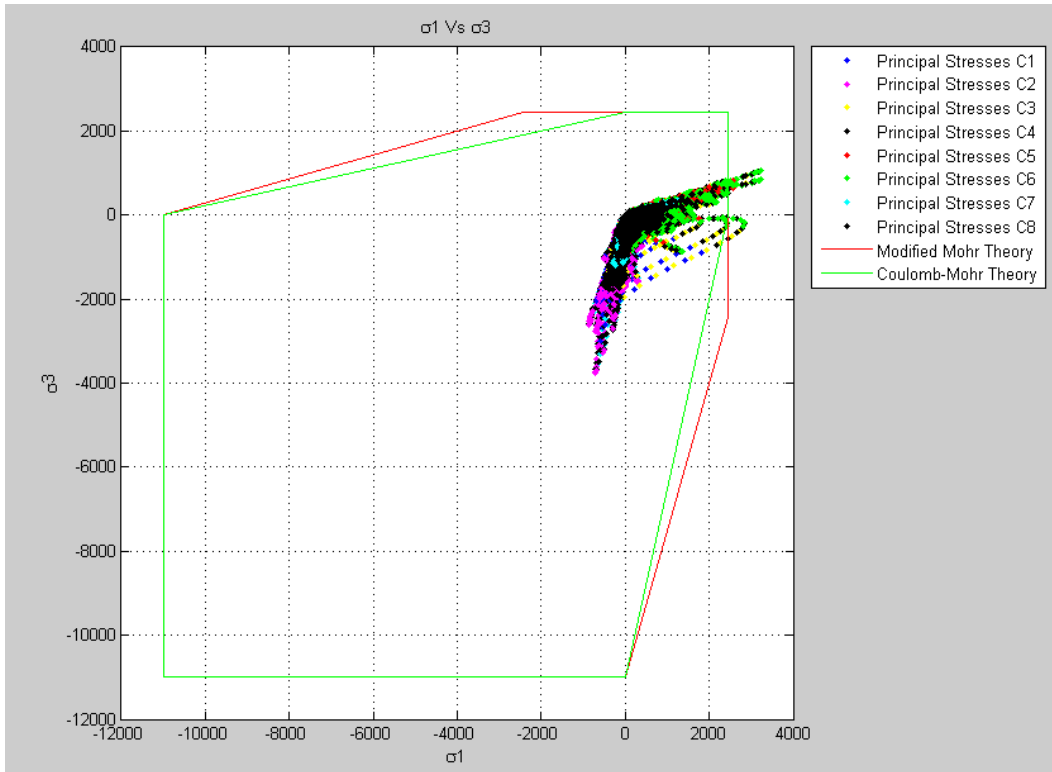


Figure 12 Analysis Results of Earthquake Loads with Fixed Supports (144 cases)

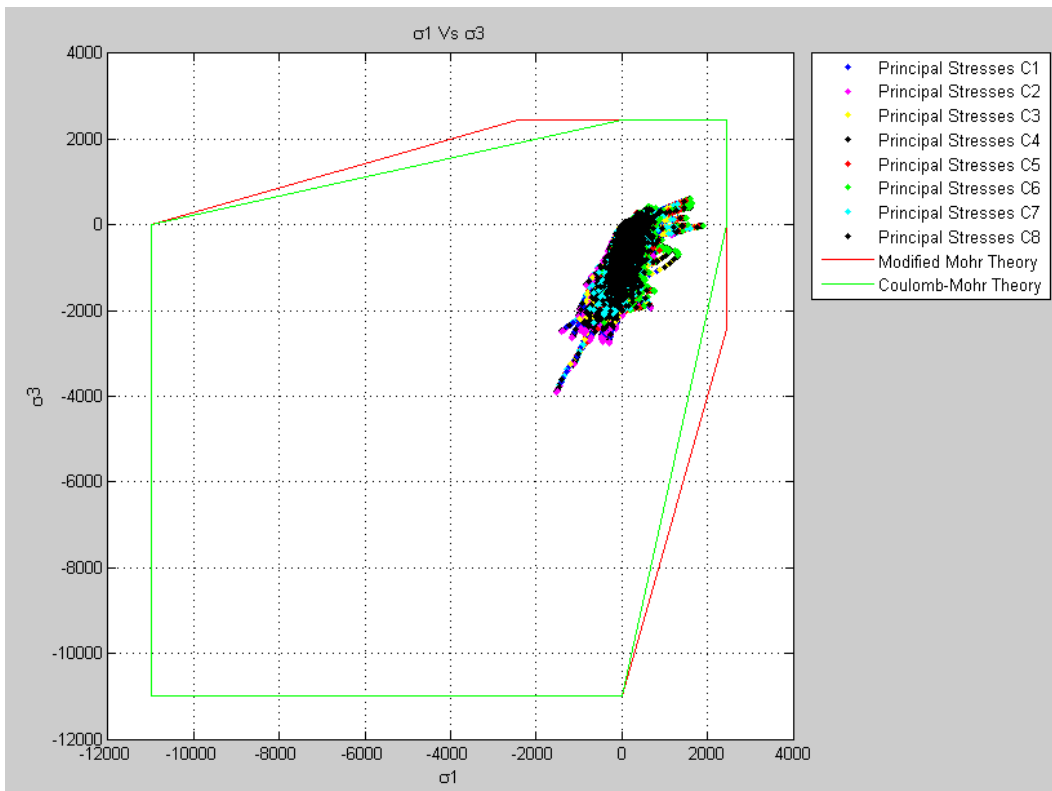


Figure 13 Analysis Results of Earthquake Loads with Springs at the base (144 cases).

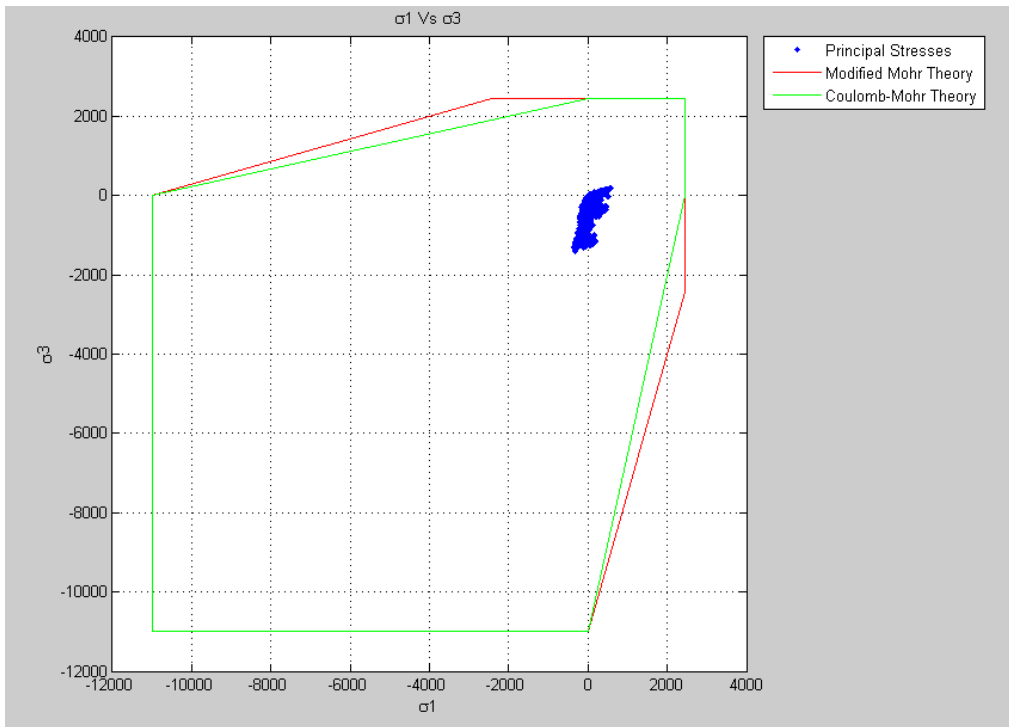


Figure 14 Analysis Results of Wind Loads (36 cases)

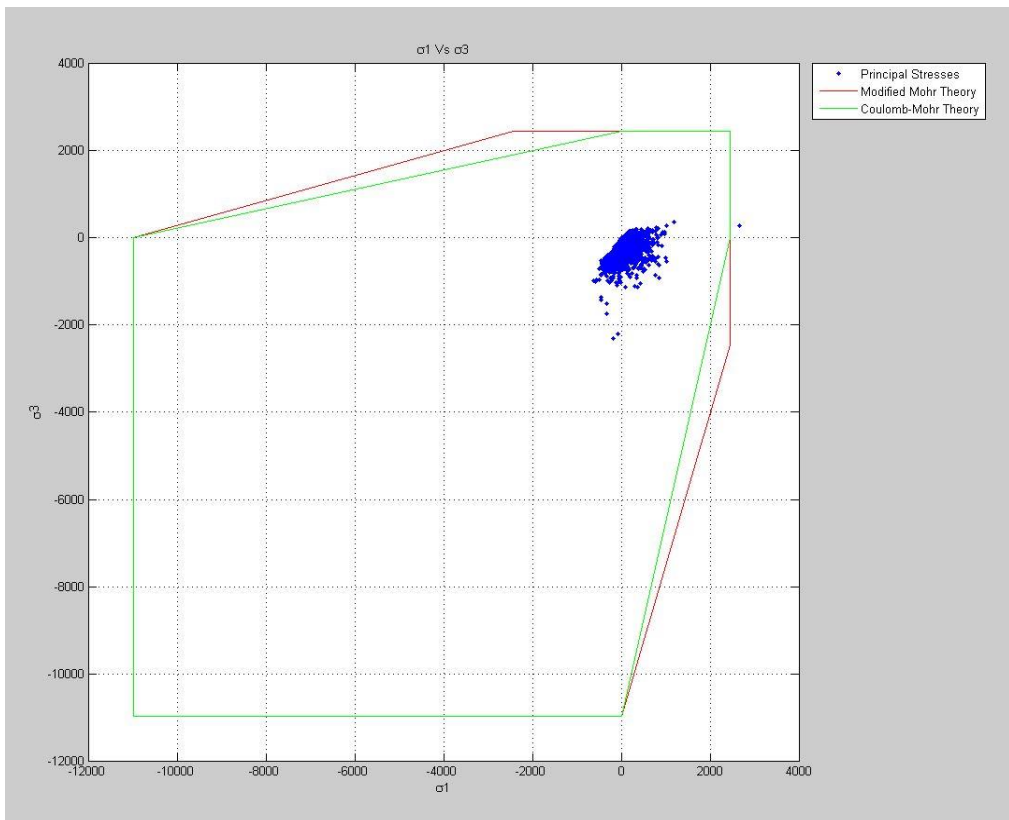


Figure 15 Analysis Results of Temperature Loads (2 cases)

In addition to the Coulomb Mohr Theory related comprehensive analyses, the stress levels for a limited number of load cases are directly obtained from SAP2000 and plotted on the castle FEM to see the distribution of stress. It should be noted that the load case results shown here are only a subset of all the combinations processed by the MATLAB code. The stress contour plots here are also used as a second check to ensure MATLAB results are reliable. As it can be seen from Figures 20 to 32, the normal stress levels (S11, S22, S33 etc) are well below the material capacity indicating that no significant damage is expected on the structure during a design earthquake or wind loading defined by the Turkish code (Figures 20-32). Figures 33 and 34 also show the Von Mises Stress results for temperature loading of $\pm 20\text{ C}^\circ$ and $+40\text{ C}^\circ$ partial temperature loading.

As a summary, although the maximum EQ stress obtained for S22 is 2.45 MPa overall stress levels are generally smaller than the tensile and compressive load capacity of the material (Figure 24). The stress directions and amplitudes are prepared in a table format and listed in Table 4. S11 stress direction is horizontal in global degrees of freedom, which is aligned with the x-axis. S33 stress direction is a vertical component in global degrees of freedom, which is aligned with the z-axis. S22 stress direction is a horizontal stress in global degrees of freedom, which is aligned with the y-axis. The maximum S22 stress of a member exceeds the tensile capacity of the material by about 10%. This member has member id # 19606 and is located towards the top of the castle with irregular shape. General stress definition of SAP2000 is shown in Figure 17 and the stress directions are shown in Figure 16.

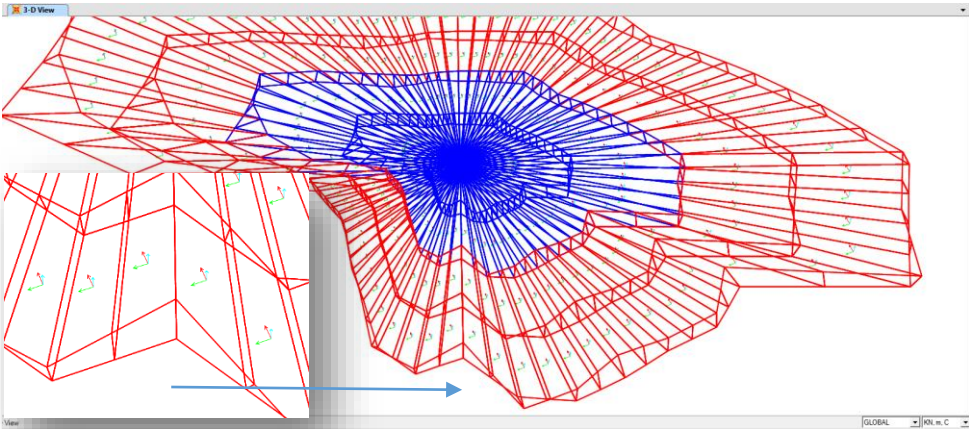
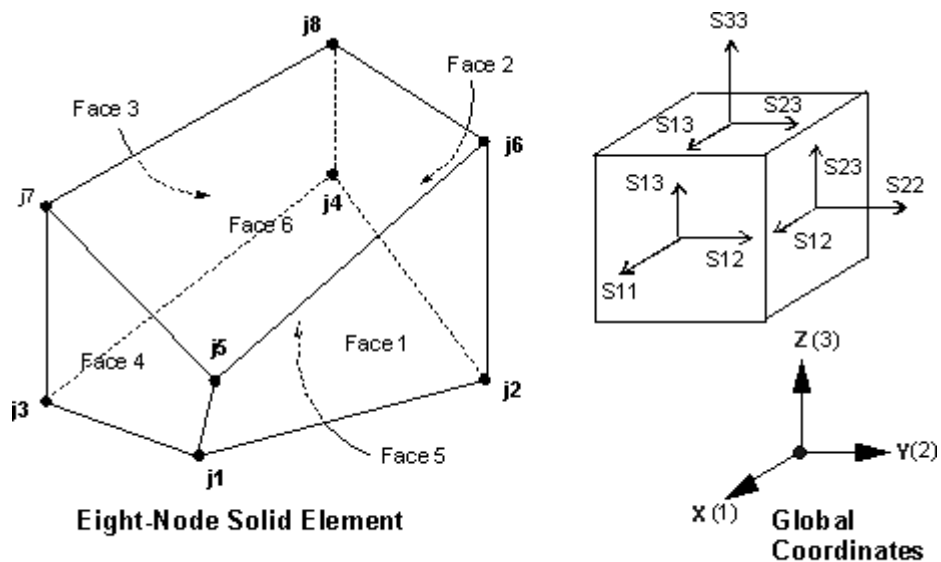


Figure 16 Global Coordinates of FEM

Table 3 Stress Results Under DL, U1, and U2

Stress direction	Min and Max stresses	Capacity check
S33	-1.81 MPa; 0.94 MPa (Figure 21-22)	>-12 MPa; <2.2 MPa
S22	-2.18 MPa; 2.45 MPa (Figure 23-24)	>-12 MPa; <2.2 MPa
S11	-2.55 MPa; 1.85 MPa (Figure 25-26)	>-12 MPa; <2.2 MPa
S12	-1.16 MPa; 1.04 MPa (Figure 27-28)	>-2 MPa; <2 MPa
S13	-0.66 MPa; 0.83 MPa (Figure 29-30)	>-2 MPa; <2 MPa
S23	-0.43 MPa; 0.43 MPa (Figure 31-32)	>-2 MPa; <2 MPa
DL	-1.29 MPa (Figure 20)	>-12 MPa; <2.2 MPa



Solid Element Stresses

Figure 17 Global Coordinates of a Solid

The calculated overall stress levels for the indicated loading directions (S11, S22, etc) are much smaller and the stress capacities as it was expected, since the castle has survived many EQs, wind, and temperature loads in its past and SAP2000 stress contours are a subset of MATLAB code checks. According to Figure 35; the percentage of damaged solid members of the Castle is 0.0047%. On the other hand; the percentage of the solids, which are in the zone whose limit is reduced by 90%, is

97.5%. This means that the Castle shows very strong behavior against earthquake loads like wind loads.

According to wind load analysis results, it is seen that the principal stresses generated by wind load has small effect compared to EQ where the maximum stress levels do not exceed more than 10% of the material capacity under wind loading. However; analysis results belong to temperature loading at SAP2000 show differences with the results calculated by hand. The values that SAP2000 found is higher at the outer solid members of the Castle. This phenomenon was investigated using higher mesh density and smaller analytical models. Although the SAP2000 coarse mesh analysis results are on the safe side, the reason for this needs to be explored: Stress distribution between the outer solid members and inner solid members is sharp. While outer solid members, whose thicknesses are 10 cm according to FEM prepared at SAP2000, have high stresses; inner solid members next to outer ones have low stress.

There are two important points to get more realistic results under temperature loading. The first one is that stress distribution between the solid members should be smooth. The second one is that minimizing the mesh size, increasing the number of members, and having proper aspect ratio for the solid members in SAP2000 is important. The second point can be achieved by obtaining optimal mesh ratio; however, obtaining optimal mesh ratio is not easy at this study because of computer's capacity used during the analyses. Figure 18 shows that the model (Figure 18a & c) with high mesh ratio gives better results than model with low mesh ratio (Figure 18b & d).

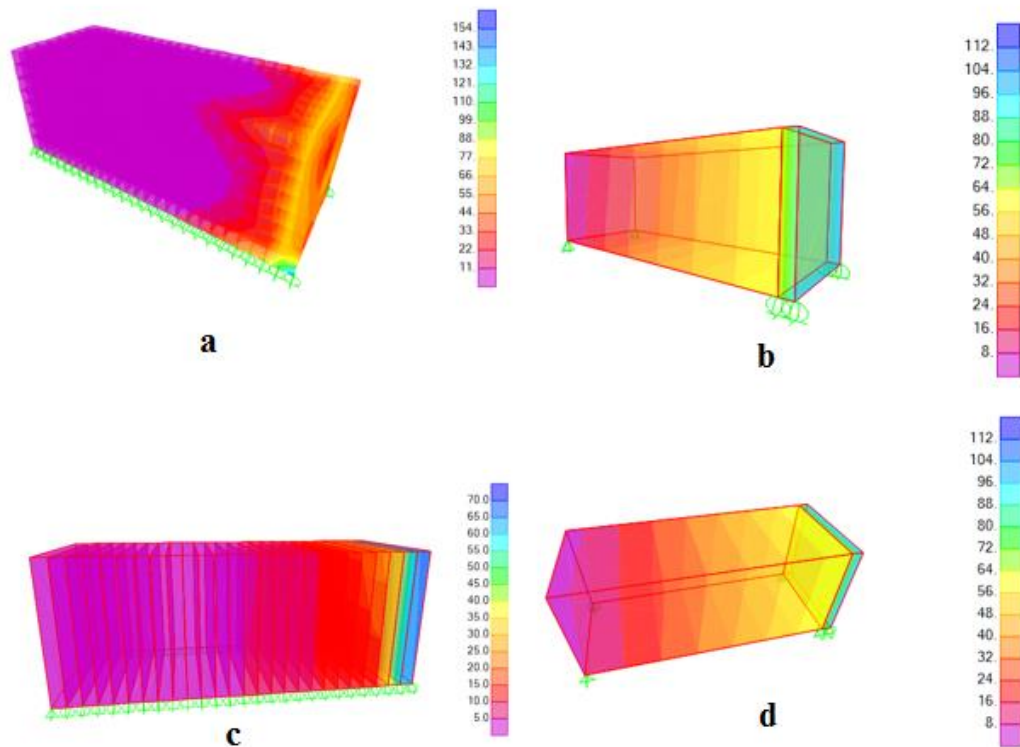


Figure 18 Temperature Load Analysis of a Rectangular Pris

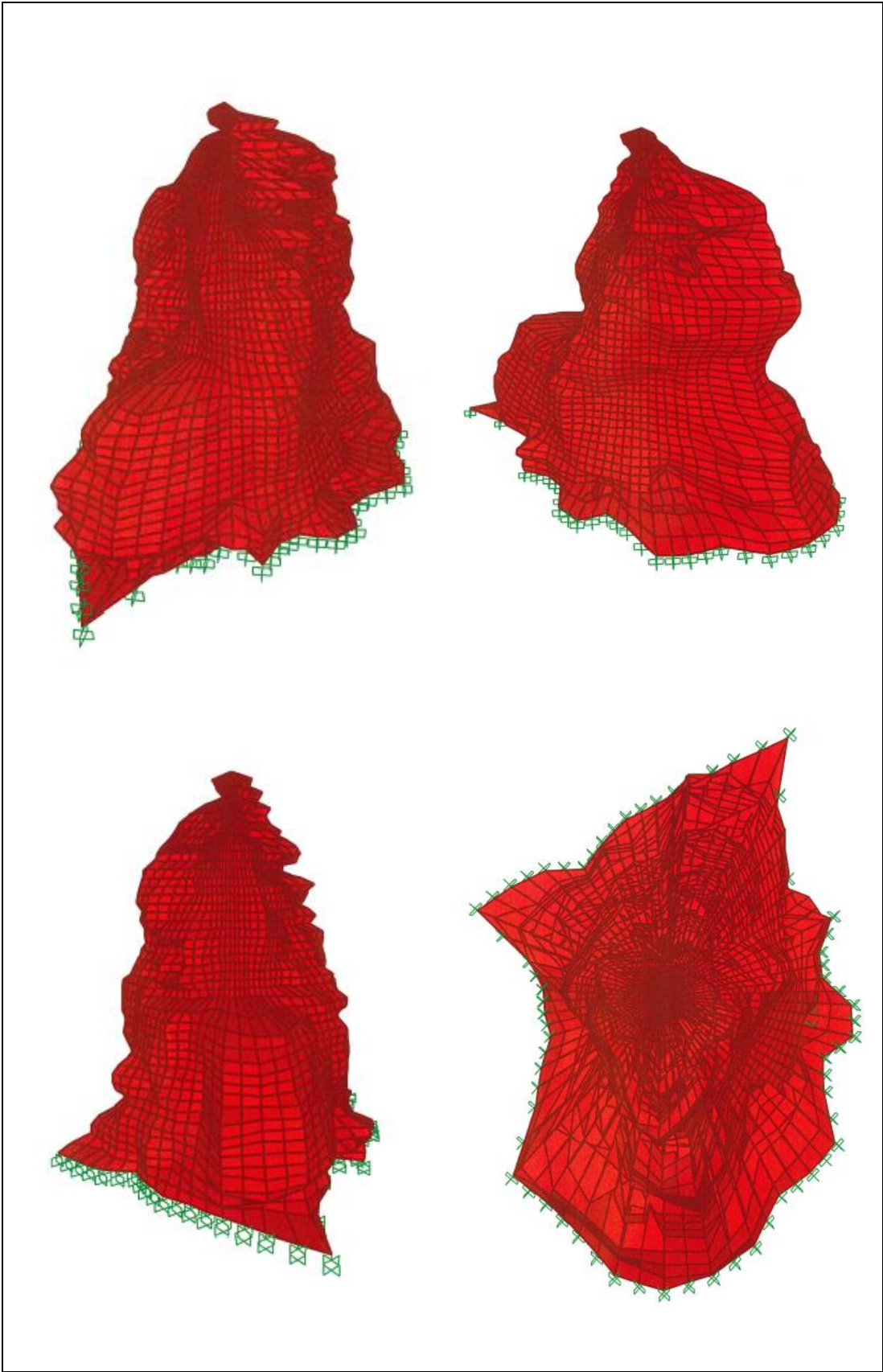


Figure 19 FEM of the Castle

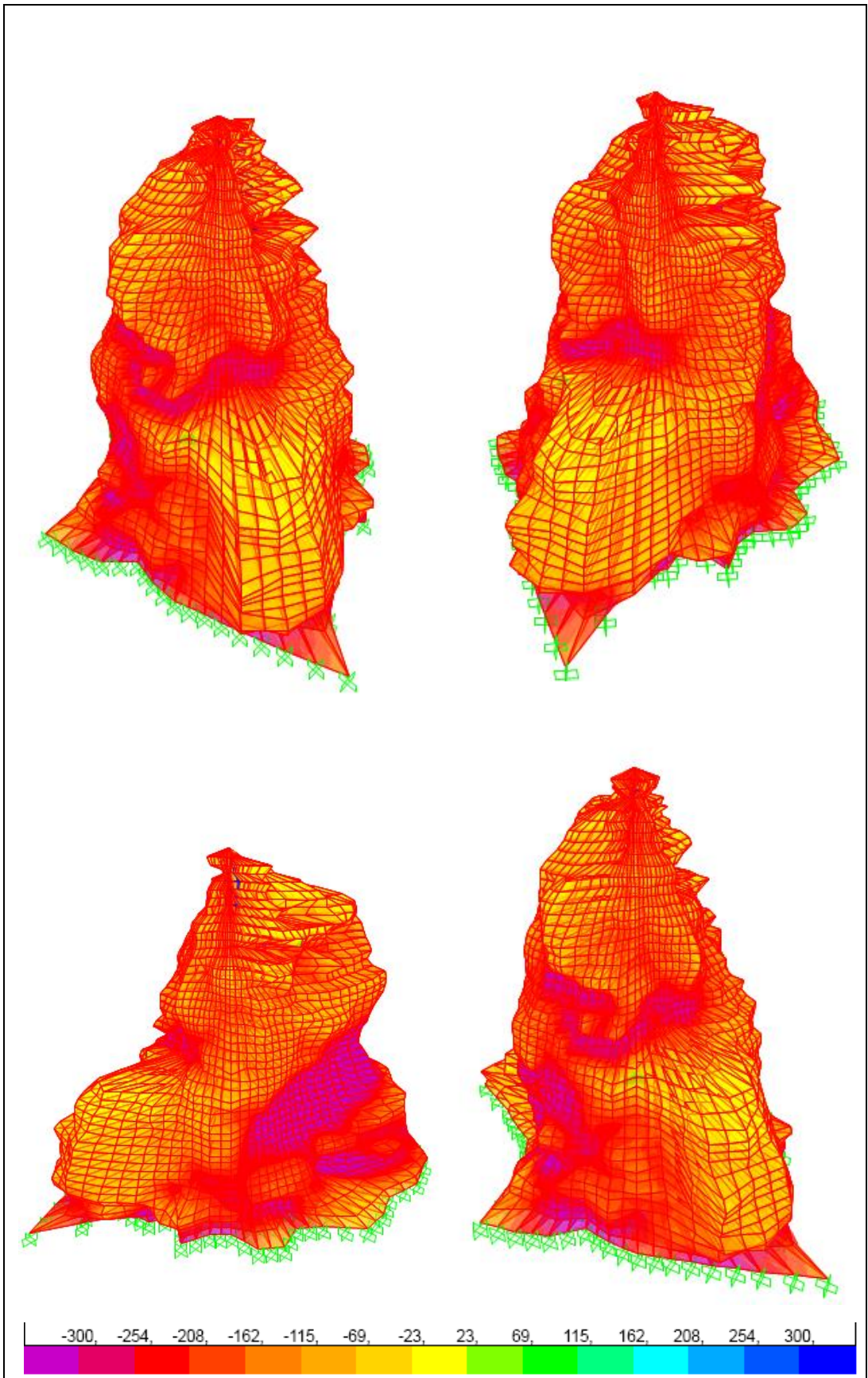


Figure 20 S33 Dead Load Stresses (kPa)

* Envelope = Max (DL;EQx;EQy;DL+1.0EQx+0.3EQy; DL+0.3EQx+1.0EQy)

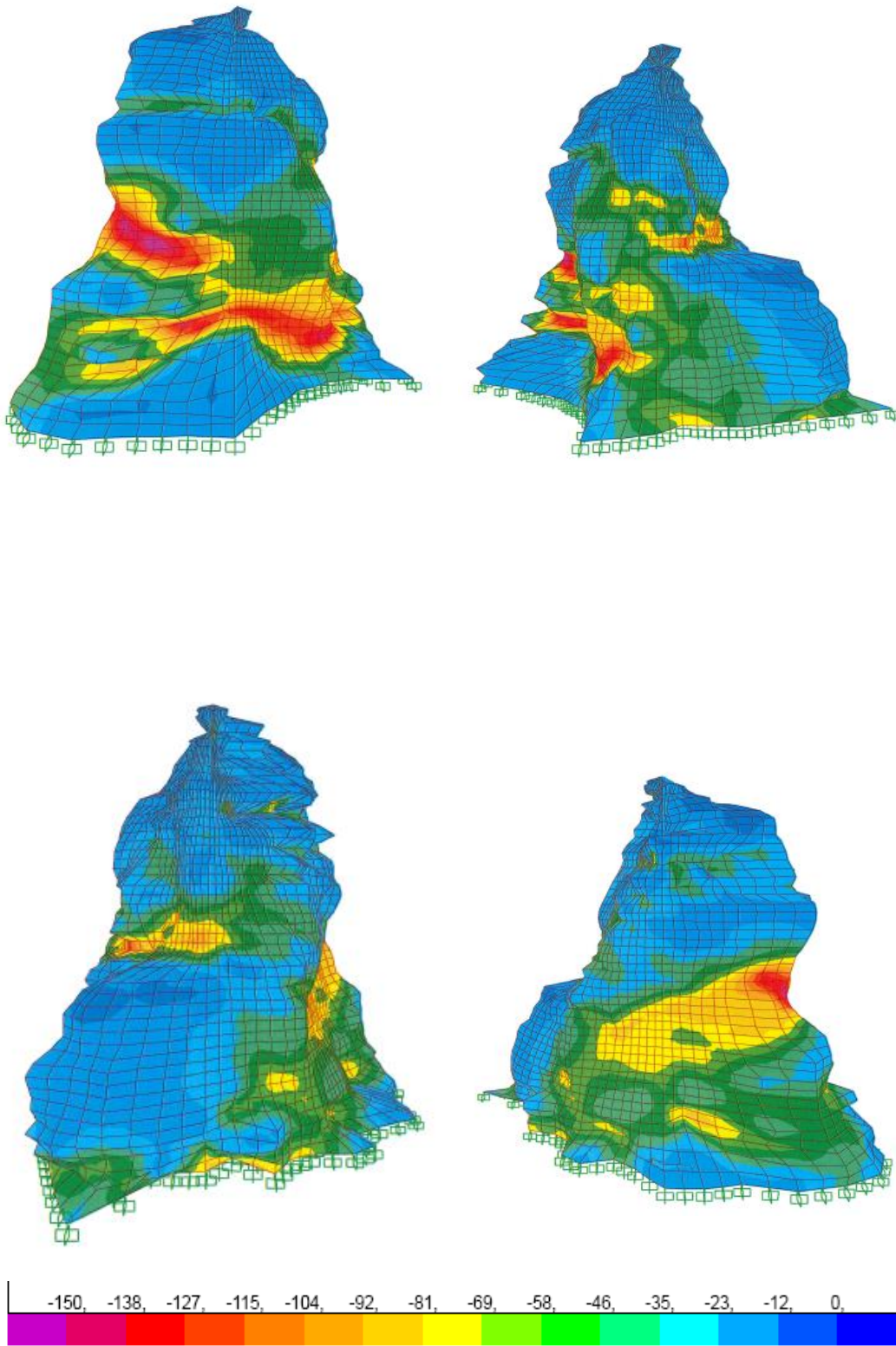


Figure 21 S33 *Envelope Min Stresses (kPa)

* Envelope = Max (DL;EQx;EQy;DL+1.0EQx+0.3EQy; DL+0.3EQx+1.0EQy)

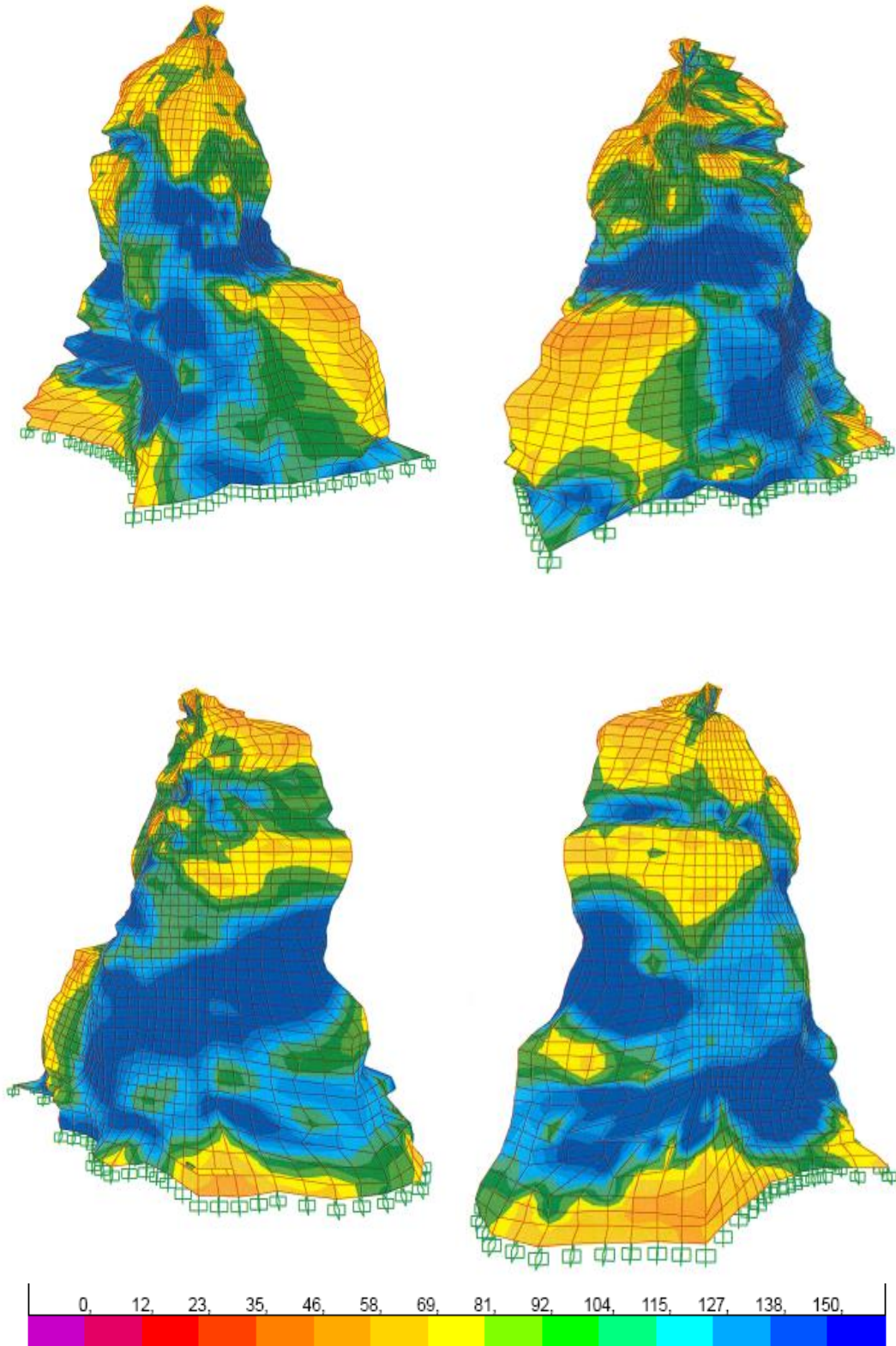


Figure 22 S33 *Envelope Max Stresses (kPa)

* Envelope = Max (DL;EQx;EQy;DL+1.0EQx+0.3EQy; DL+0.3EQx+1.0EQy)

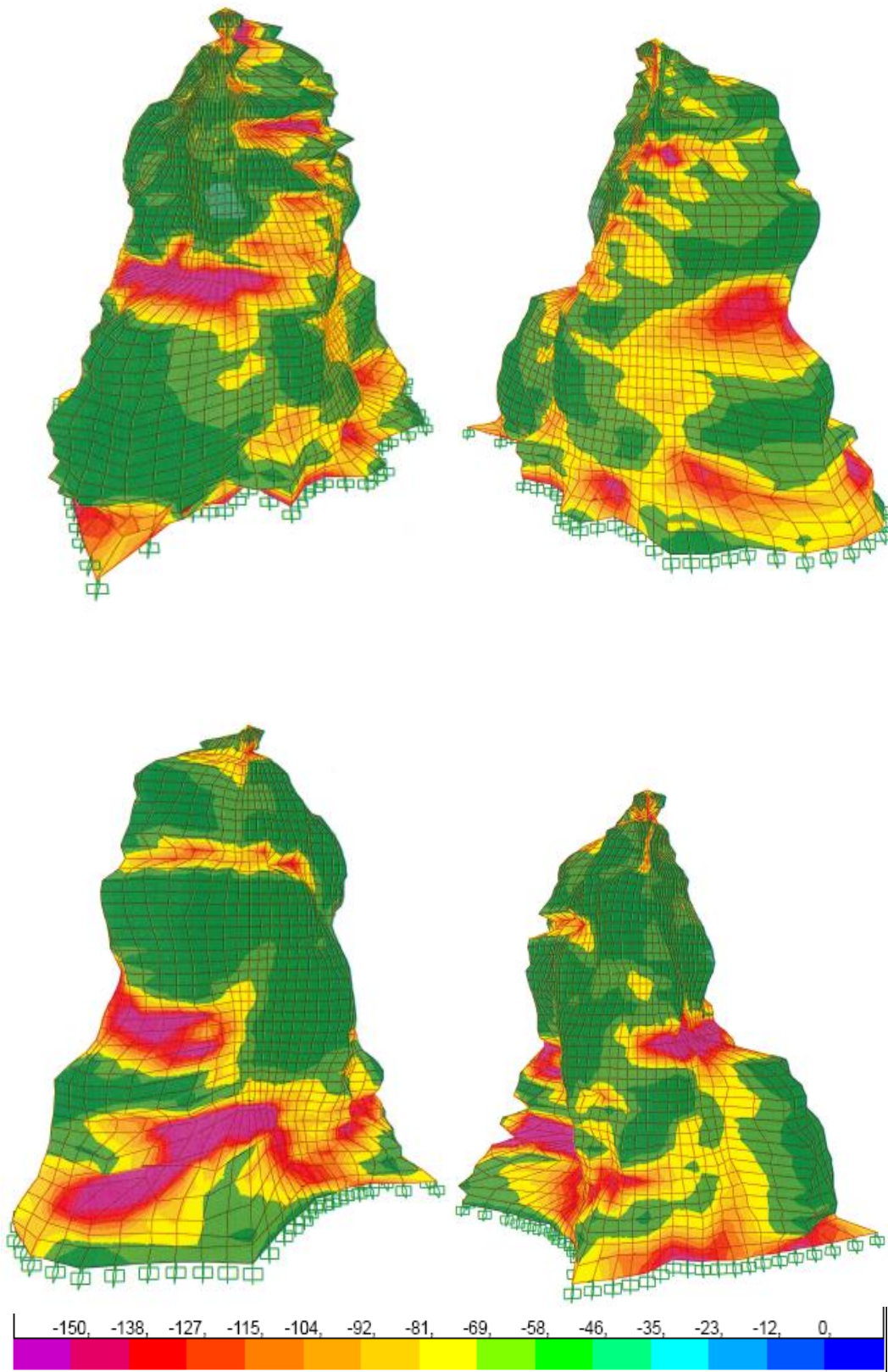


Figure 23 S22 *Envelope Min Stresses (kPa)

* Envelope = Max (DL;EQx;EQy;DL+1.0EQx+0.3EQy; DL+0.3EQx+1.0EQy)

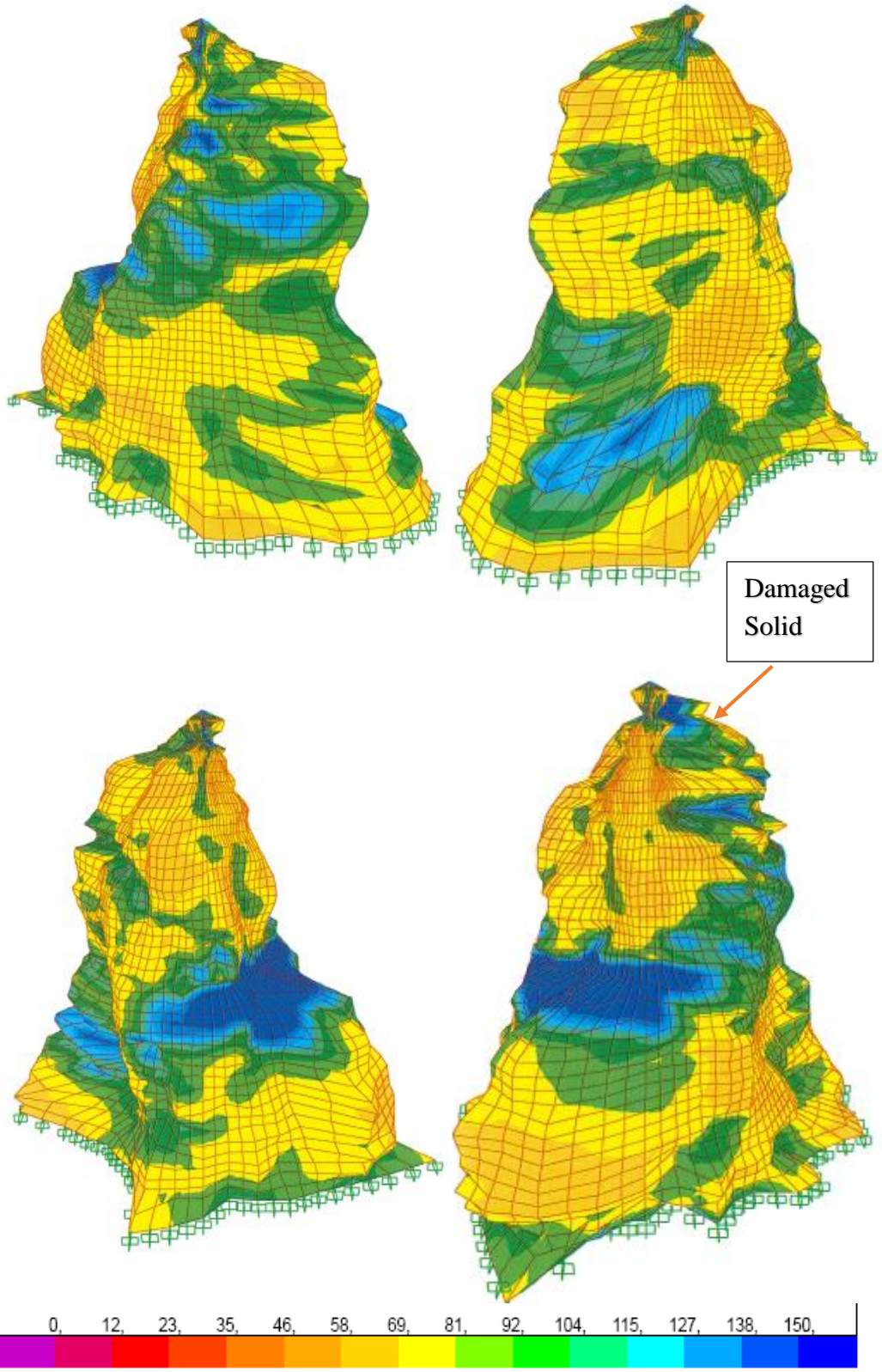


Figure 24 S22 *Envelope Max Stresses (kPa)

* Envelope = Max (DL;EQx;EQy;DL+1.0EQx+0.3EQy; DL+0.3EQx+1.0EQy)

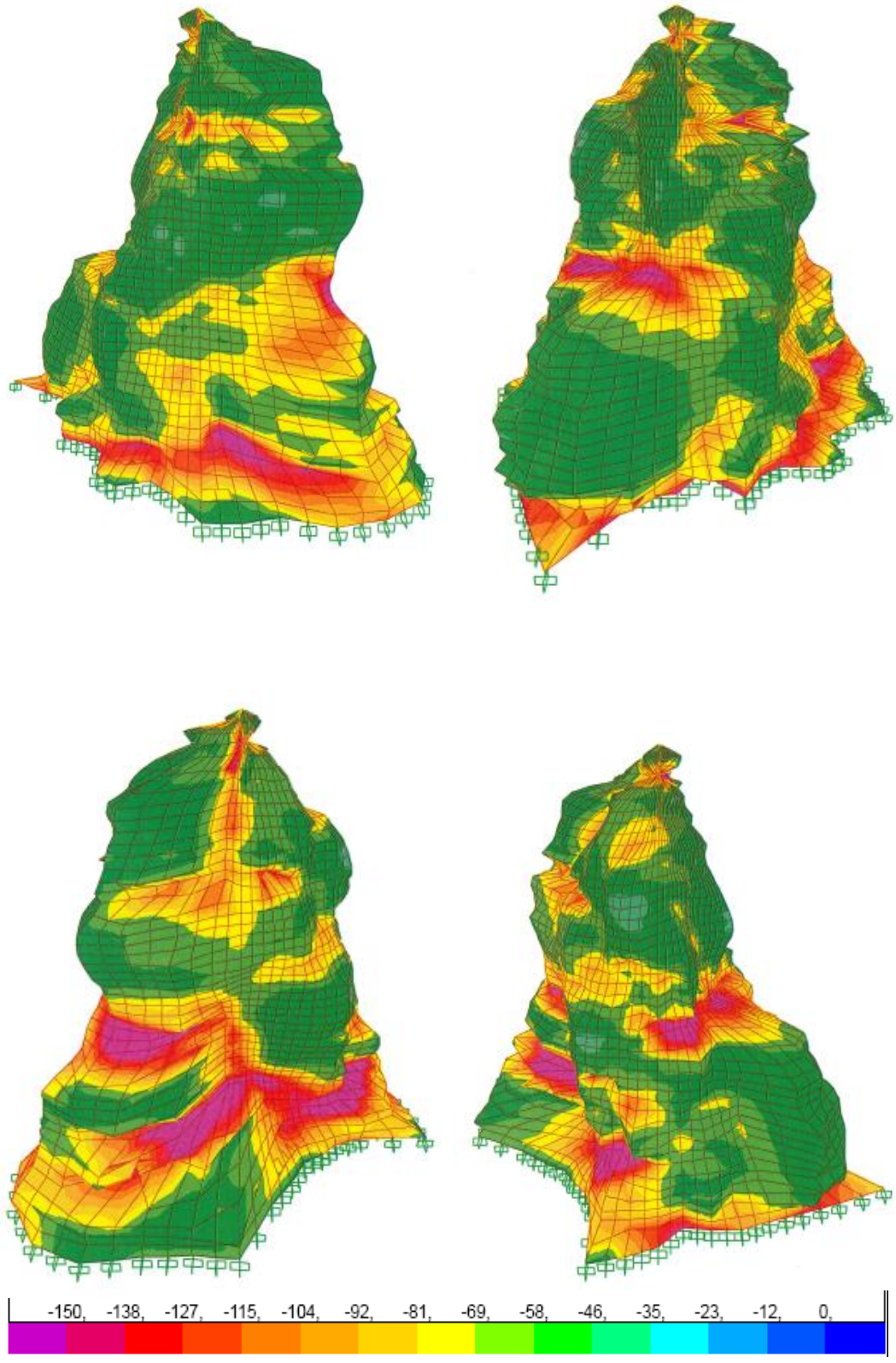


Figure 25 S11 *Envelope Min Stresses (kPa)

* Envelope = Max (DL;EQx;EQy;DL+1.0EQx+0.3EQy; DL+0.3EQx+1.0EQy)

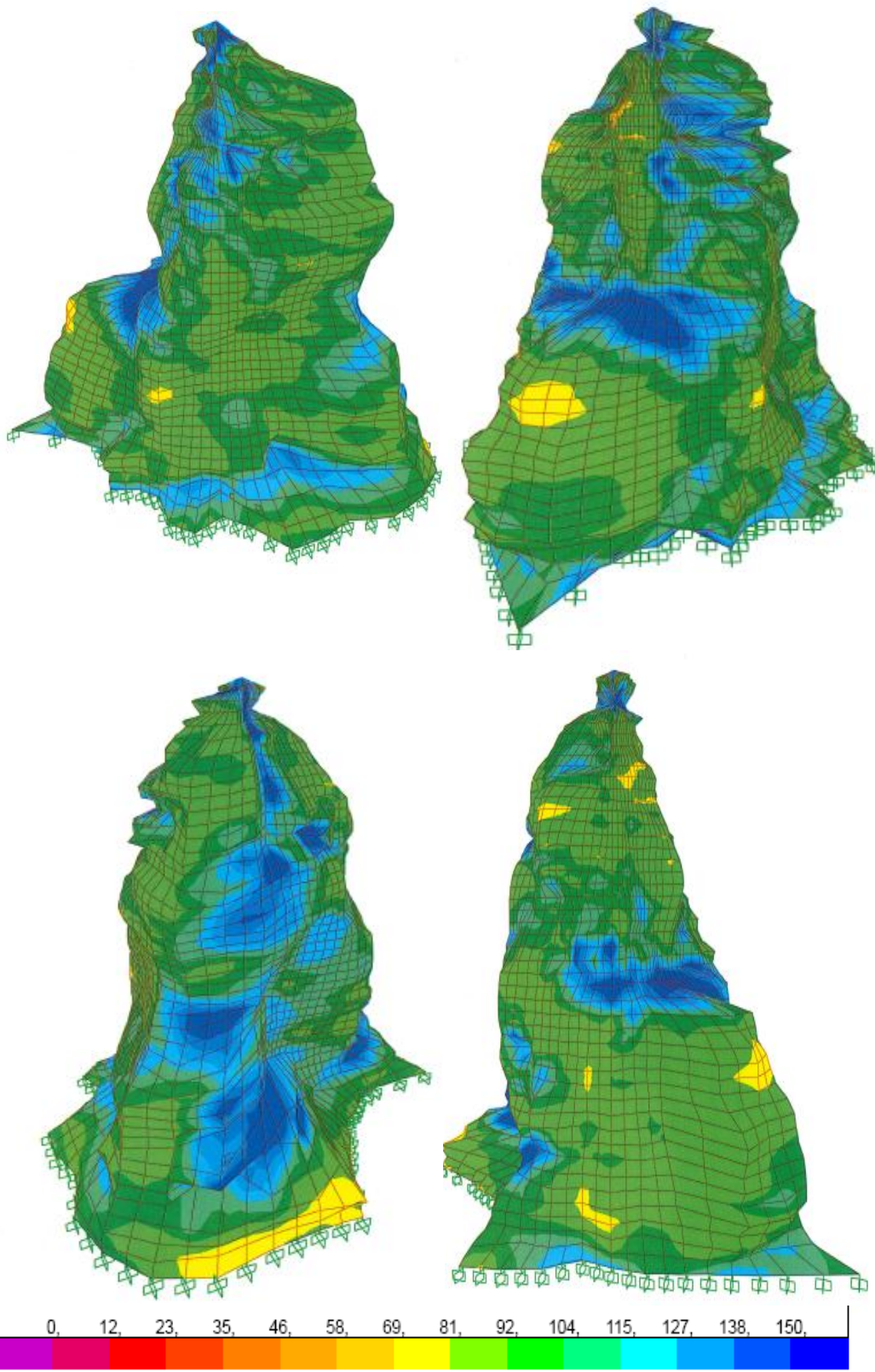


Figure 26 S11 *Envelope Max Stresses (kPa)

* Envelope = Max (DL;EQx;EQy;DL+1.0EQx+0.3EQy; DL+0.3EQx+1.0EQy)

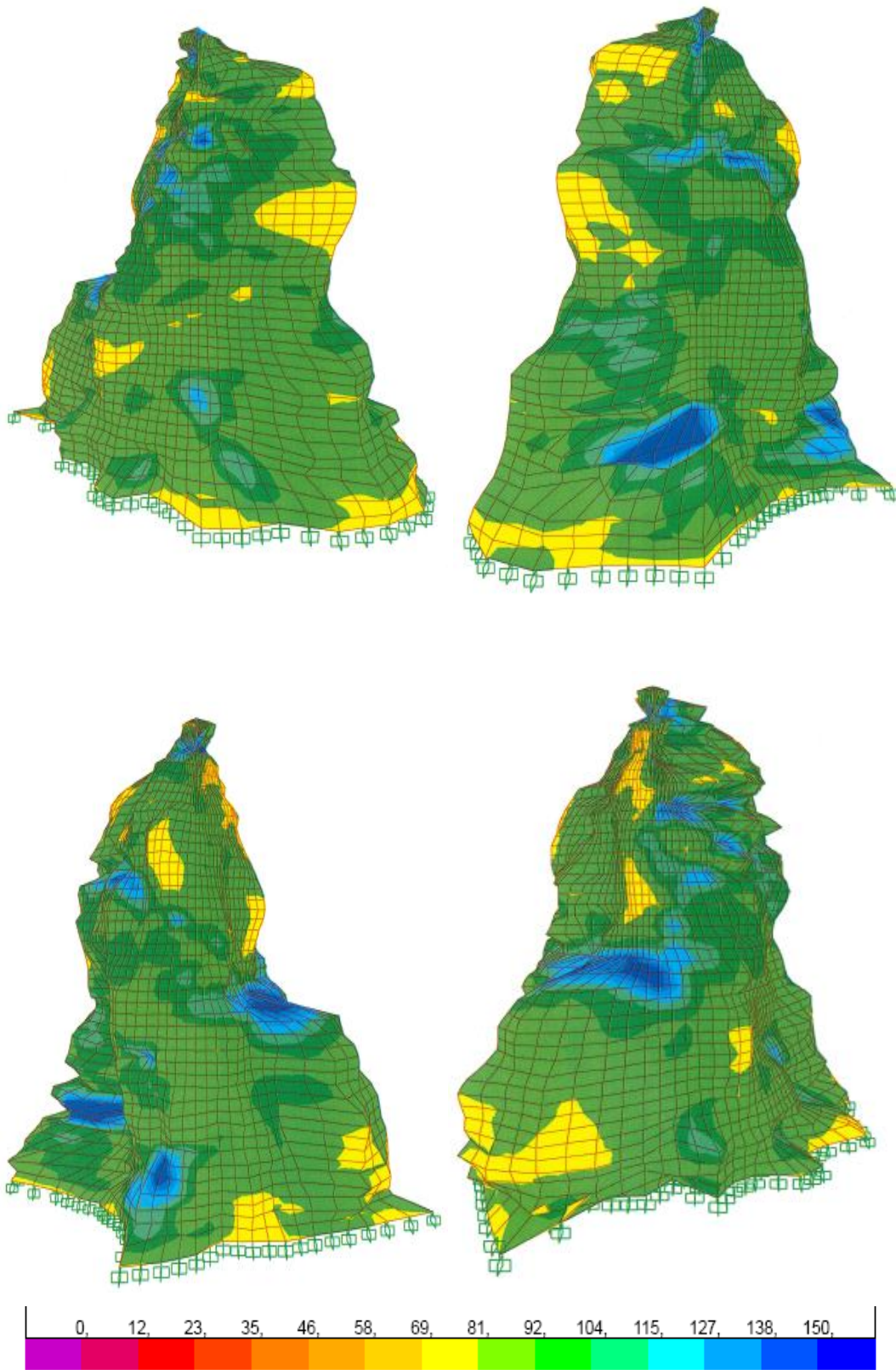


Figure 27 S12 *Envelope Max Stresses (kPa)

* Envelope = Max (DL;EQx;EQy;DL+1.0EQx+0.3EQy; DL+0.3EQx+1.0EQy)

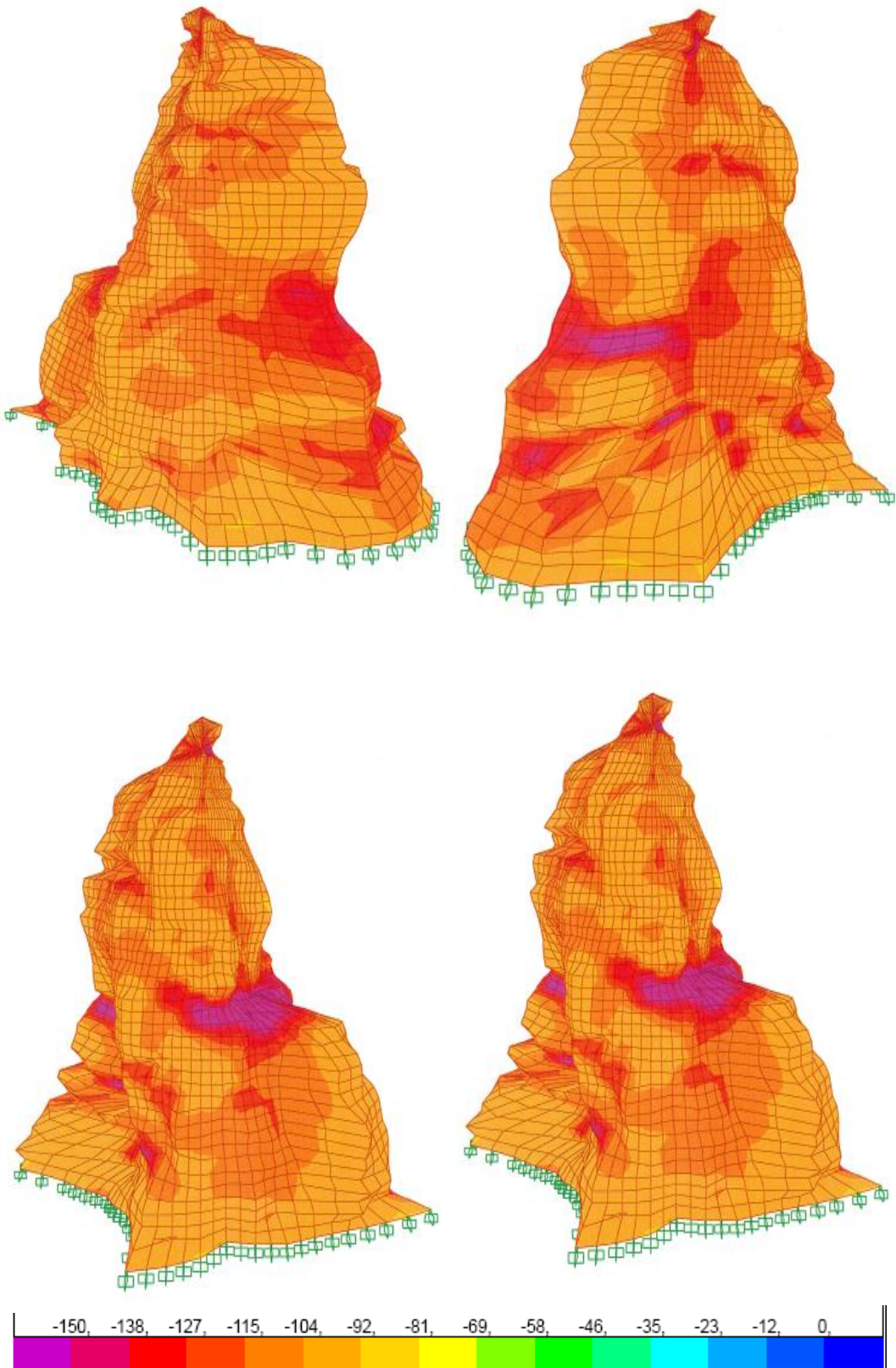


Figure 28 S12 *Envelope Min Stresses (kPa)

* Envelope = Max (DL;EQx;EQy;DL+1.0EQx+0.3EQy; DL+0.3EQx+1.0EQy)

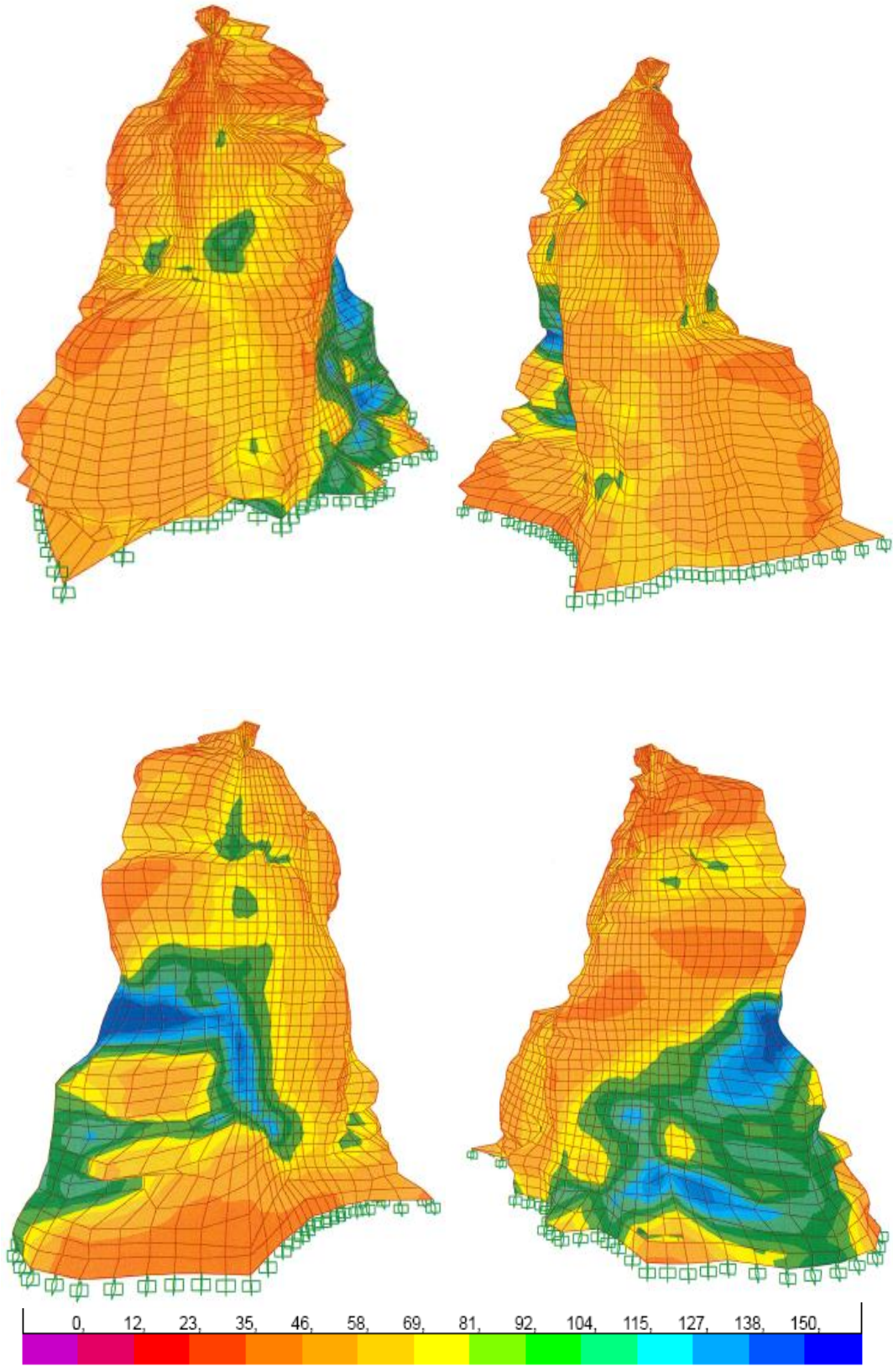


Figure 29 S13 *Envelope Max Stresses (kPa)

* Envelope = Max (DL;EQx;EQy;DL+1.0EQx+0.3EQy; DL+0.3EQx+1.0EQy)

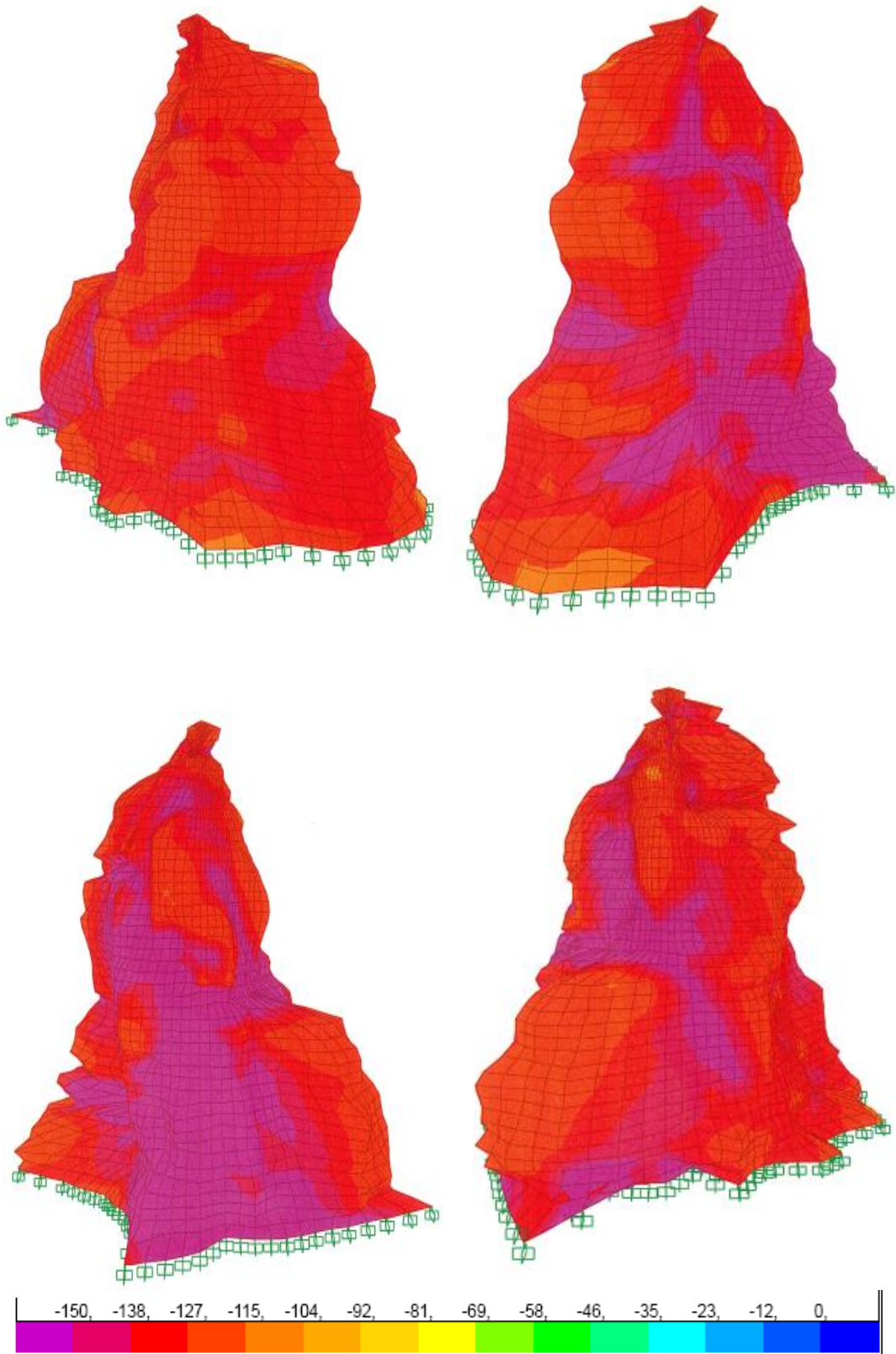


Figure 30 S13 *Envelope Min Stresses (kPa)

* Envelope = Max (DL;EQx;EQy;DL+1.0EQx+0.3EQy; DL+0.3EQx+1.0EQy)

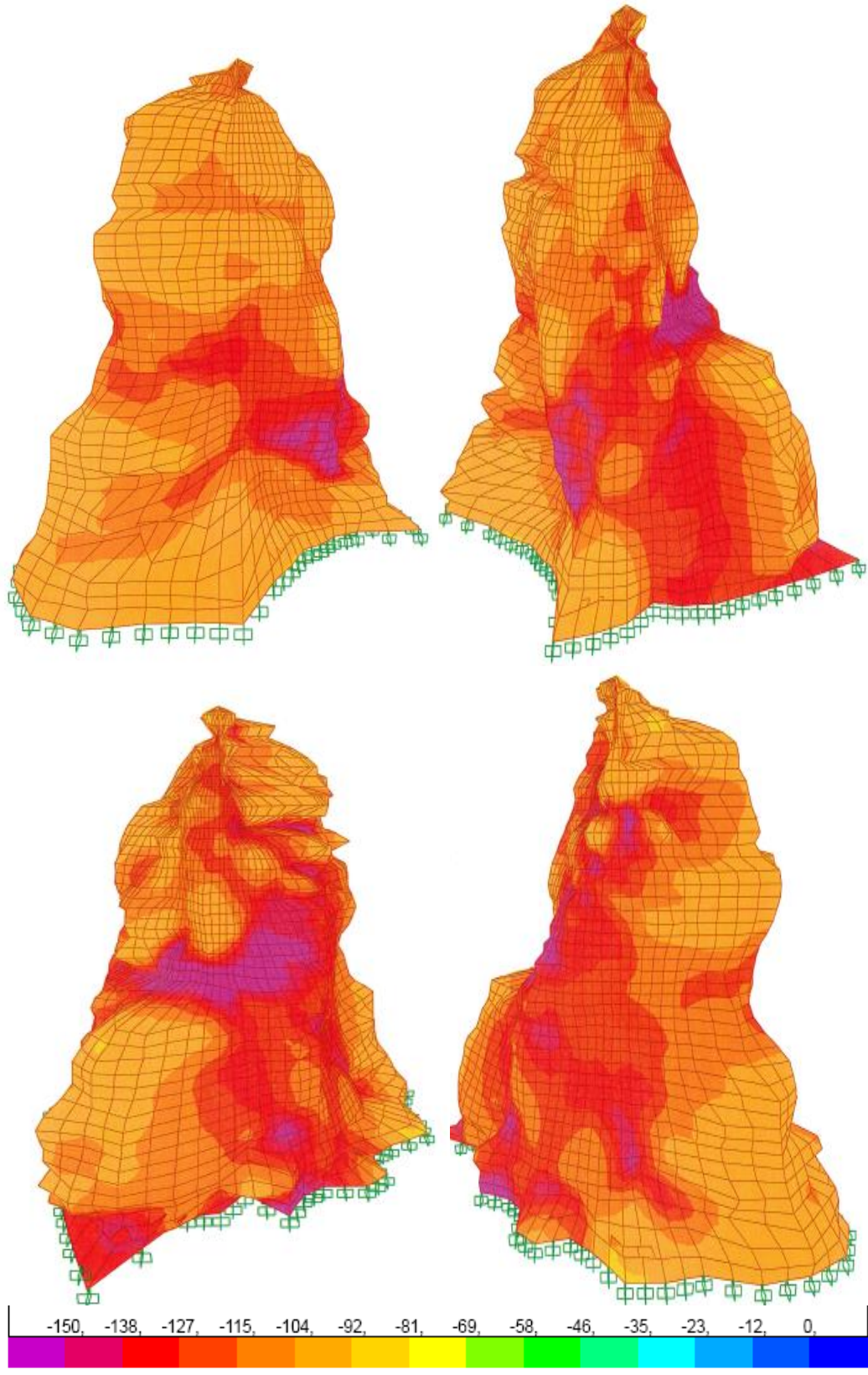


Figure 31 S23 *Envelope Min Stresses (kPa)

* Envelope = Max (DL;EQx;EQy;DL+1.0EQx+0.3EQy; DL+0.3EQx+1.0EQy)

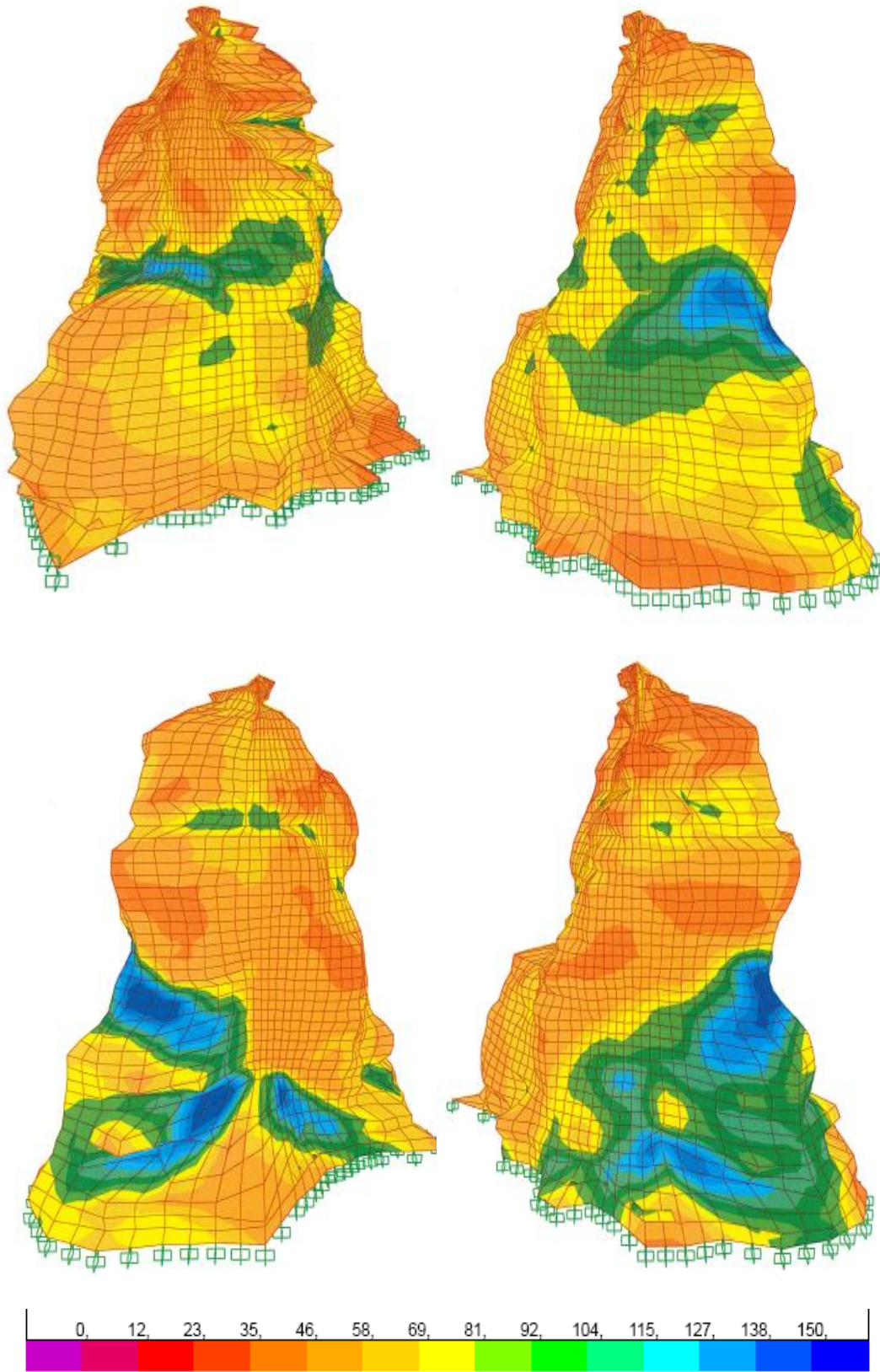


Figure 32 S23 *Envelope Max Stresses (kPa)

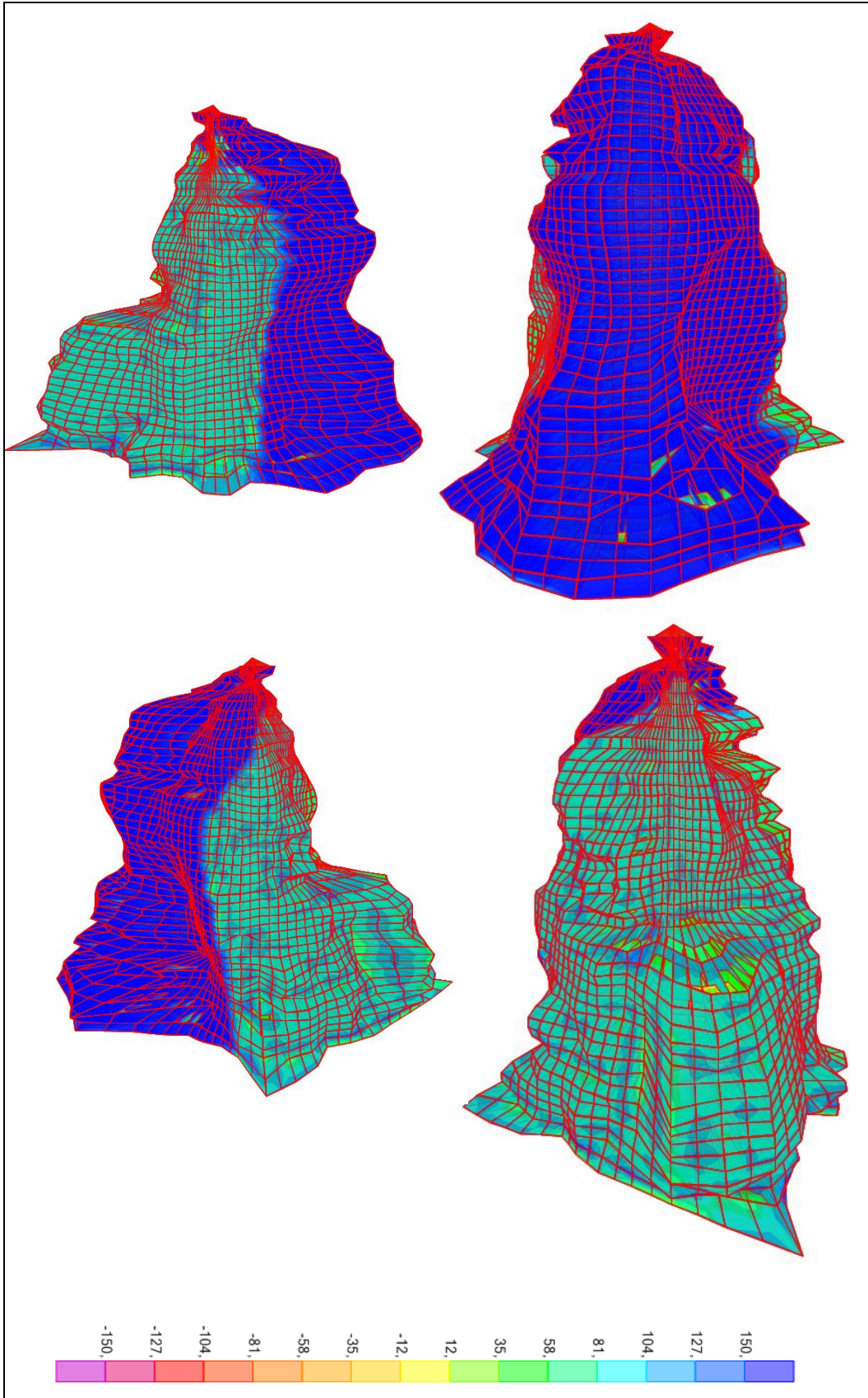


Figure 33 Von-Mises Stress Under Temperature Summer Loads

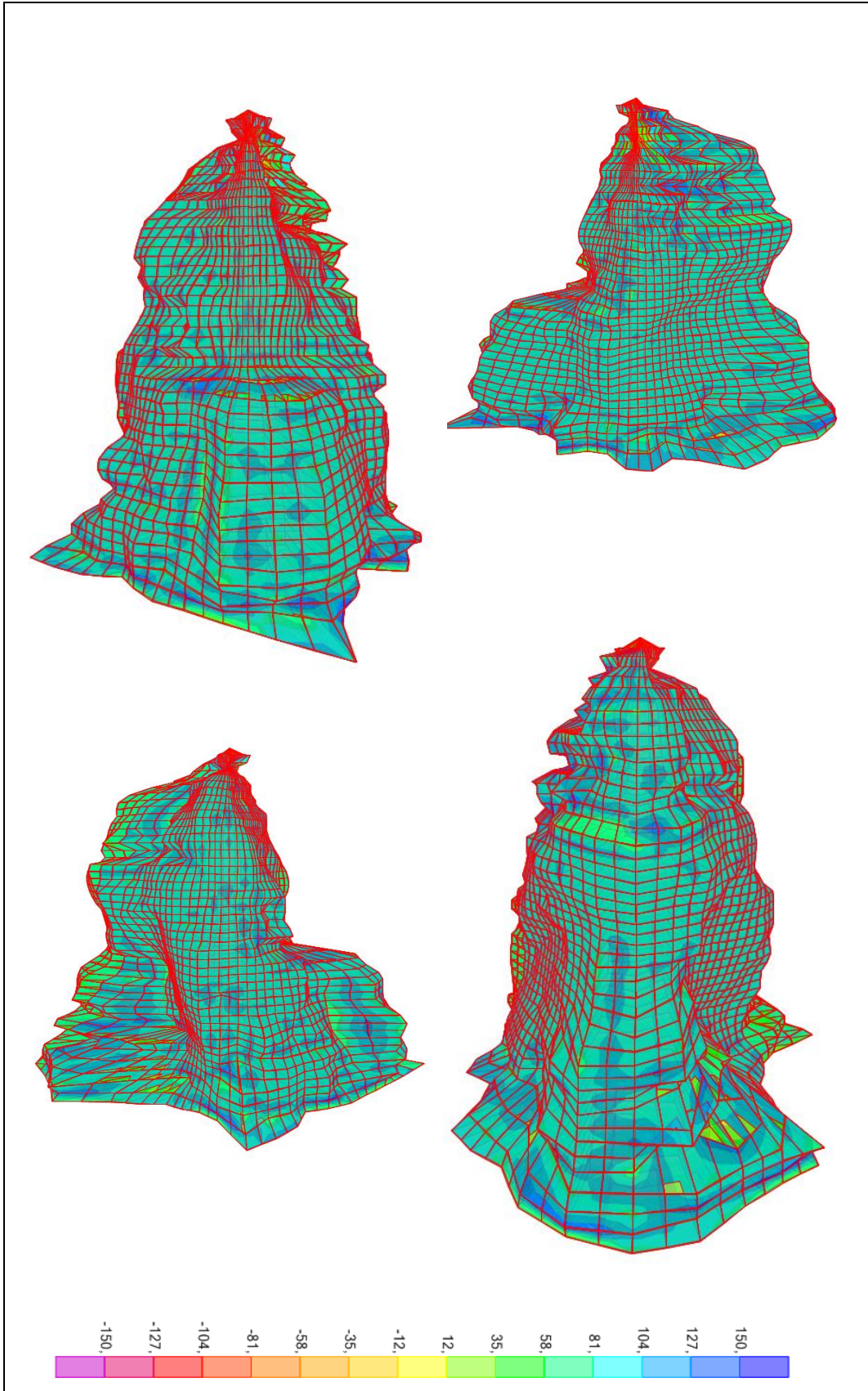


Figure 34 Von-Mises Stress Under Temperature Winter Loads

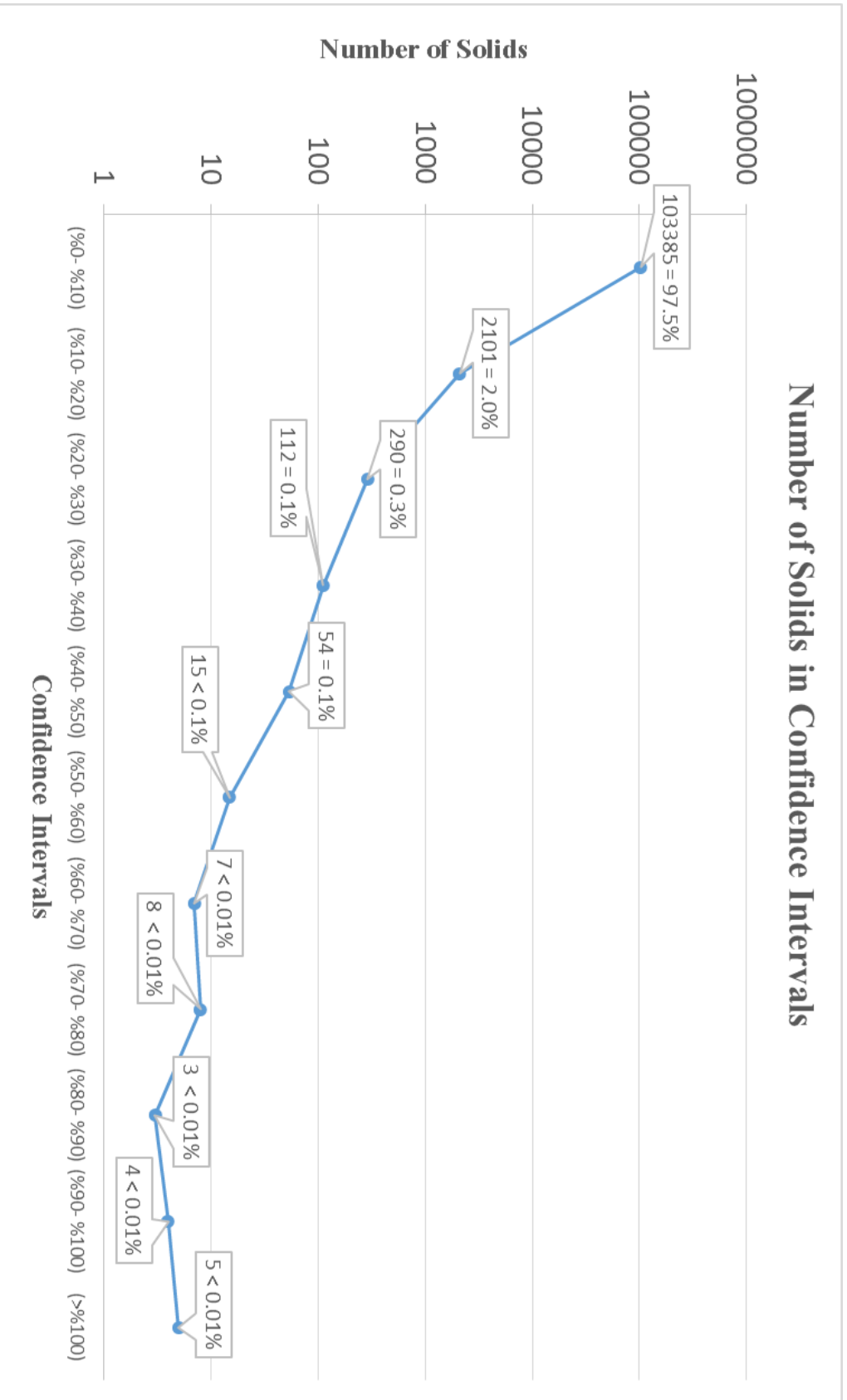


Figure 35 Number of Solids in Confidence Intervals According to Earthquake Analysis

CHAPTER 3

STRUCTURAL HEALTH MONITORING STUDIES ON THE CASTLE

3.1. Importance of Structural Health Monitoring for Historical Structures

The main reason for choosing Ortahisar Castle as a topic of study is protecting a historical structure and historical heritage. Protection of a historical structure does not only mean making analysis under several loads and determining behavior of the structure. Protection is also done by monitoring the structure and controlling structural condition of the structure for long term. Structural Health Monitoring (SHM) is subsidiary branch of structural engineering. SHM is a process of damage detection for long, short time period and, it is monitoring behavior of structures. If any damage indication was detected by SHM system, immediate measures can be taken to prevent progress of the damage to a point where the historic structure might get damaged beyond repair. The monitoring studies might also reduce the risk to public residing around or visiting the site.

There are five main reasons to monitor structures: The first reason is understanding the structures' behavior under different loads. Monitoring the current status of structural health is the second reason. The third reason is preventing any collapse by monitoring of degradations. Fourthly, learning existing structural parameters is a reason to monitor structures. Last reason is that structures with high level of importance and having important structural problems are monitored for safety. As it is mentioned at Section 1.3, there are not any structural design drawings, explained material type, and structural properties belongs to historical structures.

These types of uncertainty's increase the value of SHM for historical structures. Lima et al. (2008) mentioned that the importance of SHM is doubled up when consideration the conservation and behavior of historical heritage. Determination of damage localization for monumental historical structures can be very difficult because of extreme complexity and hyper static behavior of these structures (Damonte et al., 2007). Therefore, SHM system is installed to the Castle to monitor behavior of the Castle.

3.2. Sensor Types Used at Ortahisar Castle

Structural health monitoring system of the Castle consist of forty eight crack meters (LVDT), one accelerometer, one temperature & humidity sensor, one anemometer, one wind direction vane, one multiplexer, and one data logger.

3.2.1. Crack Meter (LVDT)

Linear Variable Differential Transformer (LVDT) is a sensor that measures change in linear motion of an object. LVDT converts mechanical motion to electrical signals to determine the linear motion. It consist of primary, secondary windings, and a core. The windings cover the core; however, there is not any connection between the windings and the core (Figure 36). When the primary winding is supplied with constant current, a magnetic region is created and position of the core is determined by created induced voltage at the secondary windings. The difference between induced voltages at the secondary windings is used to determine the change in linear motion. LPC150 is name of the model of LVDT used at the Castle. LPC150 can measure change in linear motion up to 150mm. Its linearity is $\pm 0.05\%$ and its resolution is infinite. Its working temperature is between -20°C and 80°C . Displacement speed of LPC150 is 5 m/s. It can be supplied by 28 V DC Max.



Figure 36 Inside and Outside View of LVDT

3.2.2. Accelerometer

SHM system of the Castle has one accelerometer. The accelerometer is used to find natural frequencies of the Castle. Six field tests are done to determine the natural frequencies of the Castle by using the accelerometer. Therefore, an accelerometer is used for this purpose at SHM systems. The model of the accelerometer used at the Castle is AS-5GB by Kyowa. It is a biaxial acceleration transducer. Its rated capacity is $\pm 49.03 \text{ m/s}^2$. Nonlinearity of the accelerometer is $\pm 1\%$ RO. Rated output is 0.5 mV/V . The frequency response range of AS-5GB accelerometer is DC to 100 Hz at 23°C . Sensitive accelerometers are used to measure ambient vibration for short term on-site tests, which can pick up vibrations at micro g level.

3.2.3. Anemometer

Anemometer is a structural health monitoring sensor which determines velocity of wind (Figure 37). The location of the anemometer is an important issue to get clear data about velocity of wind. At Ortahisar Castle, the anemometer is located at the top of the Castle. C3 Anemometer by Second Wind is chosen for the SHM system at the Castle. Its rated bearing pressure-velocity factor is 20. Rotor assembly moment of inertia of the anemometer is $92.2 \times 10^{-6} \text{ kg-m}^2$. Transfer Function (m/s) is $(\text{Hz} \times 0.766) + 0.324$ and its accuracy is 0.1 m/s for the range 5 m/s to 25 m/s . The anemometer at the Castle is out of order.



Figure 37 C3 Anemometer

3.2.4. Wind Direction Vane

Wind direction vane is a sensor which is only used to determine the direction of wind. A voltmeter is located in main body of the vane. The vane generates an analog voltage output whose direction is rational to the wind direction when a stable DC excitation voltage is applied to the voltmeter. Model of the wind direction vane is NRG200P (Figure 38). NRG200P can be used for wind resource assessments, meteorological studies and, environmental monitoring. Its operating temperature range is between -55°C and 60°C . Its operating humidity range starts from 0 to 100% RH and lifespan of NRG200P is 50 million revolutions.



Figure 38 NRG200P Vane

3.2.5. Temperature and Humidity Sensor

Temperature and humidity are important factors that are effecting structural conditions. Temperature and humidity sensor is used to measure temperature and humidity. The structural health monitoring system of the Castle has one temperature and humidity sensor which is located at the top of the Castle with anemometer and wind direction vane. Temperature and humidity sensor measures temperature and humidity once in an hour. The measured data is transferred to data loggers for saving. APC temperature and humidity sensor is the brand of the sensor used. Its operating temperature is between -15°C and 65°C and, its operating humidity is between 0% and 95%. These limits are suitable for the Cappadocia Region whose environmental conditions are in these limits.

3.2.6. Data logger

A data logger is a device that record the data at structural health monitoring systems. Sensors at SHM system control the condition, create the data, and send it to data loggers. Data logger can be programmable which makes data in a shape. Ortahisar Castle has two data loggers and the data loggers have been already programmed. For instance, data obtained from LVDTs shows dimensions of crack clearly.

3.3. Location of LVDTs on the Castle

LVDTs are placed on the cracks which can have a determined role to change structural condition of the Castle. The cracks are not always at easy locations to place a LVDT (Figure 39 till 41). A special team, consists of mountaineers, is used during the installation of LVDTs.

3.4. Graphical Data Obtaining From LVDTs

LVDTs measure situation of a crack at that moment which cannot be used to understand behavior of the crack without any processing. Therefore, the measurement values are processed. The first measurement value is accepted as origin and it is subtracted from other values measured after the beginning. The result gives the condition of crack from the beginning. For instance; when the first measurement data, which is measured on 25th of April 2013 at 12:30 am, is subtracted from the data measured on 14th of February 2014, the result shows the change of crack width in that time period. After the subtracted is done, the result is used to draw a graph. X-axis of the graph shows time by half-hour intervals and Y-axis shows the result of subtraction. The figures 42 to 50 show the graphs of change of crack widths.

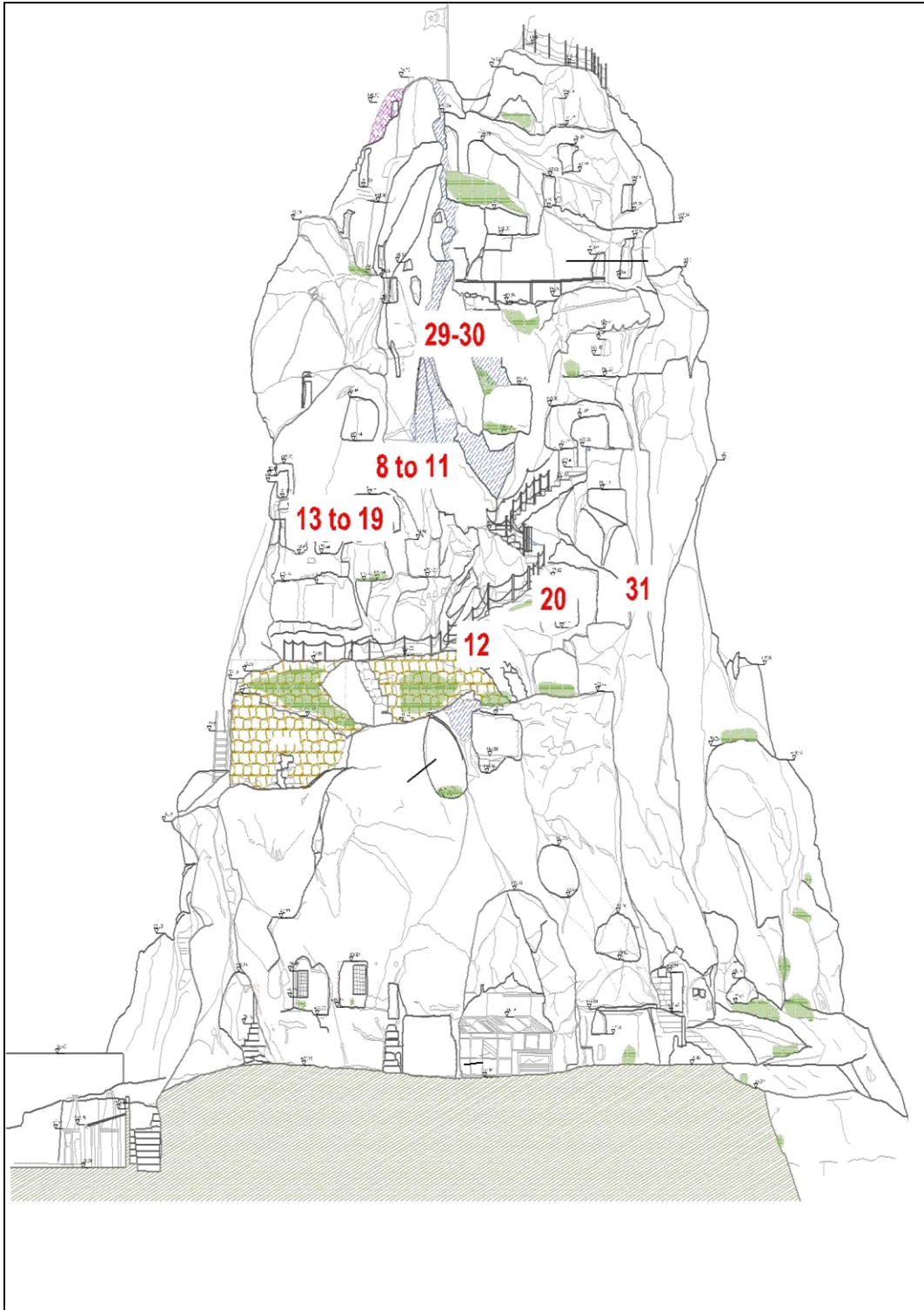


Figure 39 LVDTs Location from North of the Castle

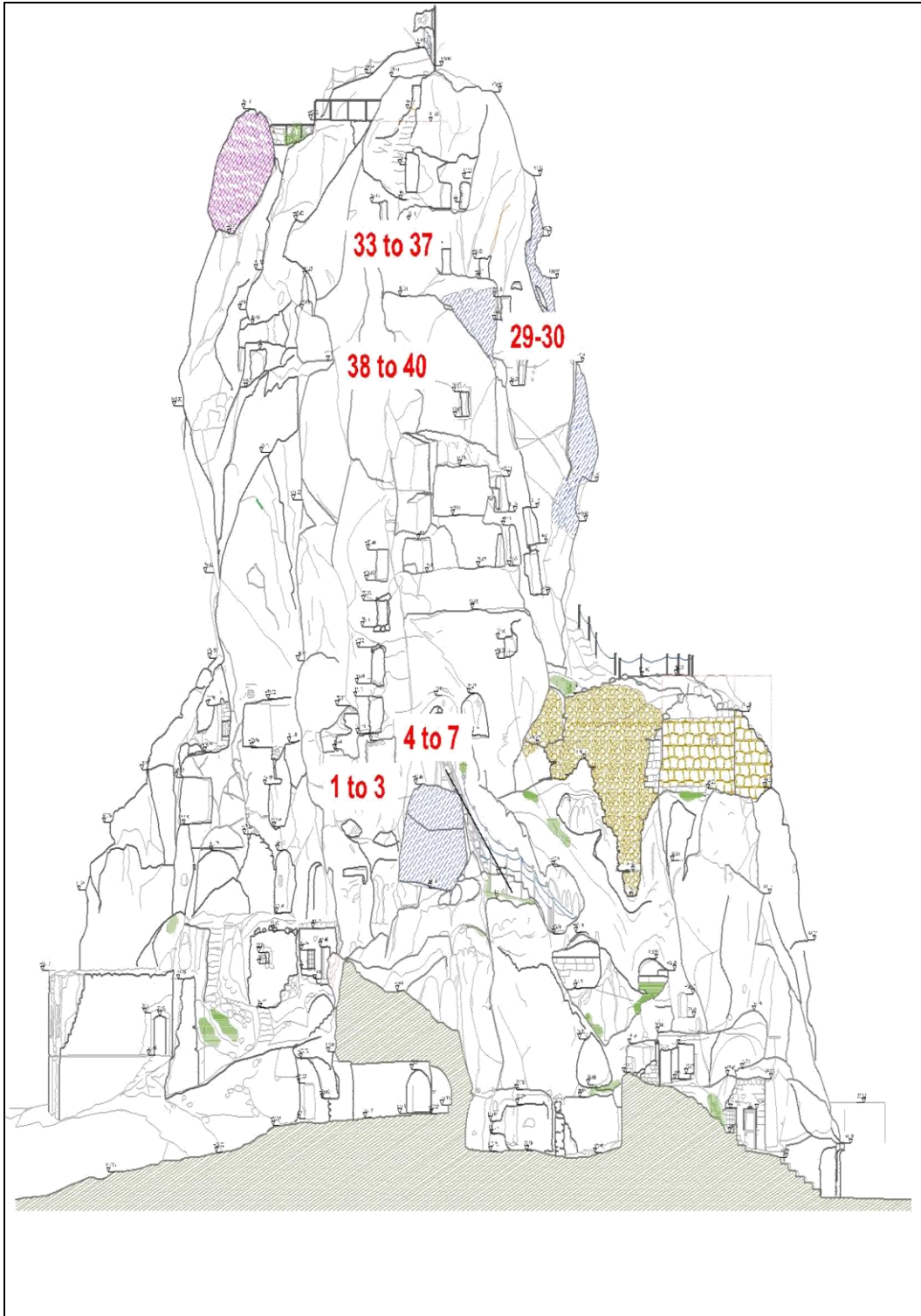


Figure 40 LVDTs Location from East of the Castle

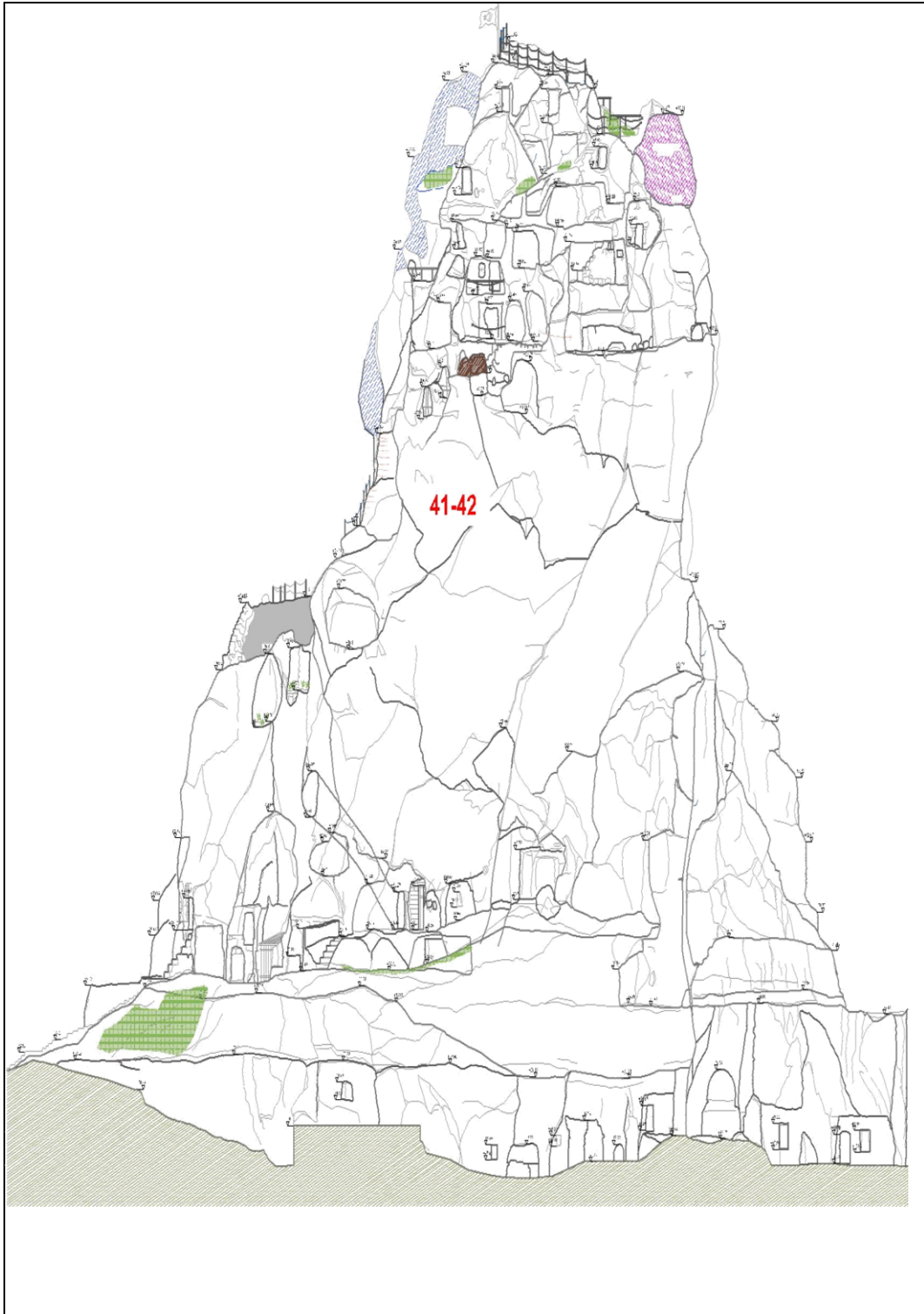


Figure 41 LVDTs Location from West of the Castle

3.5. Evaluation of Data Obtaining From LVDTs

Data obtained from LVDTs starts by 25th of April 2013 and finishes on 16th of January 2015. The LVDTs measure the crack dimensions every 30 minutes and send the measured data to the data loggers. First measurement is accepted as a starting point (origin point) and the first measured data is subtracted from other measurements, results give changes of crack widths at the provided time interval, graphs based on these change of crack widths are prepared, and evaluations are done according to the graphs.

No.1 Sensor (Figure 42) shows that the change of crack width is maximum 0.3 mm during the summer, spring, and autumn months of 2013 however on 28th of November 2013, the crack starts to enlarge 0.2 mm until 15th of December 2013 within 20 days. Since the crack width opening does not return back to its original value, it is considered to be a plastic deformation of the crack. The reason for large enlargement might be climatic change. Leaking water into the cracks would freeze in cold winter days because of low temperature and increment volume of frozen water might enlarge the crack width. After 15th of December 2013, there is not any large enlargement seen until 16th of January 2015.

The data obtained from No.2 Sensor, No.3 Sensor, No.5 Sensor, and No.31 Sensor is loud and questionable. No.10 Sensor, No.17 Sensor, and No.45 Sensor record data inaccurately. Therefore no evaluation was done for these sensors.

No.4 Sensor (Figure 42) shows that change of crack width is maximum 0.1 mm in summer, autumn, and spring. Similar to No.1 Sensor, 0.05 millimeter increment is shown in winter of 2013; however, this increment does not make plastic deformation. After winter of 2013, the crack dimensions return to normal but this return has two 0.05 millimeter increment in March of 2013 and one 0.05 millimeter increment in October of 2014. These increments thought not to cause plastic deformation. Another

0.1 mm increment is seen on 06th of January 2015, which apparently have not returned back to origin. More records for years is necessary to tell if deformations are plastic or not.

No.6 Sensor, No.8 Sensor, No.12 Sensor, and No.14 Sensor (Figures 43-44-45) show same behavior. The change of crack width is 0.1 mm again in summer, spring, and autumn. In winter of 2013 and 2014, 0.1 millimeter increment is recorded. There is one difference between two sensors which a 0.15 millimeter decreasing is shown on 10th of August 2013 at No.6 Sensor.

Recorded data by No.7 Sensor (Figure 50) is slightly noisy compared to the other sensors, which means the sensor is effected by environment while it is recording. It may be possible that the sensor is exposed to direct sunlight or cable noise problem might exist. No.7 Sensor can be accepted as a malfunctioning sensor.

The dimensions of crack, whose sensor no is 11 (Figure 44), do not show any change larger than 0.05 mm in spring, summer, and autumn months. However, 1.5 millimeter increment is detected in December of 2013. 1.5 millimeter increment ends up 1 millimeter plastic deformation which can damage the Castle in future. Moreover, 1 millimeter increment is recorded in January of 2015 again. Therefore, this crack is important and should be carefully monitored.

The obtained data from No.13 Sensor and No.18 Sensor (Figures 45 and 47) do not show any increment up to 0.10 millimeter. The change of crack width is in between -0.05 mm and 0.05 mm except from summer 2014. In summer 2014, 0.10 millimeter decreasing is recorded however this change does not result with plastic deformation which makes the change stable.

No.15 Sensor and No.16 Sensor (Figure 46) behave the same in summer, autumn, and spring months. The change of crack width belongs to that months is in between -0.1 mm and 0.1 mm. The difference between two sensors are occurred in winter months. The changes of crack width reading from No.15 Sensor is maximum 0.3 mm in winters and they are elastic deformation. However, the changes of crack width belongs to No.16 Sensor reach to 0.4 mm in winters and a permanent plastic deformation of about 0.1mm is observed between summers of 2013 and 2014.

No.19 Sensor (Figure 47) shows that the change of crack width is in between 0 mm and 0.15 mm. In winter of 2013, the change of crack width reaches the maximum value which is 0.2 mm; however, it comes back to its original values, similar to the case in in January 2015. There are no plastic deformations that can be detected.

The shapes of graphs obtaining from No.20 Sensor and No.30 Sensor (Figures 48 and 49) are similar to a sinus function. The crack widths belonging to that sensors increase in winter months and the crack width at No.20 Sensor reaches up to 0.35 mm. Similarly, the crack width at No.30 sensor reaches up to 0.50 mm in winter of 2013. On the other hand, the crack widths are decreasing in summer months up to -0.10 mm at No.30 Sensor and -0.20 mm at No.20 Sensor but these changes do not create any plastic deformations.

No.29 Sensor (Figure 48) shows that the crack width increases in winter months and decreasing in summer months. However, in summer of 2014, the crack width decreases until -0.30 mm. 0.30 mm decreasing is the highest value that all sensors record and this decreasing generates -0.1 mm plastic deformation comparing summers of 2013 and 2014.

The data obtaining from No.32 Sensor (Figure 49) is different from other sensors. The change of crack width is constant between 0.00 mm and 0.06 mm from

April, 2013 to November, 2014 and looks very noisy. On 16th of November 2014, the crack width suddenly decreases 0.10 mm. The reason for this decrease is not known but this type of changes can cause permanent damage. When cracks change very abruptly and stay in this way may also be indication of birds or other animals touching the sensors. The change of channel 32 follows the same pattern it had before the abrupt jump in November 2014.

According to readings belong to No.44 Sensor (Figure 50), the crack width changes between 0.15 mm and -0.25 mm. The crack width increases in winter months and decreases in summer months. Plastic deformation is not seen at this crack.

Sensors with numbers 9, 21, 22, 23, 24, 25, 26, 27, 28, 33, 34, 35, 36, 37, 38, 39, 40, 41, 42, 43, 46, 47, and 48 have problems. The connection between these sensors and data logger is probably missing or damaged; therefore, the data obtaining from these sensors is empty.

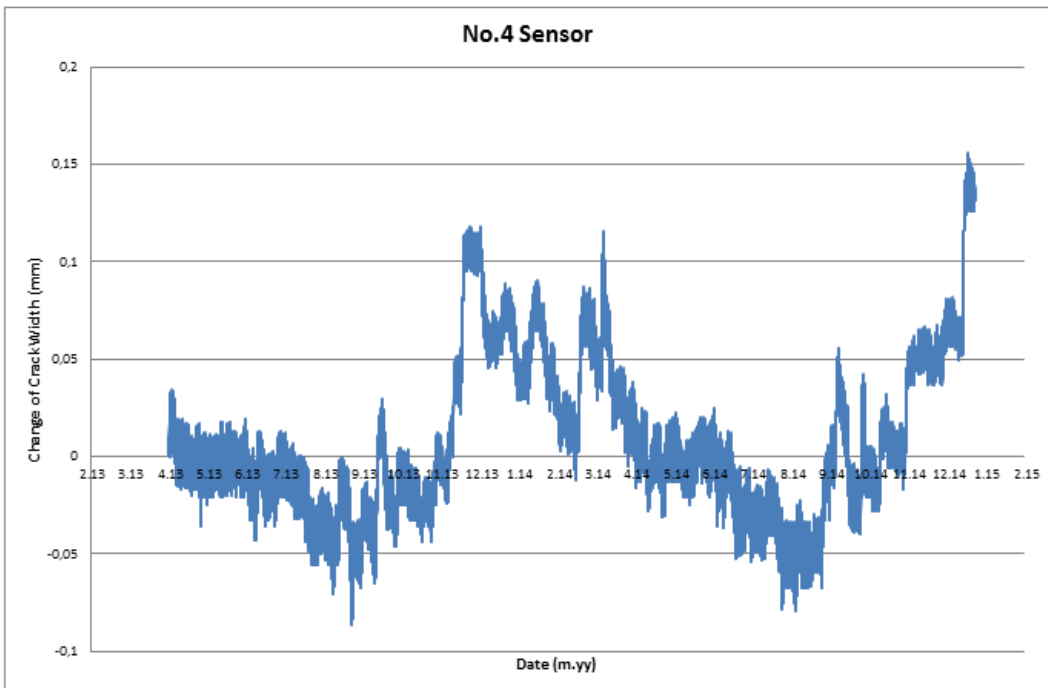
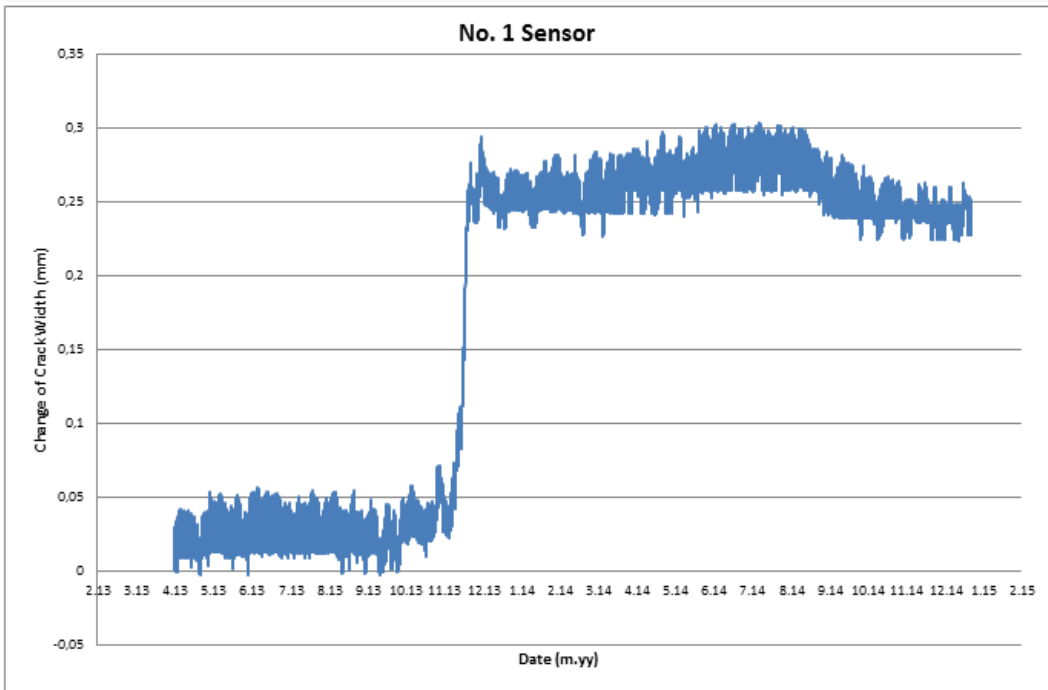


Figure 42 Sensors No.1 No.4 Change of Crack Width

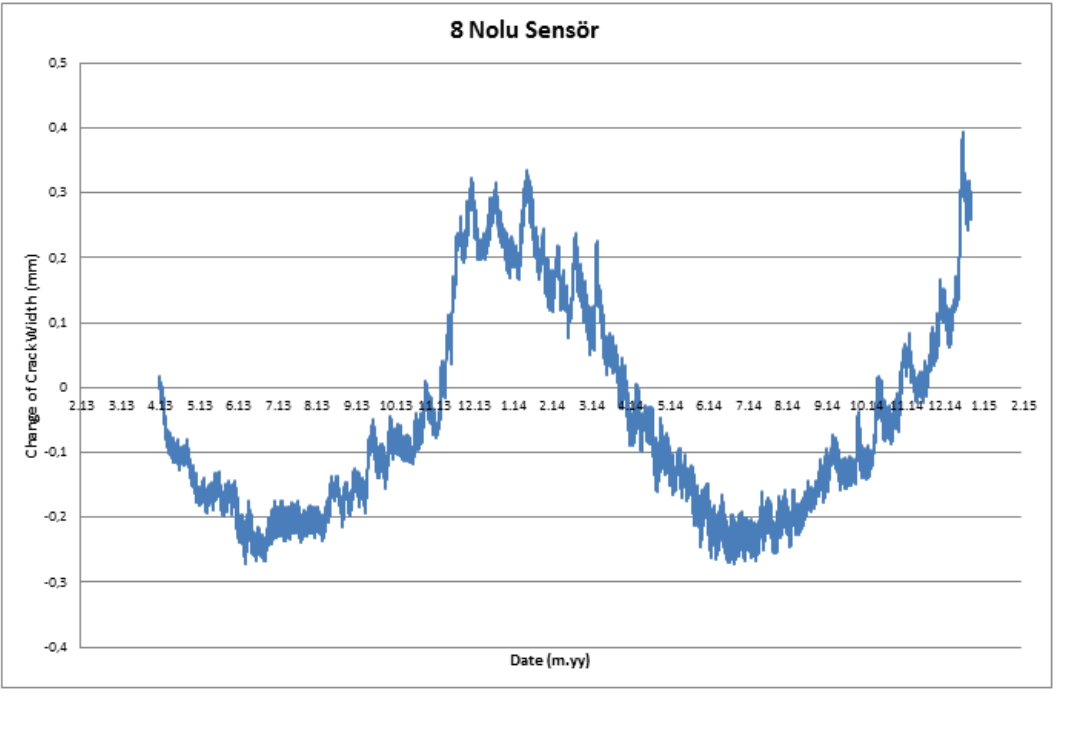
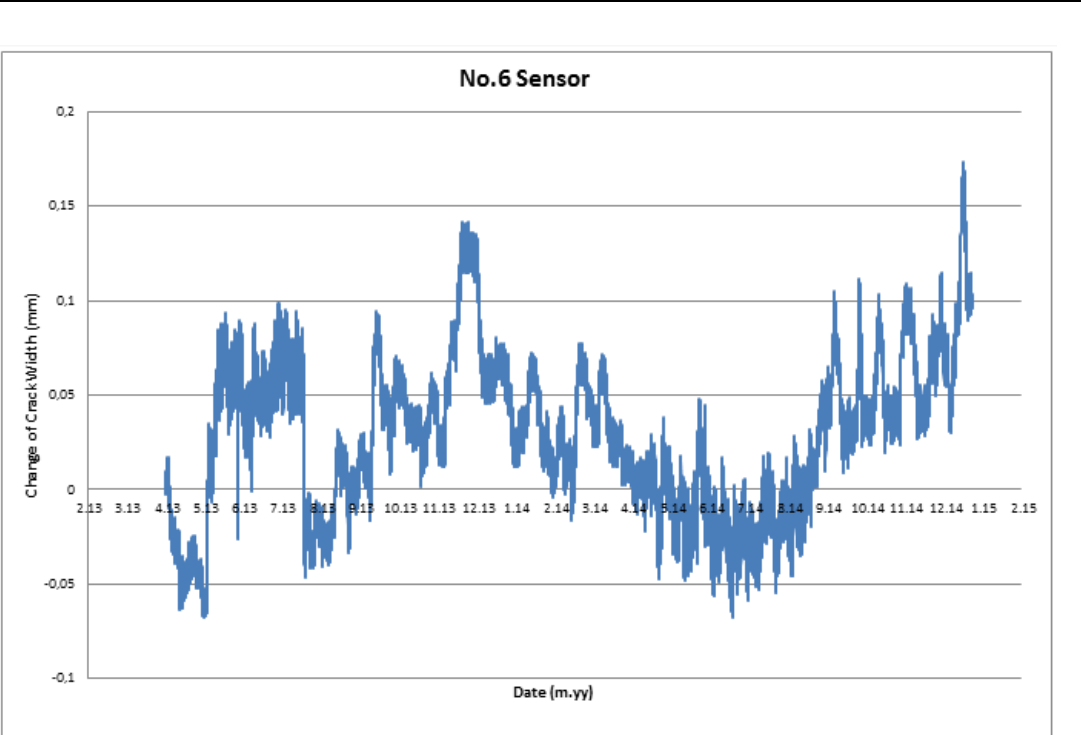


Figure 43 Sensors No.6 No.8 Change of Crack Width

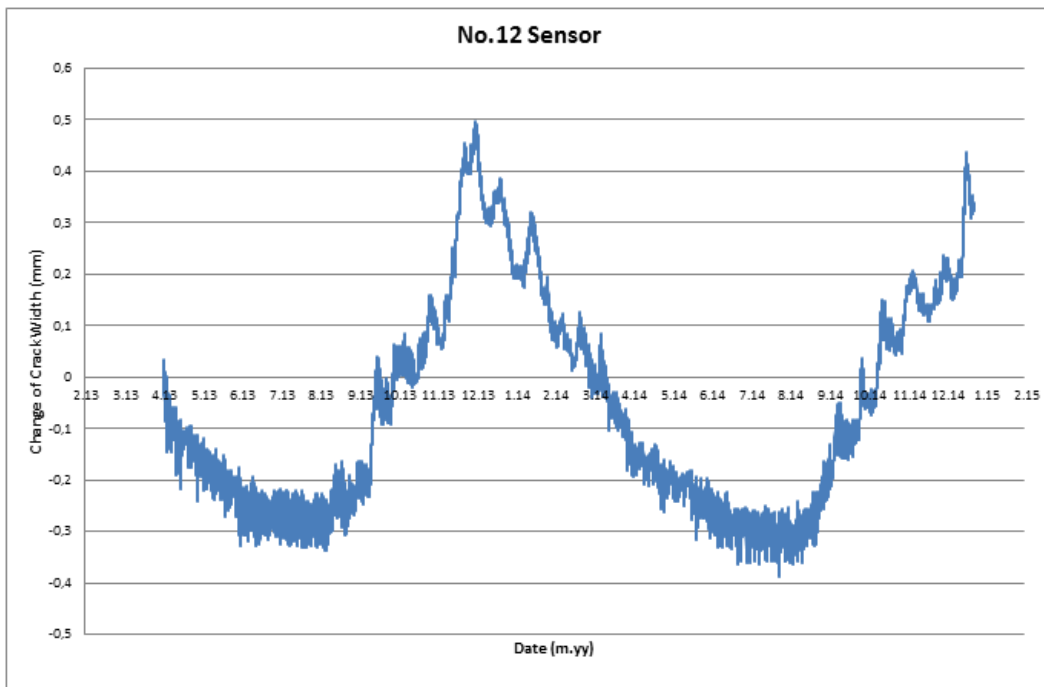
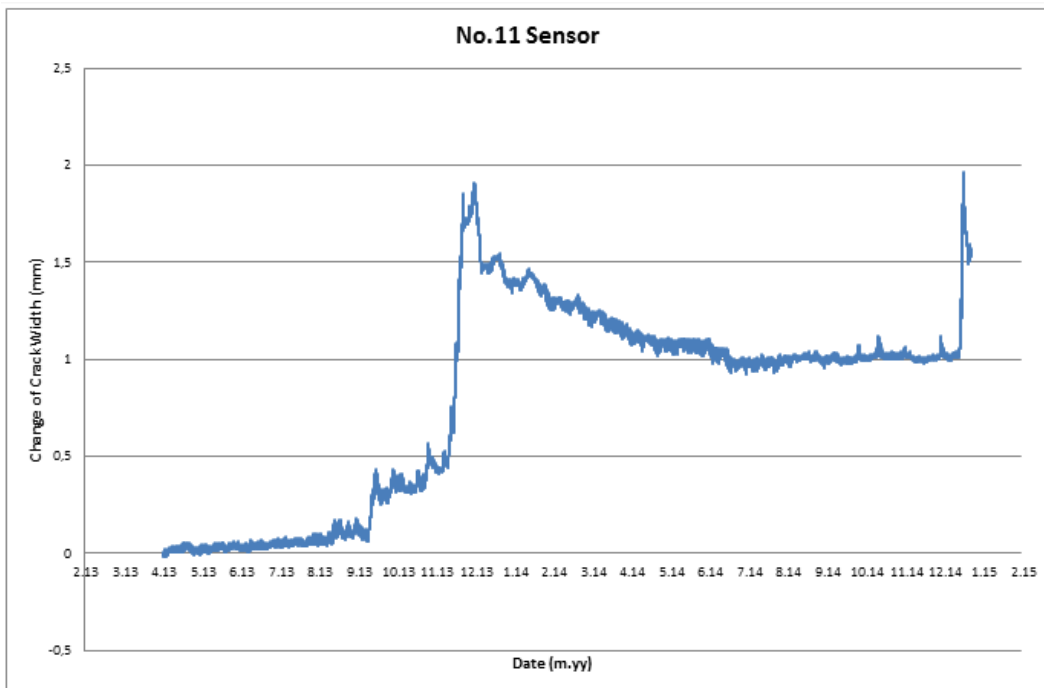


Figure 44 Sensors No.11 No.12 Change of Crack Width

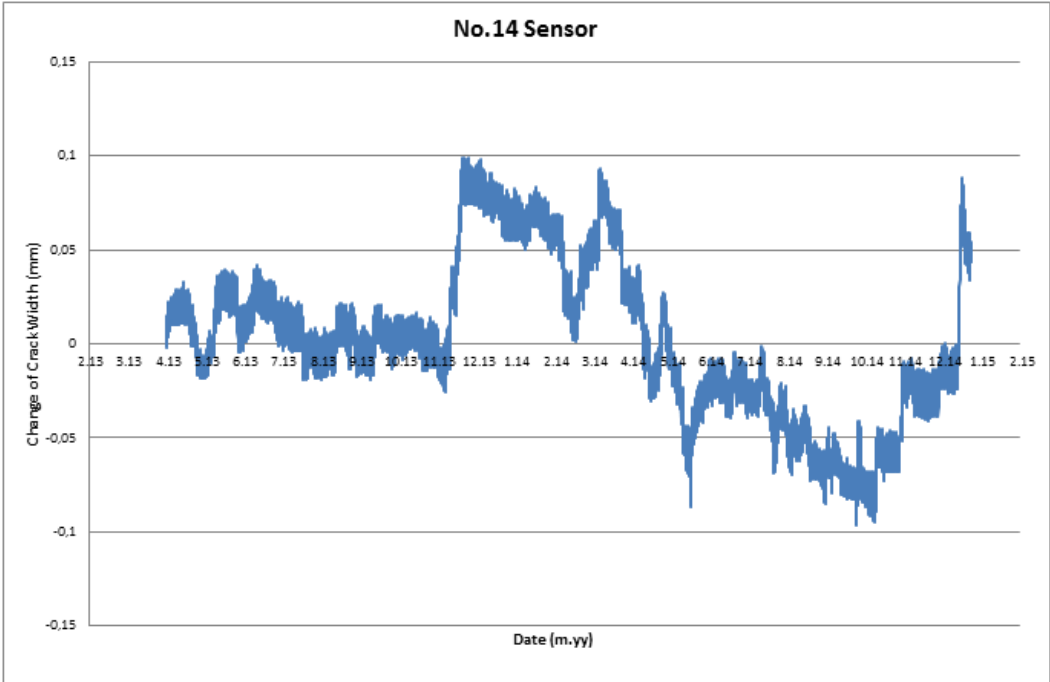
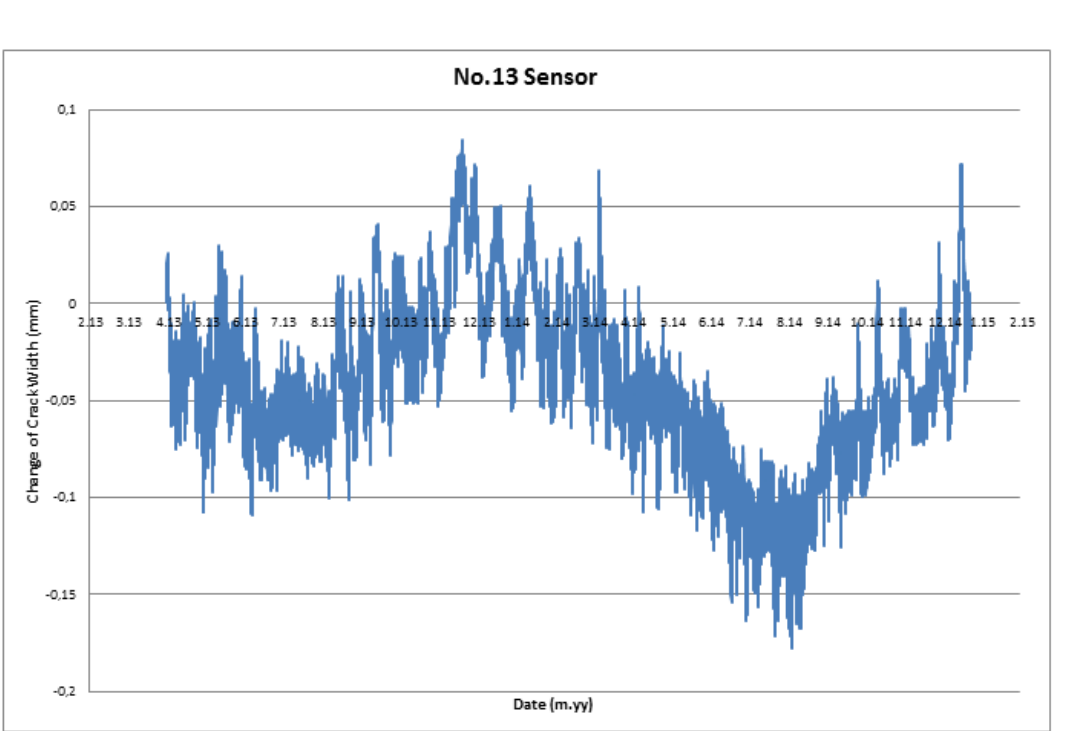


Figure 45 Sensors No.13 No.14 Change of Crack Width

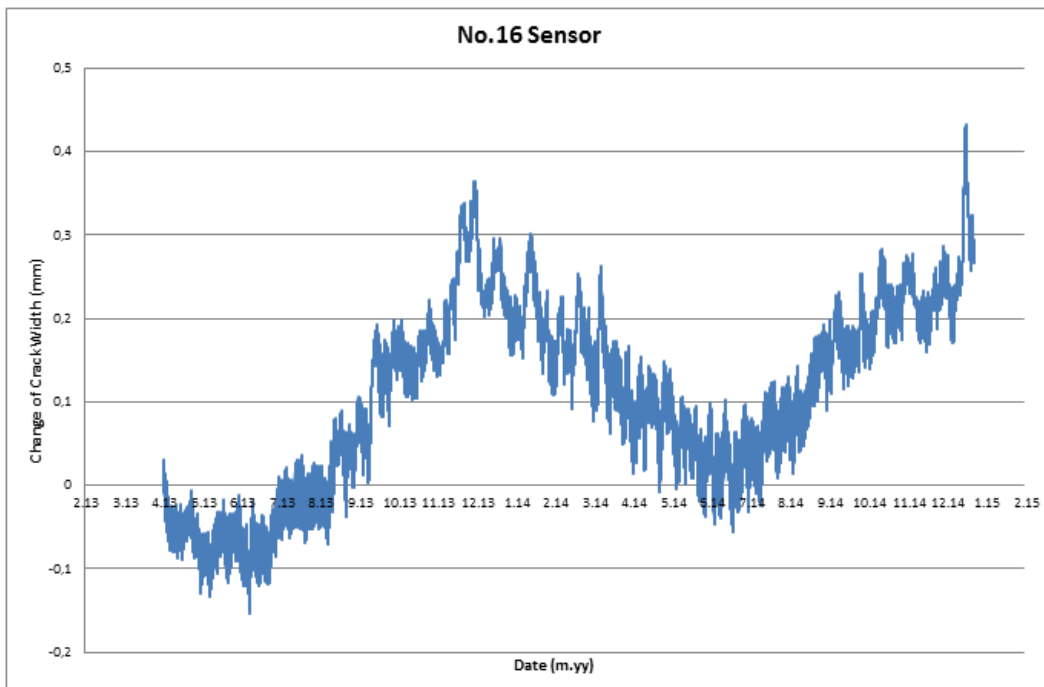
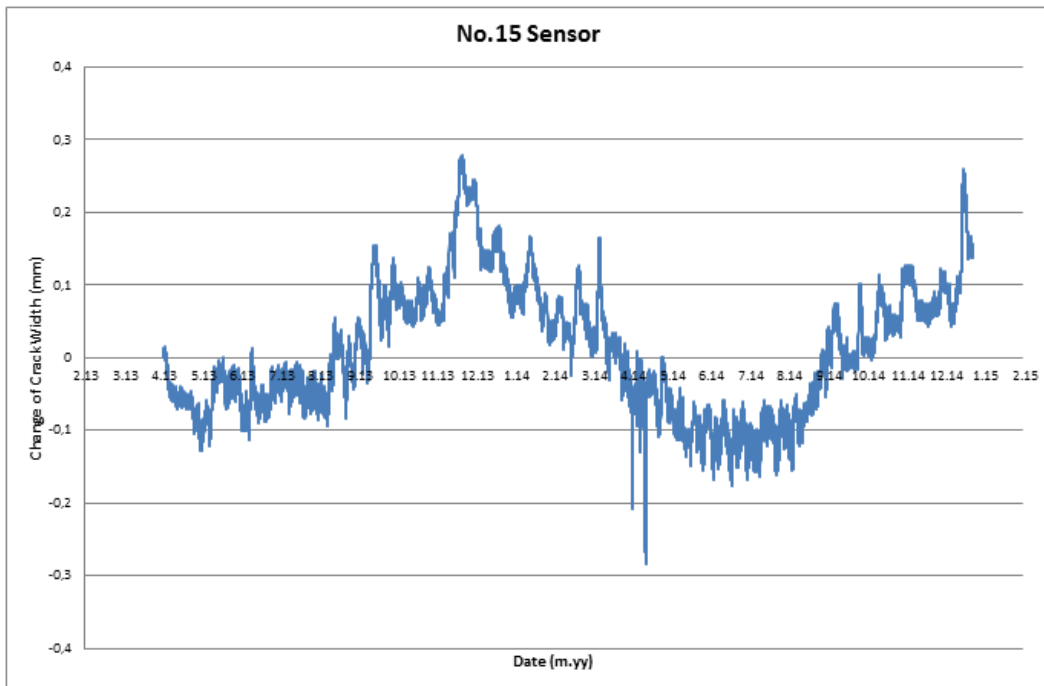


Figure 46 Sensors No.15 No.16 Change of Crack Width

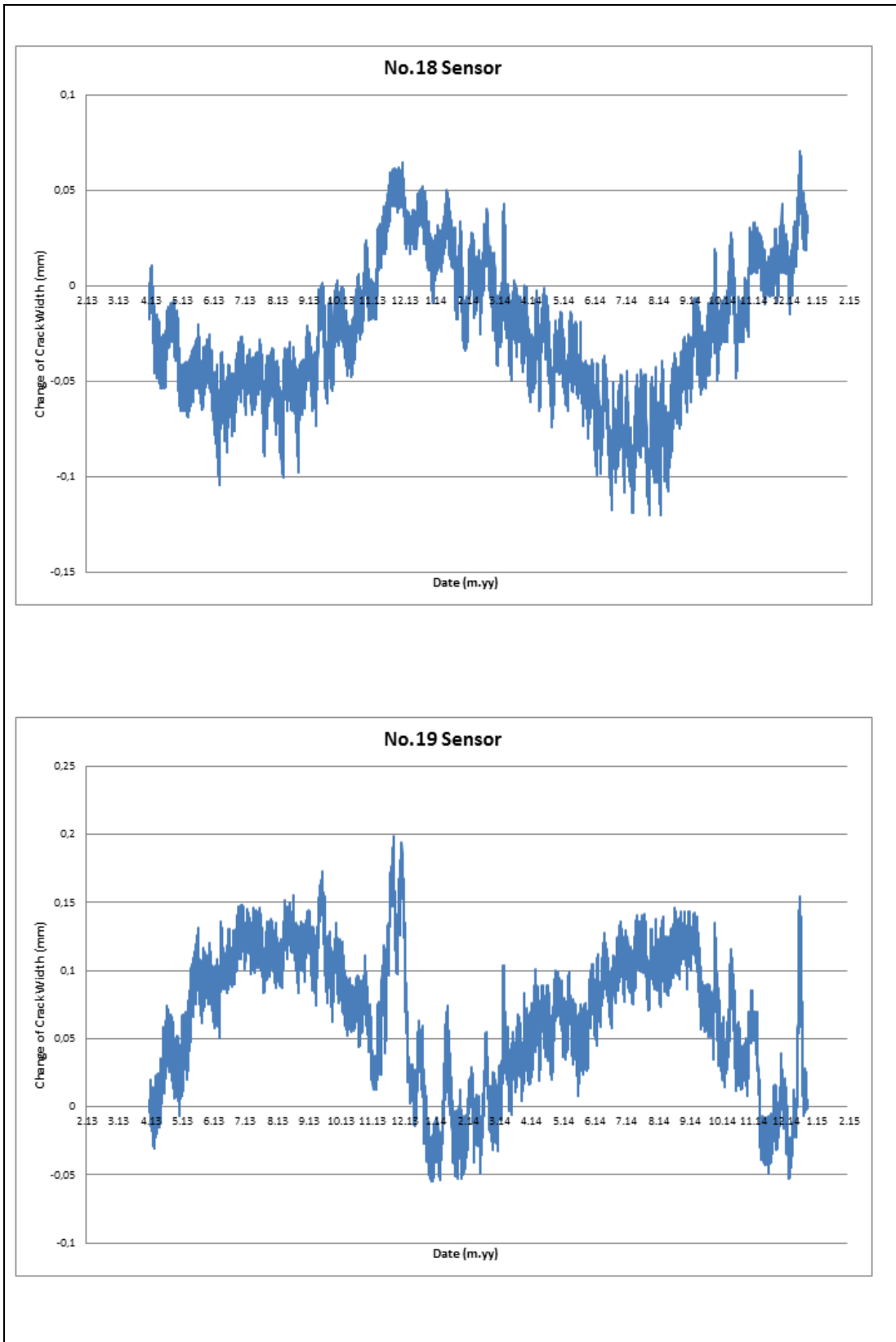


Figure 47 Sensors No.18 No.19 Change of Crack Width

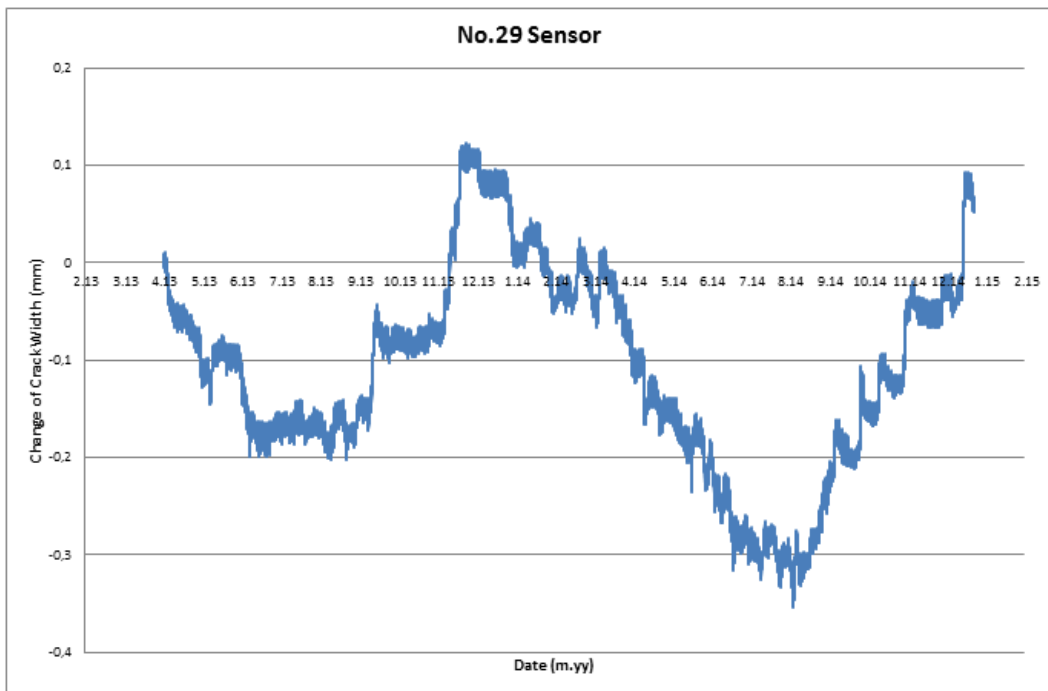
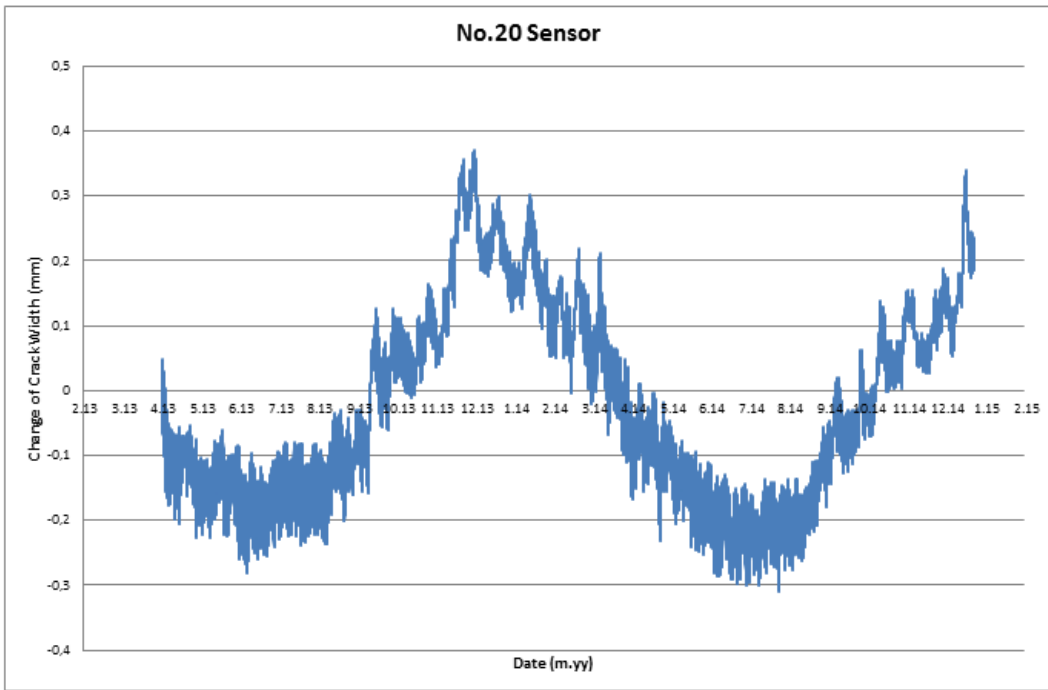


Figure 48 Sensors No.20 No.29 Change of Crack Width

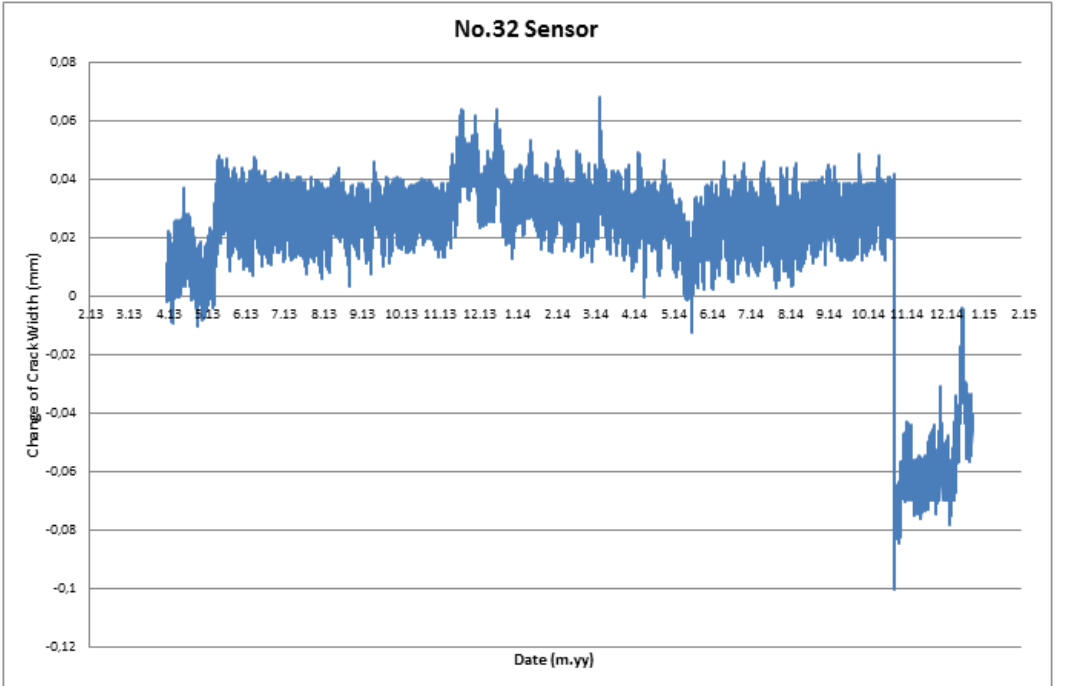
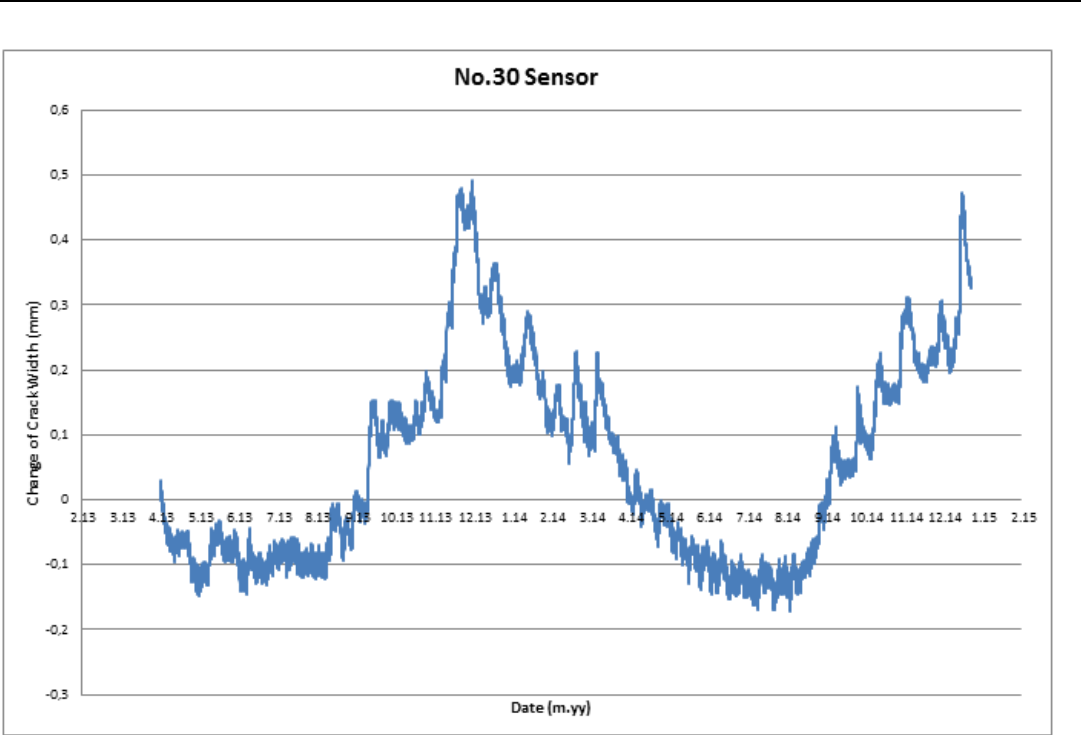


Figure 49 Sensors No.30 No.32 Change of Crack Width

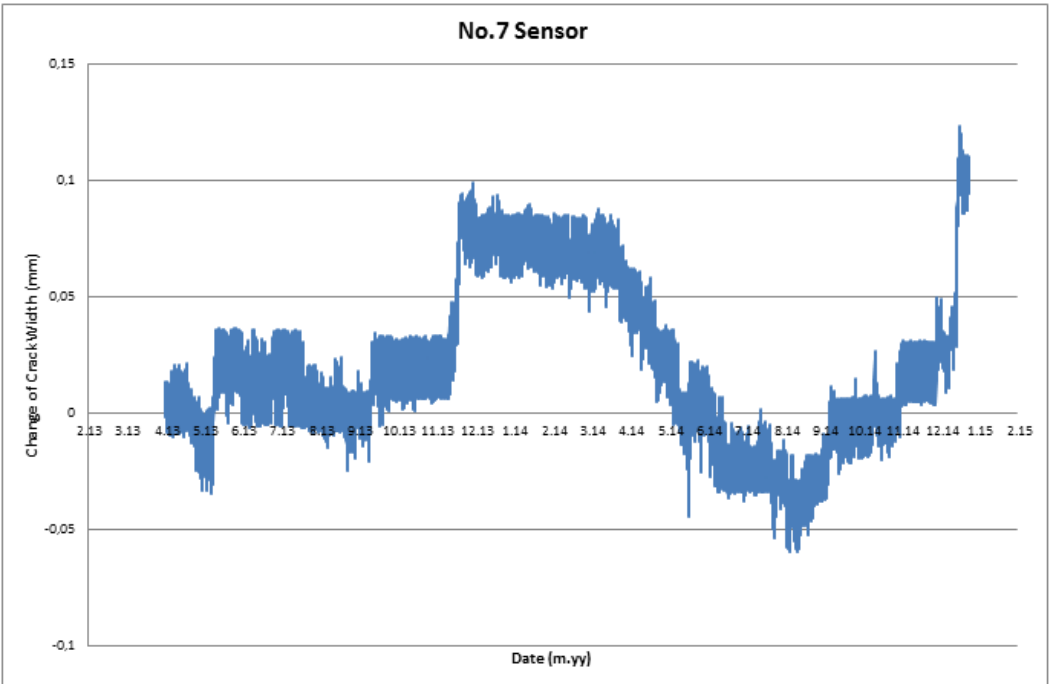
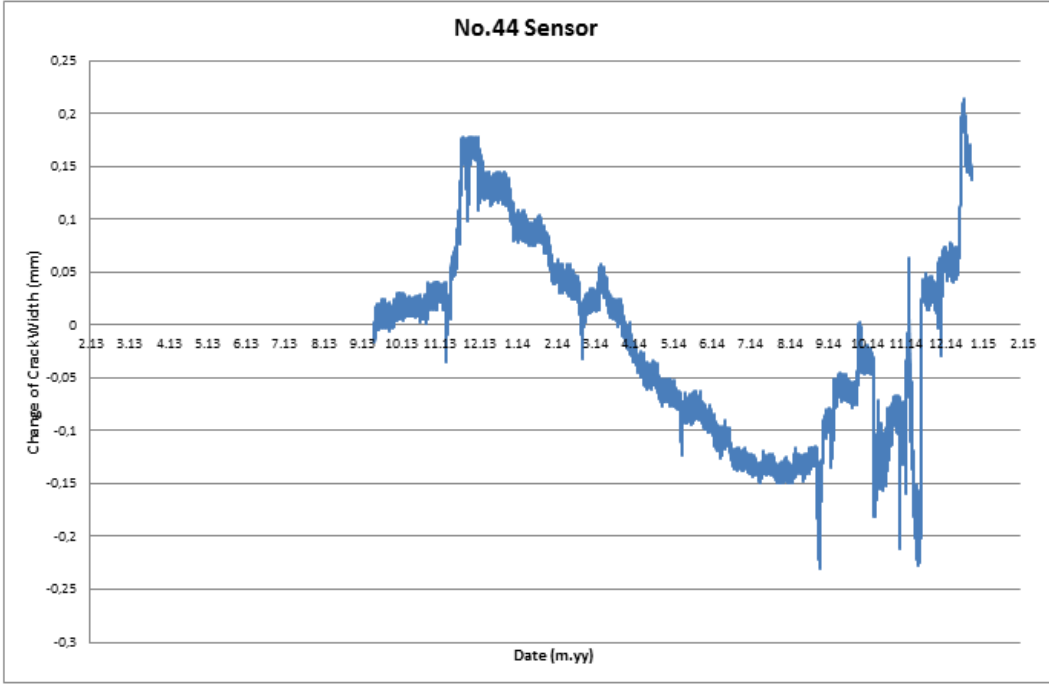


Figure 50 Sensors No.7 No.44 Change of Crack Width

CHAPTER 4

CONCLUSION

This thesis mainly consists of two main topics: The first topic is three dimensional (3D) Finite Element Modelling (FEM) of the Castle, for the purpose of structural evaluation against earthquakes, wind, and temperature forces. The second topic is the evaluation of a large sensor structural health monitoring network collected data for 48 crack meters, one accelerometer, one temperature & humidity sensor, one anemometer and one wind direction vane. For the first part of the thesis, 3D FEM of the Castle was generated by using 3D laser scanning data for dimensions of the Castle, field test results for material properties of the Castle were used, and dynamic test results to utilized to calibrate the FEM. Earthquake loads and wind loads were applied to the Castle with 183 different load combinations, which differ from each other by the applied force direction angle to the Castle. This was achieved by applying earthquake and wind loads to the Castle at every 10° angle increments. The result of the analyses were post-processed to find principal axes stresses and checked according to the Coulomb-Mohr and Modified-Mohr Theories. For the second part of the thesis, the data obtained from the sensors on the Castle were evaluated. The evaluation was mainly plotting data on time vs amplitude graphs for 48 LVDTs, which have measured the crack widths on the Castle at critical locations.

The results of the first part shows that the FEM with fixed supports have only 5 solid members out of 105984 members have slightly exceeded the principal tension capacity of the material. These members that fail at the most critical earthquake loading direction combination are located at the very top of the Castle and may cause

some stones to fall down but would not create a substantial damage to the overall integrity of the Castle since 5 out of 105984 corresponds to only 0.005% of the Castle. This is a very small percentage and the Castle can be accepted castle against earthquake. Majority of the members forming the Castle have relatively low stresses developing on them during worst possible loading scenario; 97.5% of all members have stresses smaller than 10% of their material capacity (Figure 35). Furthermore, the FE model with vertical springs at the base to model flexibility of the underlying ground has yielded no members exceeding their material capacity. Therefore, the members of the FEM forming the Castle has stresses smaller than the considered material ultimate capacity. A factor of safety (FS) evaluation is difficult to make although 97.5% of all members have less than 10% of their strength limit. Most of the members that have higher stress concentrations are located at the top of the Castle, which is in part due to the irregular shape of the members with high aspect ratios. The analytical model was also used to analyze stresses under wind loading since the height of the Castle is about 60 meters which might generate large wind loads. However, wind loading generates even smaller stresses for wind load when compared with earthquake load acting on the Castle. The results of stresses generated by temperature change during summer and winter are also considered in this study. Most of the members had stresses within limits for temperature loading made by hand calculation, small FEM, and large Castle model. Only one solid member which is located at the top of the Castle and has irregular shape has passed material tensile capacity. FEM with high mesh density has better results compared with the hand calculation but not possible to model in the Castle scale due to computer limitations. The cracks forming at the outer surface of the castle could not be linked to EQ or temperature related loads; the wind load is also irrelevant. Therefore, the crack formation can be linked to weathering effects of wetting and drying cycles, freeze and thaw cycles, and preexisting cracks in tuff material during its geological formation phase. Monitoring of crack widths over long periods would reveal more information about how they progress and what are the parameters that effect their width growth.

As it was mentioned at Chapter 1, the outer surface of the Castle has cracks, which were being monitored by use of limited number of LVDTs. LVDTs measure

the crack width changes with high precision (0.01mm) at every 30 minutes. The thesis evaluated the collected data measured between 23rd of April 2013 and 16th of January 2015, which is about 1 year and 9 months. The evaluation showed that most of the LVDTs have malfunctioned (17 working out of 48); however, the working LVDTs showed important results. The crack width changes should be monitored for the remaining life of the Castle since seasonal environmental effect play an important role on the crack width and safety of the visitors may be improved by monitoring and alarm systems. If cracks are monitored over shorter periods (such as months), seasonal changes may be misinterpreted as structural changes.

The cracks open and close on seasonal and daily cycles because of temperature changes. The cracks may also be filled by dust and small sand particles making it difficult to close and generates additional stresses. This may be another mechanism for the crack widths to increase over time. The meteorological changes also have other effects on crack width changes such as freezing and thawing, which might permanently change the crack width. The deformations that return to their original values are considered as “elastic deformation” while permanent deformations that does not return to their original values are considered as “plastic deformations”. For example, cracks of LVDT-01 (Figure 42a) and LVDT-11 (Figure 44a) show permanent plastic deformations. The malfunctioning LVDTs should be repaired or replaced, the monitoring system should be maintained and monitored continuously to detect growing cracks in time and to take timely precautions to protect the Ortahisar Castle as a valuable cultural heritage structure as well as ensure safety of visitors and local people around the castle from rock falls and similar disasters.

REFERENCES

- Akan, A. E., Özen, Ö., 2005. Bursa Yeşil Türbe'nin Sonlu Elemanlar Yöntemi ile Deprem Analizi. Deprem Sempozyumu. Kocaeli, pp. 758-762.
- AUTOCAD, 2013. AutoCAD Version 2013, Autodesk Inc.
- Aydan, Ö., Ulusay, R., 2003. Geotechnical and Geoenvironmental Characteristics of Man-made Underground Structures in Cappadocia, Turkey. Engineering Geology, 69(3), pp. 245-272.
- Bowles, J. E., 1997. "Foundation Analysis and Design", 5th Edition, Mc Graw Hill, Print.
- Chellini, G., Nardini, L., Pucci, B., Salvatore, W., & Tognaccini, R., 2014. Evaluation of Seismic Vulnerability of Santa Maria del Mar in Barcelona by an Integrated Approach Based on Terrestrial Laser Scanner and Finite Element Modeling. International Journal of Architectural Heritage, 8(6), pp. 795-819.
- Damonte, G., Podestà, S., Riotto, G., Lagomarsino, S., Magonette, G., & Marazzi, F., 2007, September. Structural Health Monitoring on Real Scale Model of a Masonry Triumphal Arch. In Key Engineering Materials Vol. 347, pp. 279-284.
- Doyuran, V., 1976. Ortahisar'ın Çevresel Jeolojik Sorunları. Bulletin of the Geological Society of Turkey, 19, pp. 83-88.
- FEMA 368, 2001a. NEHRP Recommended Provisions for Seismic Regulations for New Buildings and Other Structures , Part 1-Provisions, 2000 Edition, Building Seismic Safety Council, Washington D.C.
- FEMA 369, 2001b. NEHRP Recommended Provisions for Seismic Regulations for New Buildings and Other Structures , Part 2-Commentary, 2000 Edition, Building Seismic Safety Council, Washington D.C.
- Guarnieri, A., Milan, N., & Vettore, A., 2013. Monitoring of Complex Structure for Structural Control Using Terrestrial Laser Scanning (TLS) and Photogrammetry. International Journal of Architectural Heritage, 7(1), pp. 54-67.
- Kameroğlu, B. B., 2012. "Local Development and Conservation Priorities: The Case of Ortahisar", Graduate Thesis: Middle East Technical University, Print.
- Lima, H. F., Vicente, R. D. S., Nogueira, R. N., Abe, I., André, P. S. D. B., Fernandes, C., ... & de Lemos Pinto, J., 2008. Structural Health Monitoring of the Church of Santa

Casa da Misericórdia of Aveiro Using FBG Sensors. *Sensors Journal, IEEE*, 8(7), pp. 1236-1242.

Marazzi, F., Tagliabue, P., & Corbani, F. M., 2011. Traditional vs Innovative Structural Health Monitoring of Monumental Structures: A case study. *Structural Control and Health Monitoring*, 18(4), pp. 430-449.

MATLAB, 2013. MATLABR2013B, MathWorks Inc.

Ministry of Public Works and Settlement, 2007. "Turkish Code for Buildings in Seismic Zones, Ankara, Turkey", pp. 10-12. Print.

Muñoz, F., Peña, F., & Meza, M., 2014. Virtual Reality Models for the Structural Assessment of Architectural Heritage Buildings. *International Journal of Architectural Heritage*, 8(6), pp. 783-794.

NETCAD, 2007. NetCAD 5.1, Netcad Yazılım A.Ş.

Ramos, L. F., Marques, L., Lourenço, P. B., De Roeck, G., Campos-Costa, A., & Roque, J., 2010. Monitoring Historical Masonry Structures with Operational Modal Analysis: Two Case Studies. *Mechanical Systems and Signal Processing*, 24(5), pp. 1291-1305.

SAP2000, 2011. Structural and Earthquake Engineering Software Version 15.0, CSI.

Standartları, T., 1987. "Yapı Elemanlarının Boyutlandırılmasında Alınacak Yüklerin Hesap Değerleri (TS. 498)". Türk Standartları Enstitüsü, Print.

Tabrizi, M., Hossein M., 2010. Repair and Health Monitoring for Historical Structures. In *Advanced Materials Research Vol. 133*, pp. 205-209.

Toker, S., Ünay, A. İ., 2004. Mathematical Modeling and Finite Element Analysis of Masonry Arch Bridges. *Gazi University Journal of Science*, 17(2), pp.129-139.

Topal, T., Doyuran, V., 1994. Effect of Discontinuities on the Development of Fairy Chimneys in the Cappadocia Region (Central Anatolia- Turkey). *Tr. J. of Earth Sciences*, 4, pp. 49-54.

Tunusluoglu, M. C., Zorlu, K., 2009. Rockfall Hazard Assessment in a Cultural and Natural Heritage (Ortahisar Castle, Cappadocia, Turkey). *Environmental Geology*, 56(5), pp. 963-972.

Türer, A., 2013. Structural Health Monitoring Lecture Notes, Ankara, Turkey.

Ugural, A. C., Fenster, S. K., 2002. "Advanced Strength and Applied Elasticity", 4th Edition, Prentice Hall International, Print.

Ulusay, R., Gökçeoğlu, C., Topal, T., Sönmez, H., Tuncay, E., Ergüler, Z. A., & Kaşmer, O., 2006. Assessment of Environmental and Engineering Geological Problems for the Possible Re-use of an Abandoned Rock-hewn Settlement in Ürgüp (Cappadocia), Turkey. *Environmental Geology*, 50(4), pp. 473-494.